

UC San Diego

UC San Diego Electronic Theses and Dissertations

Title

Rostrocaudal Diversification of Spinal Neurons Confers Segment-Specific Spinal Network Architectures

Permalink

<https://escholarship.org/uc/item/8r06f54n>

Author

Hayashi, Marito

Publication Date

2016

Peer reviewed|Thesis/dissertation

UNIVERSITY OF CALIFORNIA, SAN DIEGO

Rostrocaudal Diversification of Spinal Neurons Confers
Segment-Specific Spinal Network Architectures

A dissertation submitted in partial satisfaction of the
requirements for the degree Doctor of Philosophy

in

Biology

by

Marito Hayashi

Committee in charge:

Professor Samuel L. Pfaff, Chair
Professor Martyn D. Goulding
Professor Yishi Jin
Professor Franck Polleux
Professor Massimo Scanziani
Professor Binhai Zheng

2016

Copyright

Marito Hayashi, 2016

All rights reserved.

The Dissertation of Marito Hayashi is approved, and it is acceptable in quality and form for publication on microfilm and electronically:

Chair

University of California, San Diego

2016

DEDICATION

To the memory of my brother, Takuji,
who taught me compassion and wonders of life.

To my family and friends near and far,
for instilling in me a sense of curiosity and adventure.

To all of my mentors in science,
for sharing your joy and passion in scientific explorations,
and for your investment in my scientific development.

TABLE OF CONTENTS

Signature Page	iii
Dedication.....	iv
Table of Contents	v
List of Figures.....	vi
List of Abbreviations.....	vii
Acknowledgements.....	xi
Vita	xiii
Abstract of the Dissertation	xiv
Chapter 1 Introduction: Spinal cord patterning	1
Chapter 2 Rostrocaudal diversification of spinal neurons confers segment-specific spinal network architectures	22
Introduction	23
Results	25
Discussion	52
Author Contributions.....	57
Acknowledgements	58
References	58
Methods.....	63
Chapter 1 Methods.....	64
Chapter 2 Methods.....	64

LIST OF OF FIGURES

Figure 1.1 The black box of spinal cord circuitry	3
Figure 1.2 Cartesian coordinate system framework of spinal cord development.	4
Figure 1.3 Shh regulates gene expression through modulation of GLI activity	6
Figure 1.4 Rostrocaudal identity is defined by <i>Hox</i> genes	7
Figure 1.5 Examples of classical signaling cascades involved in spinal cord patterning.	8
Figure 1.6 Generation of progenitor domains.	10
Figure 1.7 Transcriptional cross-repression sharpens boundaries between progenitor domains . .	11
Figure 1.8 Example of a combinatorial transcription factor code	12
Figure 1.9 Diverse neuronal identities are specified by combinatorial transcription factor codes.	15
Figure 2.1: Basic characterization of V2a INs	26
Figure 2.2: V2a spinal neurons are glutamatergic ventrally projecting neurons both in cervical and lumbar segments.	27
Figure 2.3: V2a interneurons exhibit distinct anatomical connectivity schemes in different spinal segments.	30
Figure 2.4: Distinct MN-V2a connectivity between cervical and lumbar segments	31
Figure 2.5: Activation of lumbar V2a interneurons results in more robust motor outputs than cervical V2a interneurons.	34
Figure 2.6: Contralateral stimulations.	35
Figure 2.7: V2a interneurons exhibit distinct genetic signatures between cervical and lumbar segments.	38
Figure 2.8: Supplemental RNA-seq data	39
Figure 2.9: Conventional V2a interneuron marker CHX10 is differentially expressed between cervical and lumbar segments at a single cell level.	41
Figure 2.10: Characterization of the V2a IN diversification.	43
Figure 2.11: Other V2a interneuron marker genes are differentially expressed between cervical and lumbar segments.	46
Figure 2.12: Molecular diversification of V2a interneurons corresponds to brainstem-projecting status	50
Figure 2.13: Rabies infection control experiment.	51

LIST OF ABBREVIATIONS

AAV	Adeno-associated virus
ACSF	Artificial cerebrospinal fluid
ALS	Amyotrophic lateral sclerosis
bHLH	Basic helix–loop–helix transcription factor
Bhlhb5	Class B basic helix-loop-helix transcription factor
BMP	Bone morphogenetic protein
C	Cervical
CAG	CAG promoter
ChAT	Choline acetyltransferase
ChR2	Light-activated cation channel Channelrhodopsin 2
Chx10	Visual System Homeobox 2
CNQX	6-Cyano-7-nitroquinoxaline-2,3-dione
CNS	Central nervous system
CPG	Central pattern generator
Cre	Cre recombinase
dI1	Dorsal interneuron Class 1
dI2	Dorsal interneuron Class 2
dI3	Dorsal interneuron Class 3
dI4	Dorsal interneuron Class 4
dI5	Dorsal interneuron Class 5
dI6	Dorsal interneuron Class 6
dILA	Late-born dorsal interneuron class A
dILB	Late-born dorsal interneuron class B
e	Mouse embryonic day
En1	Engrailed Homeobox 1
ESC	Embryonic stem cell
ESC-MN	ESC-derived motor neuron
FACS	Fluorescence-activated cell sorting

G	Glycoprotein
GABA	Gamma aminobutyric acid
GAD	Glutamate decarboxylase
Gata3	GATA Binding Protein 3
GFP	Green fluorescent protein
GlyT2	Glycine transporter 2
GS	Gastrocnemius
Hb9	Motor Neuron And Pancreas Homeobox 1
HMC	Hypaxial motor column
Hox	Homeobox
iPS	Induced pluripotent stem cell
Isl	Islet
L	Lumbar
Lhx3	LIM homeobox 3
Lhx4	LIM homeobox 4
LIM-HD	LIM homeodomain transcription factor
LMC	Lateral motor column
LMCl	LMC lateral division
LMCm	LMC medial division
Lmx1b	LIM homeobox transcription factor 1-beta
LSL	Lox-stop-lox
mESC	Mouse embryonic stem cell
Min	Minute
MMC	Medial motor column
MN	Motor neuron
NMDA	N-Methyl-D-aspartic acid
OLP	Oligodendrocyte precursor
P	Mouse postnatal day
p0	V0 interneuron progenitor domain

p1	V1 interneuron progenitor domain
p2	V2 interneuron progenitor domain
p3	V3 interneuron progenitor domain
Pax2	Paired box gene 2
PCR	Polymerase chain reaction
pdI1	dI1 dorsal interneuron progenitor domain
pdI2	dI2 dorsal interneuron progenitor domain
pdI3	dI3 dorsal interneuron progenitor domain
pdI4	dI4 dorsal interneuron progenitor domain
pdI5	dI5 dorsal interneuron progenitor domain
pdI6	dI6 dorsal interneuron progenitor domain
pdIL	dILA–dILB late-born interneuron progenitor domain
PGC	Preganglionic motor column
pMN	Motor neuron progenitor domain
polyA	Polyadenylation tail
R26	Rosa locus
RA	Retinoic acid
Rab	Rabies virus
Rosa	Rosa locus
SAG	Smoothened agonist
Sec	Second
Shh	Sonic hedgehog
Shox2	Short stature homeobox 2
Sim1	Single-minded family bHLH transcription factor 1
SMA	Spinal muscular atrophy
Sox14	SRY-box 14
Syn-Tom	Synaptophysin-TdTomato fusion protein
Syp	Synaptophysin
T	thoracic

TdTomato	Tandem Tomato fluorescent protein
V	Ventral interneuron class
V0	Ventral interneuron Class 0
V1	Ventral interneuron Class 1
V2	Ventral interneuron Class 2
V3	Ventral interneuron Class 3
vGlut2	Vesicular glutamater transporter 2
μV	microvolt

ACKNOWLEDGEMENTS

I would like to thank my fellow graduate students: Neal, Kathryn, Matt, Wes, Sagar, Peter and Tiffany. You are my lab siblings whom I wish nothing but happiness and success in your own way. I feel extremely fortunate to have gotten to know you during graduate school, and I have learned so much from you. Thank you for all the laughs that we got to have together and all the stimulating discussions we had during and outside of graduate student discussions. Ariel and Chris, thank you for being great mentors and friends in the lab. I sincerely appreciate your investment in my scientific development and your contagious drive in science. Lukas, thank you for your friendship and sharing the new perspective that you have brought into the Pfaff lab. Your drive and curiosity in science have inspired me tremendously in the lab. Dario, thank you for sharing your keen insights. Karen, Miriam, Nick, Laura, and G, your support has tremendously facilitated my scientific explorations in the Pfaff lab. The rest of the Pfaff lab, past and present: thank you everyone for your help and creating a fun environment that I look forward to conducting scientific research everyday in. I would also like to thank Martyn and the Goulding lab for their technical help and friendship.

I would also like to express my gratitude to my dissertation committee members, Martyn, Jin, Franck, Massimo and Binhai for their guidance and support over the years. Thank you for your contribution to better my dissertation work by generously sharing your expertise during and outside of committee meetings.

I am deeply grateful to my previous supervisors and mentors in science: Drs. Jing Wang (UCSD), Haruko Kazama (ICU), Hiroshi Chiura (ICU), Daichi Kawaguchi (UTokyo), and Yukiko Gotoh (UTokyo) for helping shape me as a scientist today. Thank you for your encouragement and support.

Sam, I cannot thank you enough for your guidance, support, and patience over the years. You have provided me with the resources to expand my perspective as a scientist as well as a person, and I thank you for creating a lab environment that I enjoy conducting research in. I have witnessed your generosity countless times, but I learned how much you care about the lab environment particularly when you repeatedly gave up your office to provide us with more space

over the years. I am sincerely thankful for the training opportunities that you have given me, and I look forward to further developing the scientific inquiry skills that you have instilled in me for the years to come.

Chapter 1, in full, is a reprint of the material as it appears in Gifford, W.D., Hayashi, M., Sternfeld, M.J., Tsai, J., Alaynick, W.A., & Pfaff, S.L. (2013). Chapter 7 - Spinal Cord Patterning. Patterning and Cell Type Specification in the Developing CNS and PNS: Comprehensive Developmental Neuroscience (Vol. 1). Academic Press. <http://doi.org/10.1016/B978-0-12-397265-1.00047-2>.

Chapter 2 is an adaptation of a manuscript being prepared for submission. The working citation is: Hayashi, M., Hinckley, C.A., Driscoll, S.P., Levine, A.J., Hilde, K.L., Sharma, K., Pfaff, S.L. Rostrocaudal diversification of spinal neurons confers segment-specific spinal network architectures. The authors would like to thank K. Lettieri, M. Gullo, L.C. Bachmann, M.J. Sternfeld, N.D. Amin, P.J. Osseward, Salk GT3 core (L. Lisowski, J. Naughton, J. Marlet, R. Armendariz, C. Ly), FCCF core (C. O'Connor, C. Fitzpatrick), NGS core (M. Ku) for technical support and advice; M. Goulding and R. Johnson for providing reagents. M.H. was supported by the Timken-Sturgis Foundation and the Japanese Ministry of Education, Culture, Sports, Science, and Technology Long-Term Student Support Program. C.A.H. was supported by a U.S. National Research Service Award Fellowship from U.S. National Institutes of Health NINDS. A.J.L. was supported by George E. Hewitt Foundation for Medical Research and Christopher and Dana Reeve Foundation. K.L.H. was supported as a National Science Foundation Graduate Research Fellow and by the Chapman Foundation. S.L.P. is supported as a Howard Hughes Medical Institute Investigator and as a Benjamin H. Lewis chair in neuroscience. This research was supported by funding from the Howard Hughes Medical Institute, the Marshall Foundation and the Sol Goldman Charitable Trust.

VITA

- 2003-2007 International Christian University
Bachelor of Arts - Liberal Arts/Biology
- 2005-2006 Education Abroad Program. University of California, San Diego
- 2007-2008 Institute of Molecular and Cellular Biosciences, University of Tokyo
- 2008-2016 University of California, San Diego
The Salk Institute for Biological Studies
Doctor of Philosophy - Biology

PUBLICATIONS

Peer Reviewed Original Research

Hayashi, M., Hinckley, C.A., Driscoll, S.P., Levine, A.J., Hilde, K.L., Sharma, K., Pfaff, S.L. Rostrocaudal diversification of spinal neurons confers segment-specific spinal network architectures. *in preparation*.

Hilde, K.L., Levine, A.J., Hinckley, A.C., **Hayashi, M.**, Montgomery, J.M., Gullo, M., Driscoll, S.P., Grosschedl, R., Kohwi, Y., Kohwi-Shigematsu, T., Pfaff, S.L. Satb2 is required for the development of a spinal exteroceptive circuit node that modulates limb position. *Neuron*. 91 (4), 763-776. 2016

Hinckley, C.A., Alaynick, W.A., Gallarda, B.W., **Hayashi, M.**, Hilde, K.L., Driscoll, S.P., Dekker, J.D., Tucker, H.O., Sharpee, T.O., Pfaff, S.L. Spinal Locomotor Circuits Develop Using Hierarchical Rules Based on Motorneuron Position and Identity. *Neuron*. 87 (5), 1008-1021. 2015.

Hsu, C., White, N.M., **Hayashi, M.**, Lin, E.C., Poon, T., Banerjee, I., Chen, J., Pfaff, S.L., Macagno, E., Dorrestein, P.C. Microscopy Ambient Ionization Top-Down Mass Spectrometry Reveals Developmental Patterning. *Proc. Natl. Acad. Sci. U.S.A.* 110 (37), 14855-14890. 2013.

Peer Reviewed Literature Review

Gifford, W.D., **Hayashi, M.**, Sternfeld, M.J., Tsai, J., Alaynick, W.A., & Pfaff, S.L., Chapter 7 - Spinal Cord Patterning, *Patterning and Cell Type Specification in the Developing CNS and PNS*, edited by John L.R. Rubenstein Pasko Rakic, Academic Press, Oxford, 2013, Pages 131-149, <http://dx.doi.org/10.1016/B978-0-12-397265-1.00047-2>.

ABSTRACT OF THE DISSERTATION

Rostrocaudal Diversification of Spinal Neurons Confers
Segment-Specific Spinal Network Architectures

by

Marito Hayashi

Doctor of Philosophy in Biology
University of California, San Diego, 2016
Professor Samuel L. Pfaff, Chair

The spinal cord represents the final stage of generating motor behaviors, where descending commands or sensory inputs must be transformed into behaviorally-relevant pattern of motor neuron activity. Networks along the rostrocaudal axis of the spinal cord regulate diverse motor behaviors such as respiration, forelimb, trunk, and hindlimb movements, mediated by stringent innervations of motor neurons to muscle fibers. However, how the network properties of the central nervous system enable these diverse motor outputs remains elusive. To address this

question, we set out to investigate whether a cardinal class of spinal cord neurons are diversified in different spinal segments.

This dissertation describes a series of original work that aims to elucidate the diversification of spinal neurons in different segments of the spinal cord. The first chapter is an introduction into the developmental processes of spinal cord development.

The second chapter proceeds from this review to explore whether spinal neurons are further diversified in different spinal segments to underlie distinct network operation and motor outputs. In particular, we studied V2a interneurons as a model to address this question. Using viral tracing and RNA-sequencing, we uncovered how V2a interneurons exhibit distinct anatomical connectivity schemes and distinct genetic signatures in forelimb regulating- and hindlimb regulating-segments of the spinal cord. It is my hope that our studies establish a framework of how diversification of spinal neurons along the rostrocaudal axis underlies distinct intrinsic network properties in different spinal segments that ultimately contribute to diverse motor outputs that the spinal cord regulates.

Chapter 1

Introduction: Spinal cord patterning

CHAPTER

7

Spinal Cord Patterning

W.D. Gifford, M. Hayashi, M. Sternfeld, J. Tsai, W.A. Alaynick, S.L. Pfaff
Howard Hughes Medical Institute, La Jolla, CA, USA; Salk Institute for Biological Studies, La Jolla, CA, USA

O U T L I N E

7.1 Introduction	132	7.5.3 Establishing Neural Identities through a Combinatorial Code	140
7.2 Major Concepts of Spinal Cord Patterning	132	7.6 Cell–Cell Interactions	141
7.3 Dorsoroventral Patterning	134	7.6.1 Notch–Delta Signaling	141
7.3.1 Dorsoroventral Patterning: Shh	134	7.6.2 Retinoid Signaling	142
7.3.2 Dorsoroventral Patterning: BMPs	134	7.7 Glia in the Spinal Cord	142
7.3.3 Dorsoroventral Patterning: Wnts	135	7.7.1 Astrocytes	142
7.3.4 Other Aspects of Dorsoroventral Patterning	135	7.7.2 Oligodendrocytes	143
7.4 Rostrocaudal Patterning	136	7.8 Human Diseases of Spinal Cord Patterning	143
7.4.1 Rostrocaudal Patterning: RA, FGFs, Gdf11, and the Hox Code	136	7.9 Lessons from Spinal Cord Patterning for Disease Modeling and Regenerative Medicine	145
7.4.2 Rostrocaudal Patterning: Hox Expression in MNs	137	7.10 Summary and Unanswered Questions	146
7.5 LIM/bHLH Factors and the Combinatorial Code	138	Glossary	147
7.5.1 LIM Homeodomain Factors	138	References	147
7.5.2 bHLH Factors	140		

Nomenclature

ALS Amyotrophic lateral sclerosis
bHLH Basic helix–loop–helix transcription factor
BMP Bone morphogenetic protein
CNS Central nervous system
dI1 Dorsal interneuron Class 1
dI2 Dorsal interneuron Class 2
dI3 Dorsal interneuron Class 3
dI4 Dorsal interneuron Class 4
dI5 Dorsal interneuron Class 5
dI6 Dorsal interneuron Class 6
dIL_A Late-born dorsal interneuron class A
dIL_B Late-born dorsal interneuron class B
E9.5 Embryonic day 9.5
ESC Embryonic stem cell
ESC-MN ESC-derived motor neuron
HMC Hypaxial motor column
iPS Induced pluripotent stem cell

LIM-HD LIM homeodomain transcription factor
LMC Lateral motor column
LMCI LMC lateral division
LMC_m LMC medial division
MMC Medial motor column
MN Motor neuron
OLP Oligodendrocyte precursor
p0 V0 interneuron progenitor domain
p1 V1 interneuron progenitor domain
p2 V2 interneuron progenitor domain
p3 V3 interneuron progenitor domain
pdI1 dI1 dorsal interneuron progenitor domain
pdI2 dI2 dorsal interneuron progenitor domain
pdI3 dI3 dorsal interneuron progenitor domain
pdI4 dI4 dorsal interneuron progenitor domain
pdI5 dI5 dorsal interneuron progenitor domain
pdI6 dI6 dorsal interneuron progenitor domain
pdIL dIL_A–dIL_B late-born interneuron progenitor domain
PGC Preganglionic motor column

pMN Motor neuron progenitor domain
 Shh Sonic hedgehog
 SMA Spinal muscular atrophy
 V0 Ventral interneuron Class 0
 V1 Ventral interneuron Class 1
 V2 Ventral interneuron Class 2
 V3 Ventral interneuron Class 3

7.1 INTRODUCTION

The vertebrate spinal cord serves two basic functions for the organism. First, it relays sensory information from the periphery along a number of white matter tracts to the brain, where it is processed and informs the organism about the internal state of the body and position in space (interoception, proprioception) and the influences of the outside world upon the body (somatosensation). Second, it transmits motor information from the brain along white matter tracts to control the stability and movement of the body in space. However, the concept of the spinal cord as simply a collection of axonal conduits between the brain and the periphery is both factually oversimplified and a poor metaphor because the spinal cord is a highly complex neuronal structure that actively processes and modulates ascending and descending information and mediates compound reflexes (Figure 7.1). In fact, the spinal cord performs a number of sensorimotor computations, most notably those required for the proper control of movement. Classical experiments have demonstrated that a decerebrated cat preparation, when suspended above a treadmill, is capable of coordinated locomotion despite loss of descending control from the brain (Brown, 1911). It is now well accepted that the spinal cord contains the basic circuitry responsible for proper species-specific coordination of left versus right, flexor versus extensor, and forelimb versus hindlimb movement. For recent reviews on spinal locomotor circuitry, the reader is referred elsewhere (Goulding, 2009; Grillner and Jessell, 2009).

How does the spinal cord develop in the embryo? While a full answer to this question requires extensive scientific characterization at the molecular, cellular, and circuit levels, as well as an understanding of the roles that neural activity and experience play on developmental processes, this chapter focuses primarily on the generation of the distinct cell types that are specified by patterns of morphogen gradients. This focus can be explained by the wealth of information that has come out of studies over the last 20 years that were aimed at describing the basis for behaviors mediated by the spinal cord at the cellular level. Because of this work, a framework that assigns neuronal identity and diversity in the spinal cord based upon expression of transcription factors has now reached a more mature state and can be used to inform studies of other central nervous system (CNS) regions (Alaynick et al., 2011). Other developmental neuroscience topics



FIGURE 7.1 The black box of spinal cord circuitry. The spinal cord receives descending input from the brain and ascending information from the periphery, which it can modulate or process accordingly. Additionally, it has been shown that the spinal cord has the ability to produce movements independently of these inputs. The capacity to carry out diverse functions relies on the generation of many cell types that arise from an elegant system of patterning and transcriptional control, which is described in this chapter. These findings have helped to illuminate many components in this black box.

important for understanding spinal cord function, such as early neural tube formation, neurogenesis, axon guidance, and postnatal developmental processes, are discussed elsewhere.

The molecular mechanisms of neuronal specification in this chapter have been the product of over a century of research using a variety of model systems. The six most widely used organisms in this regard are mouse, chicken, frog, zebra fish, fly, and worm. Each of these model organisms provides unique experimental tools that can be leveraged to better understand spinal cord patterning, such as mammalian genetics in mouse and optically accessible vertebrate development in zebra fish. Importantly, while many findings made in these organisms apply to human spinal cord development, this has not been directly demonstrated in most cases. Future work using fetal material and human embryonic stem cells (ESCs) may prove informative in this regard.

7.2 MAJOR CONCEPTS OF SPINAL CORD PATTERNING

A fundamental concept of spinal cord patterning is that the early embryonic neural tube is comprised of a largely unspecified pool of immature cells that are

7.2 MAJOR CONCEPTS OF SPINAL CORD PATTERNING

capable of differentiating into any one of the many unique cell types in the spinal cord. Spinal cord organization results from uncommitted progenitor cells responding to positional cues that come from neighboring tissues that instruct the cells. These instructions come first in the form of morphogen gradients along three orthogonal axes: mediolateral, dorsoventral, and rostrocaudal. In effect, these axes define a three-dimensional Cartesian coordinate system in which each 'point' represents an uncommitted spinal cord cell that receives a unique complement of signals based upon its particular point in space (Figure 7.2). While there is a biological basis for considering these axes independently, it should be remembered that there is a complex interplay of factors across these axes over time.

The signals that act on the naïve spinal progenitor cells take one of two general forms. First, there are long-range secreted factors that are released from neighboring tissues and diffuse to their targets. These factors

include sonic hedgehog (Shh) from the ventral notochord, bone morphogenetic proteins (BMPs), and wingless MMTV integration site proteins (Wnts) from the overlying ectoderm, and retinoic acid (RA) produced by the activity of retinaldehyde dehydrogenase (*Raldh*) in the paraxial mesoderm. A second short-range signaling strategy arises from membrane-bound molecules that mediate local cell-cell interactions, such as the Notch-Delta pathway (Figure 7.4). Some factors, like Shh, induce different cellular responses in a graded, concentration-dependent manner. Others, like Notch signaling, function with a binary (on/off) mechanism. The consequence for a particular cell depends on (1) the unique combination and concentration of secreted and fixed signals it receives from its environment; and (2) the extent to which prior signaling has rendered the cell competent to receive or integrate new signals.

These signaling molecules can exert lasting effects through signaling cascades that regulate the expression of transcription factors that produce gene expression changes capable of specifying cell fate. Borders between adjacent classes of cells (which receive roughly equivalent fate-instructive signals) must be clearly defined to avoid hybrid identities. This is accomplished by the elegant strategy of cross-repression, which has been well characterized in the ventral spinal cord. With this system, fate-specifying transcription factors of bordering cell types act to reciprocally repress one another. As a result, when a cell-type-specific transcription factor is expressed, it will directly inhibit the expression of other transcription factors that could serve to alter the identity of that cell. If two cross-repressive transcription factors are under the control of a single morphogen (such as Shh), then both factors may be briefly coexpressed. But the 'winner-takes-all' process of cross-repression ensures that only one specific cell identity is ultimately generated (Figure 7.7).

While signaling molecules set up a coarse coordinate system within the spinal cord that is refined by transcriptional cross-repression, generating a specific cell type results from the coactivation of a unique combination of transcription factors. Such combinations of transcription factors can interact at the protein level to form higher-order complexes that then recognize distinct DNA regulatory elements. This increased level of complexity, shaped by binding partners, allows for diverse transcription factor-binding characteristics and gene expression profiles.

The remainder of this chapter will survey research from many studies of spinal cord patterning with particular attention to features that are well studied. At the end of the chapter, human diseases of spinal cord patterning and the implications of the lessons learned from spinal cord patterning for regenerative medicine will be discussed.

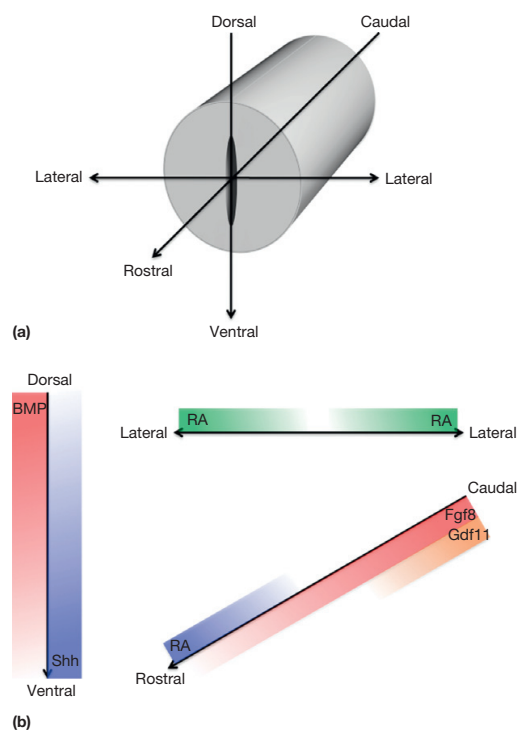


FIGURE 7.2 Cartesian coordinate system framework of spinal cord development. (a) The embryonic spinal cord tissue can be mapped in space along three axes: dorsoventral, rostrocaudal, and mediolateral. (b) Along these principal axes, gradients of morphogens induce cell-type-specific patterns of gene expression. High concentrations of Shh induce ventral cell fates while high concentrations of BMPs induce dorsal cell fates. Similarly, RA, FGF8, and Gdf11 regulate positional identity along the rostrocaudal axis.

7.3 DORSOVENTRAL PATTERNING

The dorsal portion of the spinal cord is primarily composed of interneurons that receive and process sensory input from peripheral neurons of the dorsal root ganglia, while the ventral spinal cord is generally thought to be dedicated to the processing of motor output. This gross dorsoventral division in sensory and motor function reflects the dorsoventral-patterning mechanisms in early spinal cord development. Within the ventricular zone of the spinal cord, many progenitor domains are established which give rise to distinct neuronal and glial lineages. As these progenitors mature during midgestation, they stop dividing, express further transcriptional programs important for differentiation, and migrate to stereotypic locations in the mantle layer (Jessell, 2000; Shirasaki and Pfaff, 2002).

Based on the expression patterns of various marker genes along the dorsoventral axis, six interneuron progenitor domains (dp1–6) have been designated in the dorsal spinal cord, while five progenitor domains have been designated in the ventral spinal cord (p0–3, pMN). Each of these progenitors then gives rise to a corresponding neuron population, dI1–dI6 interneurons in the dorsal spinal cord, and V0–V3 interneurons and motor neurons (MNs) in the ventral spinal cord (Alaynick et al., 2011; Goulding, 2009; Jessell, 2000; Shirasaki and Pfaff, 2002). This diversity in progenitor domains and their corresponding mature neural subtypes can be seen in Figures 7.6 and 7.9. The principle signals important for generating these diverse cell types along the dorsoventral axis are Shh, BMPs, and Wnts.

7.3.1 Dorsoventral Patterning: Shh

The transduction of morphogen signaling through second messenger systems to regulate specific gene expression programs is a general feature of spinal cord patterning. The most well-studied morphogen, Shh, is expressed and secreted from the notochord, which then induces Shh expression from the floor plate (Jessell, 2000). As a result of this secretion pattern, local Shh concentration is high in the ventral cord and diminishes dorsally. Many experiments have shown the importance of this Shh gradient. For example, studies conducted by Ericson and colleagues using spinal cord explants showed that induction of V1-specific genes required lower Shh concentrations than induction of V2- or MN-specific genes. These levels of Shh corresponded to the relative dorsoventral positions of the progenitor domains (Ericson et al., 1997a,b). Furthermore, studies of *Shh* knockout mice have shown that the floor plate fails to develop and genes that are normally transcribed only in the dorsal region of the spinal cord expand their

expression domains into the ventral spinal cord (Chiang et al., 1996). More recent work has shown that, in addition to the Shh concentration gradient, the duration of exposure and an additional gene regulatory network appear to be critical for induction of downstream genes in response to Shh (Balaskas et al., 2012; Dessaud et al., 2007).

To signal downstream genes, in the canonical Shh pathway, Shh binds to its receptor, patched-1 (PTCH1). In the absence of Shh, PTCH1 inhibits the transmembrane protein, smoothed (SMO; Figure 7.4(a)). When Shh binds to PTCH1, SMO is released from inhibition by PTCH1, possibly mediated by transfer of an oxysterol from PTCH1 to SMO (Corcoran and Scott, 2006). SMO is then free to activate the transcription factors GLI1–GLI3, which, in turn, regulate the expression of downstream genes (Fuccillo et al., 2006; Rahnama et al., 2006).

The concentration gradient of Shh (high ventrally to low dorsally) causes differential expression of various downstream genes in progenitors along the dorsoventral axis, and this is thought to be a major factor responsible for the diversification of spinal cord progenitor domains. So how do the different local concentrations of Shh result in differing downstream gene expression effects? As described earlier, three GLI proteins serve as intermediaries in the Shh pathway. In the most ventral spinal cord, Shh is found at its highest levels. At this location, GLI1 and GLI2 transcriptionally activate their targets, while GLI3 repressor activity is low. In more dorsal regions, where Shh concentration is lower, GLI1 and GLI2 are not readily active, while GLI3 actively represses its targets. The combined activity of all three GLI proteins results in differential expression of downstream genes, based on the concentration of Shh (Figure 7.3; Fuccillo et al., 2006).

7.3.2 Dorsoventral Patterning: BMPs

In the dorsal spinal cord, BMPs and other TGF β family members (Bmp2, 4, 7, growth differentiation factor 7, activin, dorsalin) are secreted from the overlying ectoderm (Liem et al., 2000; Liu and Niswander, 2005). Binding of BMPs to their receptors (BMPRs) results in receptor phosphorylation. Phosphorylated BMPRs subsequently phosphorylate Smad proteins which associate with additional Smad mediator proteins facilitate either activation or repression of downstream genes (Liu and Niswander, 2005).

The importance of TGF β family proteins in determining dorsal fates of spinal cord progenitors during development was demonstrated experimentally in a manner similar to the Shh work. In BMPR knockout mice, the most dorsal interneuron population (dI1) was not present, the dI2 population was significantly reduced, and

7.3 DORSOVENTRAL PATTERNING

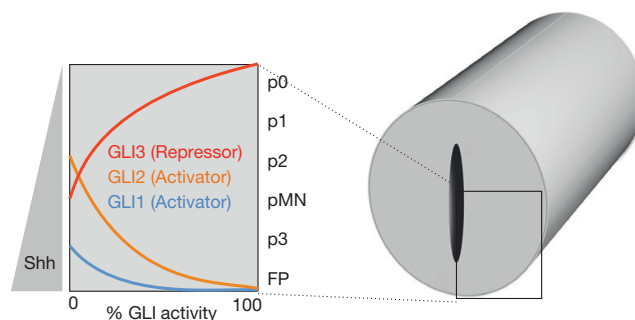


FIGURE 7.3 Shh regulates gene expression through modulation of GLI activity. Shh regulates the activity of the three GLI proteins. At the highest levels of Shh near the floor plate, for example, GLI1 and GLI2 transcriptionally activate their targets while GLI3 repressor activity is low. Reciprocally, at low levels of Shh, more dorsally, GLI1 and GLI2 are not readily active while GLI3 actively represses its targets. The net effect of differential GLI activity results in the induction of different sets of downstream genes. Gradients of other morphogens regulate their respective gene targets through similar intracellular machinery as that shown here for Shh. Adapted with permission by Macmillan Publishers Ltd from Fuccillo M, Joyner AL, and Fishell G (2006) *Morphogen to mitogen: The multiple roles of hedgehog signalling in vertebrate neural development*. Nature Reviews Neuroscience 7: 772–783.

the dI3 and dI4 domains expanded dorsally, suggesting that BMP signaling is required for specification of the dorsal spinal cord (Wine-Lee et al., 2004). In a series of experiments, dorsal interneuron marker genes were shown to be upregulated in spinal cord explants by the application of various TGF β family proteins (Liem et al., 1997). This was also observed when a constitutively active BMPR was ectopically expressed in chick spinal cords (Timmer et al., 2002).

Do the morphogens from the floor plate and roof plate specify the ventral cell fate and the dorsal cell fate independently, or do they interact to specify and refine cell fates? A study showed that in the presence of BMPs, ventral spinal cord marker genes induced by Shh were downregulated, and normally dorsal genes were upregulated, suggesting that Shh and BMPs interact (directly or indirectly) to specify progenitor cell fate. Furthermore, application of a BMP inhibitor together with Shh promoted greater expression of ventral marker genes than Shh alone (Liem et al., 2000).

7.3.3 Dorsoventral Patterning: Wnts

Apart from Shh, BMP and other TGF β family members, Wnt signaling is also known to participate in cell specification in the spinal cord, particularly in the dorsal regions where Wnt1 and Wnt3a are found (Parr et al., 1993). In *Wnt1/3a* double knockout mice, the number of dI4–6 marker gene-positive neurons increased at the expense of dI1–3, suggesting that Wnt1 and Wnt3a are necessary for the specification of the dI1–3 dorsal progenitor domains. The intact expression patterns of BMP signaling components in this mutant mouse suggest that the changes in cell fate specification in this context were achieved directly by Wnt

signaling rather than through modulation of BMP activity (Muroyama et al., 2002).

The role of Wnts in dorsal spinal cord patterning appears to be mediated by the canonical Wnt signaling pathway: once Wnt binds to its receptor Frizzled, initiating a downstream signaling cascade, β -catenin translocates into the nucleus where it interacts with TCF/LEF transcription factors to effect gene expression (Figure 7.4(b)). Consistent with this signaling pathway, ectopic expression of a constitutively active form of β -catenin in the chick spinal cord results in expansion of dorsal marker genes. Conversely, a dominant negative form of TCF3 facilitates the expression of the ventral marker genes, and was shown to suppress the expression of GLI3, a negative regulator of the Shh pathway. Taken together, these studies suggest that Wnt signaling specifies the dorsal spinal cord fate and can modulate Shh signaling (Alvarez-Medina et al., 2008).

7.3.4 Other Aspects of Dorsoventral Patterning

In addition to relative position with respect to Shh, BMP, and Wnt signaling centers, the timing of differentiation also contributes to the diversity of spinal neurons along the dorsoventral axis. For instance, the dIL spinal cord progenitor domain produces unique ‘late-born’ interneuron populations, dIL_A and dIL_B, between E12.0 and E13.5 in mice, while all other dorsal neural subtypes are generated between E10 and E11.5 (Mizuguchi et al., 2006). Furthermore, toward the end of neurogenesis, the progenitor cell programming switches from neurogenesis to gliogenesis, producing astrocytes and oligodendrocytes (Lee and Pfaff, 2001). A recent study suggests that the diversity of neurons along the dorsoventral axis may also be a general feature of glia subtypes (Hochstim

7.4 ROSTROCAUDAL PATTERNING

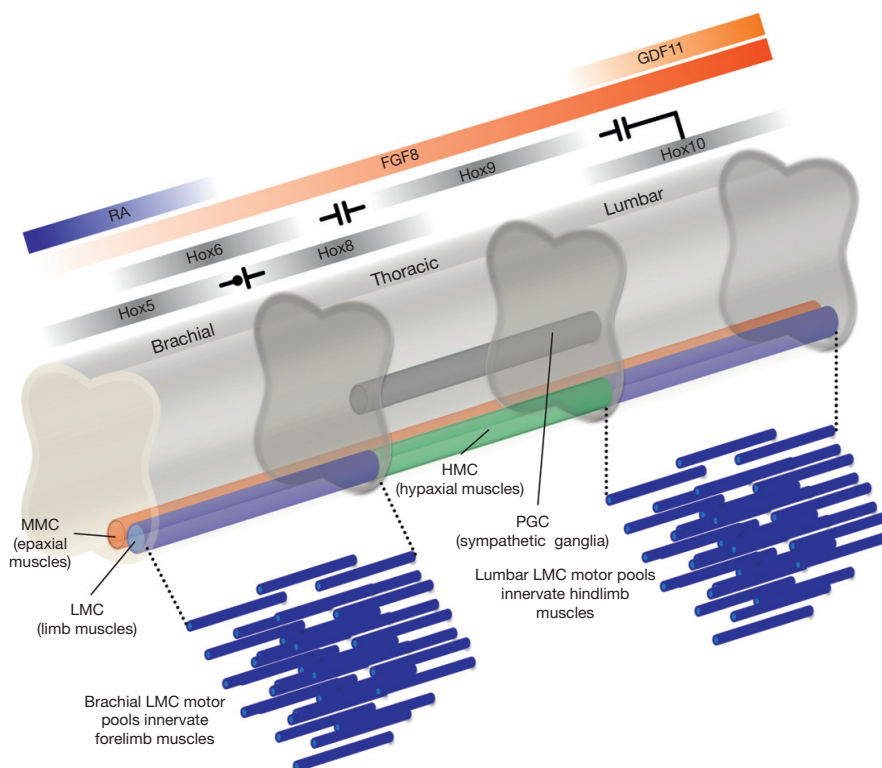


FIGURE 7.5 Rostrocaudal identity is defined by *Hox* genes. The morphogens FGF8, Gdf11, and RA are found in rostrocaudal gradients along the length of the spinal cord. These factors induce the expression of specific *Hox* genes, which serve to demarcate the spinal cord into rostrocaudal divisions. High levels of RA induce *Hox* genes that specify rostral spinal cord fates while high levels of FGF8 and Gdf11 induce *Hox* genes that specify caudal cell fates. Cross-repression between particular *Hox* genes defines the brachial, thoracic, and lumbar levels. This also specifies the rostrocaudal extent of each of the motor neuron columns. The MMC is found throughout the rostrocaudal extent of the spinal cord, the HMC is restricted to thoracic levels, the PGC is found in thoracic and upper lumbar levels, while the LMC is found at limb levels (brachial and lumbar spinal cord). The LMC is further subdivided into motor pools, each responsible for innervating a single limb muscle.

high concentrations of FGF to ensure the appropriate expression of specific *Hox* genes (Liu et al., 2001).

In addition to the Gdf11 and FGF signaling needed for proper spinal *Hox* expression caudally, RA drives the expression of *Hox* genes at rostral spinal levels (Dasen and Jessell, 2009). RA is expressed by somites in the paraxial mesoderm alongside the rostral spinal cord, influencing *Hox* patterning in the cervical and brachial levels (Figure 7.5; Liu et al., 2001). RA also affects hindbrain *Hox* expression, and it imposes its influence here by binding the nuclear hormone receptor, RAR (Dasen and Jessell, 2009; Duester, 2008). In addition to shaping *Hox* expression patterns in the rostral spinal cord, RA is also responsible for antagonizing FGF signals from the caudal mesoderm (Dasen and Jessell, 2009; Duester, 2008), possibly helping to define borders of *Hox* expression. The combined signaling of RA, Gdf11, and FGF leads to 3' *Hox* expression (*Hox4–Hox8*) at cervical and brachial levels, *Hox8* and *Hox9* expression at

thoracic levels, and 5' *Hox* expression (*Hox10–Hox13*) at lumbar levels (Dasen and Jessell, 2009).

7.4.2 Rostrocaudal Patterning: *Hox* Expression in MNs

While systematic studies comparing interneurons of a single class across rostrocaudal levels in the spinal cord have not been conducted, the MN populations along the rostrocaudal axis have been shown to differ with respect to *Hox* gene expression. In the spinal cord, there are four different columns of MNs: the lateral motor column (LMC), the medial motor column (MMC), the hypaxial motor column (HMC), and the preganglionic motor column (PGC). The MMC runs the length of the cord and innervates dorsal epaxial musculature, while the LMC is limited to the brachial and lumbar levels where MNs innervate the limbs. The MNs of the HMC target intercostal and abdominal wall hypaxial musculature.

7. SPINAL CORD PATTERNING

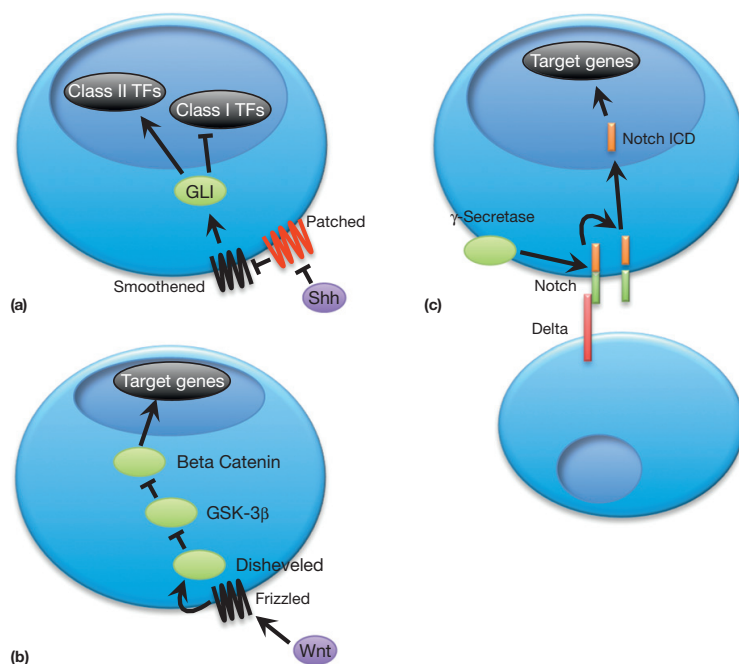


FIGURE 7.4 Examples of classical signaling cascades involved in spinal cord patterning. Several signaling pathways are induced by morphogen gradients or cell-cell interactions that induce the expression of target genes, such as transcription factors. These transcription factors and transcriptional modulators then express cell fate specification genetic programs. (a) The canonical Shh pathway. Shh binds to the patched receptor, thus disinhibiting Smoothedown. This then activates GLI factors responsible for regulating downstream genes. (b) The canonical Wnt signaling pathway. Wnt binds to the Frizzled receptor and the following intracellular signaling cascade results in transcriptional changes. (c) The canonical Notch–Delta signaling pathway. Physical proximity of two adjacent cells allows the two transmembrane proteins Delta and Notch to interact. This binding event allows γ -secretase to cleave Notch, releasing the Notch intracellular domain (ICD), which then translocates into the nucleus to effect transcription.

et al., 2008). Future work is expected to uncover glial subtype-specific functions (see Section 7.7).

7.4 ROSTROCAUDAL PATTERNING

While many studies have focused on dorsoventral patterning of the spinal cord, much less effort has been put into understanding rostrocaudal diversity and specification. However, recent studies have shown that homeobox (*Hox*) transcription factor genes are differentially expressed along the spinal cord under the influence of RA, fibroblast growth factors (FGFs), and growth and differentiation factor 11 (Gdf11) (a TGF β family member) (Figure 7.5).

7.4.1 Rostrocaudal Patterning: RA, FGFs, Gdf11, and the *Hox* Code

Hox genes are responsible for the rostrocaudal segmentation seen in animals. They are found arrayed in gene clusters, of which there are four in mammals. Typically, the *Hox* genes located at the 3' end of a particular cluster are expressed in more rostral areas, while genes at the 5' end of the cluster are most often active in caudal regions of the organism, though exceptions exist (Lemons and McGinnis, 2006). FGF signaling is

responsible for the initial expression of *Hox* genes along the spinal cord and then continually influences their caudal expression through its secretion from the primitive knot (or Hensen's node/Spemann's organizer in various species) and the presomitic mesoderm. During development, these two areas move farther caudally, resulting in the caudal regions of spinal cord being exposed to higher concentrations of FGF, and for a longer period of time, relative to the rostral cord (Bel-Vialar et al., 2002; Dasen et al., 2003; Dubrulle and Pourquie, 2004; Liu et al., 2001). How FGF influences the expression of *Hox* genes is not clear, but altering expression of vertebrate caudal homeobox (*Cdx*) genes can mimic aberrant expression of FGF (Bel-Vialar et al., 2002). This finding, and the possibility that *Cdx* could bind directly to *Hox* regulatory elements, has led to the hypothesis that FGF may act through *Cdx* activity to regulate *Hox* gene expression (Dasen and Jessell, 2009).

Though FGF expression is responsible for *Hox* patterning in most regions of the spinal cord, it alone is insufficient to drive the entire *Hox* expression pattern seen in the spinal cord (Carpenter, 2002; Dasen and Jessell, 2009). For instance, in caudal areas of the spinal cord, Gdf11, a specific TGF β family member, is required for proper *Hox* expression (Figure 7.5). Like FGF, Gdf11 is expressed by the primitive knot, which leads to its high caudal-to-rostral gradient (Dasen and Jessell, 2009). In these caudal regions, Gdf11 works in conjunction with

The MNs in the PGC, located in the thoracic and upper lumbar levels, target sympathetic ganglia (Dasen and Jessell, 2009). *Hox* genes appear to be responsible for setting up these columns as it has been found that *Hox6* is restricted to the brachial LMC neurons, *Hox9* to the thoracic PGC neurons, and *Hox10* to the lumbar LMC neurons (Choe et al., 2006; Dasen and Jessell, 2009; Dasen et al., 2003; Lance-Jones et al., 2001; Liu et al., 2001). Furthermore, *Hox9* is cross-repressive with both *Hox6* and *Hox10*, ensuring distinct boundaries between the brachial, thoracic, and lumbar segments (Dasen et al., 2003; Figure 7.5).

In addition to establishing rostrocaudal boundaries of motor columns, *Hox* genes can act with accessory factors to promote the diversification of MNs. Recently, it was discovered that *FoxP1*, whose expression is in part controlled by *Hox* genes, promotes MN segregation and motor pool specification. In studies by Dasen and colleagues (2008) and Rousso and colleagues (2008), formation of the LMC and PGC were found to be dependent on the expression of *FoxP1*. Elimination of *FoxP1* in mice resulted in the loss of the PGC and LMC, resulting in a more primitively structured spinal cord with a more homogeneous MN population throughout its length (Dasen et al., 2008). *FoxP1*'s effect on the generation of these columns appears to be expression-level-dependent, where a lower level of the protein promotes a PGC fate while the LMC is generated at higher levels of *FoxP1* (Dasen et al., 2008).

The loss of the LMC and PGC in *FoxP1* knockout mice is not because LMC and PGC progenitors are not generated, but rather due to a change in cell fate for these MNs as they differentiate (Rousso et al., 2008). Studies examining the axonal projections of these transformed neurons showed that gross nerve branches were still present and the proper muscles were still innervated. It was noted, however, that the normal arborization within specific muscles was lost. In addition, while dorsal and ventral projecting MNs normally tend to be found in a medial to lateral position, respectively, back-fill labeling from limbs in *FoxP1* knockout mice showed this topography to be randomized (Dasen et al., 2008; Rousso et al., 2008). Further work has examined downstream effectors of *FoxP1*. One example, *Dab1*, appears to have a role in the migration of MN somata (Palmesino et al., 2010). Studies to identify other factors that control the expression of *FoxP1* are ongoing and new layers of regulatory complexity are emerging. For instance, a miRNA, *miR-9* appears to play an important regulatory role (Otaegi et al., 2011).

In the brachial and lumbar LMCs, *FoxP1* acts as a permissive factor to gate the expression of additional *Hox* genes that drive motor pool formation. The specific combinations of *Hox* genes are a result of the unique rostrocaudal expression patterns of each *Hox* gene

(Carpenter, 2002). However, these termination zones are not as well defined as those between *Hox9*, *Hox6*, and *Hox10* (Dasen and Jessell, 2009). One model states that LMC motor pool formation is due to the overlapping expression of more than one *Hox* gene within a MN. Because *Hox* genes can cross-repress and compete for dominance within each MN, a mosaic of MNs expressing distinct sets of transcription factors is produced. This model suggests that once a *Hox* expression profile has been established, similar neurons coalesce into a defined pool, with each pool dedicated to innervating a specific muscle (Dasen and Jessell, 2009; Dasen et al., 2005).

7.5 LIM/bHLH FACTORS AND THE COMBINATORIAL CODE

As mentioned earlier, several progenitor domains express unique sets of transcription factors in response to morphogen gradients. A 'map' that serves to catalog the various combinations of transcription factors expressed in each cell type is shown in Figure 7.6. Most of these transcription factors defining the progenitor domains are LIM homeodomain (LIM-HD) transcription factors, though some are basic helix-loop-helix (bHLH) proteins (Jessell, 2000; Shirasaki and Pfaff, 2002).

7.5.1 LIM Homeodomain Factors

LIM-HD proteins have two LIM domains, each composed of two zinc fingers at the N-terminal, allowing for protein-protein interactions responsible for modulating the function of transcription factors, while the homeodomain, located at the center of the amino acid sequence, specifies the DNA sequence motif to which it binds (Hunter and Rhodes, 2005). LIM-HD factors found within the spinal cord are classified as either Class I or Class II transcription factors depending on their response to Shh signaling (Briscoe and Novitsch, 2008; Jessell, 2000; Shirasaki and Pfaff, 2002). Class I transcription factors are repressed by Shh, while Class II transcription factors are induced by Shh (Figure 7.7). Additionally, the expression of the transcription factors within each class is dependent on differential sensitivity to Shh signaling (mediated by GLI), resulting in distinct dorsal and ventral boundaries for transcription factors within the same class. One example of this is the differential expression of two Class I transcription factors, *Pax6* and *Irx3*. *Irx3* is more sensitive to repression by Shh, and therefore has a more dorsal boundary than *Pax6*. At the same time, Class II, Shh-activated, transcription factors that are less sensitive to Shh are less likely to be activated in more dorsal areas of the cord.

7.5 LIM/bHLH FACTORS AND THE COMBINATORIAL CODE

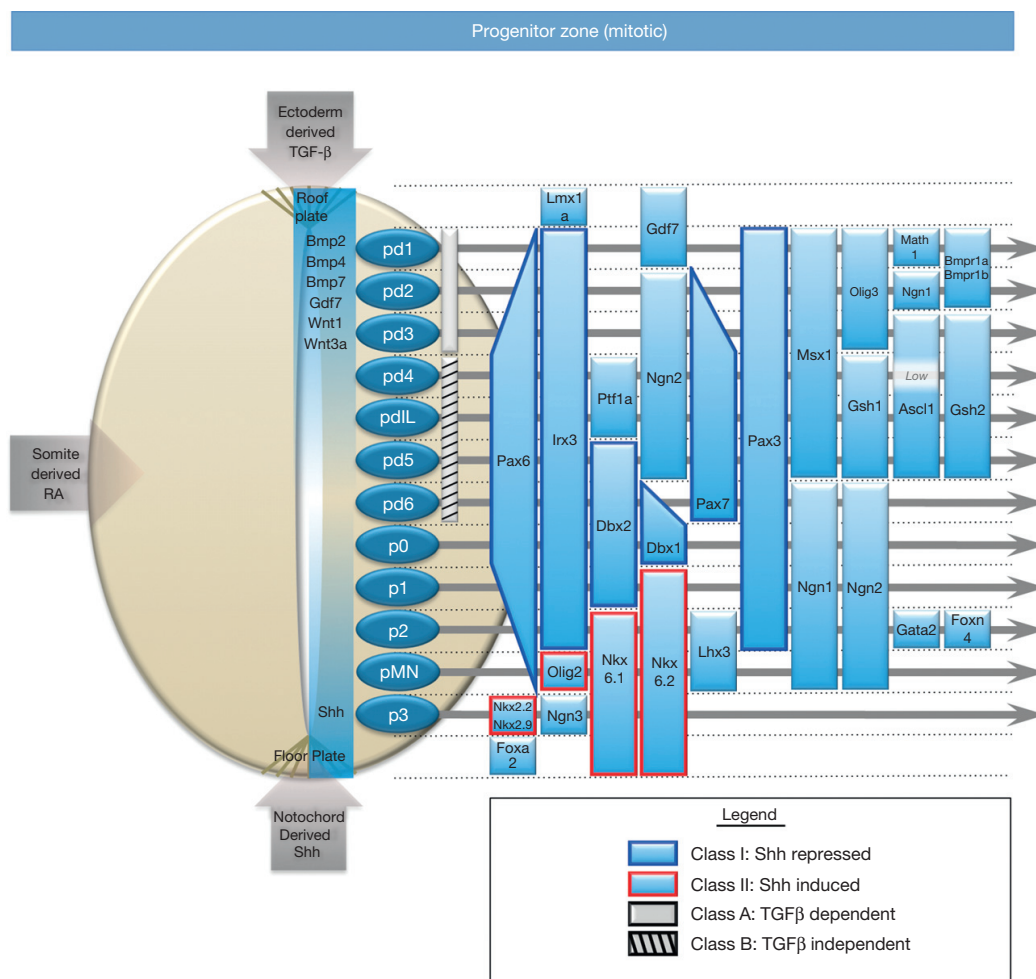


FIGURE 7.6 Generation of progenitor domains. At least 12 progenitor domains have been defined by their expression of unique combinations of transcription factors. This image depicts an idealized spinal cord section. As cells from these progenitor domains differentiate, they express additional, unique sets of postmitotic transcription factors, depicted in Figure 7.9. Adapted with permission of Elsevier from Alaynick WA, Jessell TM, and Pfaff S (2011) *SnapShot: Spinal cord development*. Cell 146: 178-178.e1.

For example, Nkx2.2 and Nkx6.1, both Class II transcription factors, differ in their dorsal termination point because Nkx2.2 is less sensitive to Shh, preventing it from extending as far dorsally as the more sensitive Nkx6.1 (Figure 7.7).

Furthermore, when the ventral limit of a Class I transcription factor shares the dorsal limit of a Class II transcription factor, such as the Class I Dbx2 and Class II Nkx6.1, the two transcription factors have often been found to display reciprocal inhibition, a concept known as cross-repression (Figure 7.7; Briscoe and Novitsch, 2008; Jessell, 2000; Lewis, 2006; Shirasaki and

Pfaff, 2002). This cross-repression results by the binding of a transcription factor to a regulatory element of its opposing factor. Such cross-repression, also seen with *Hox* genes discussed earlier, leads to sharp, delineated boundaries between expression zones. The direct silencing action of many of these transcription factors is accomplished by Engrailed homology-1 (eh1) domains, a conserved region of the Engrailed transcriptional repressor (Muhr et al., 2001). Transcription factors containing the eh1 domain recruit Groucho/TLE corepressors to suppress transcription. Disruption of Groucho/TLE function leads to the loss of the sharp

7. SPINAL CORD PATTERNING

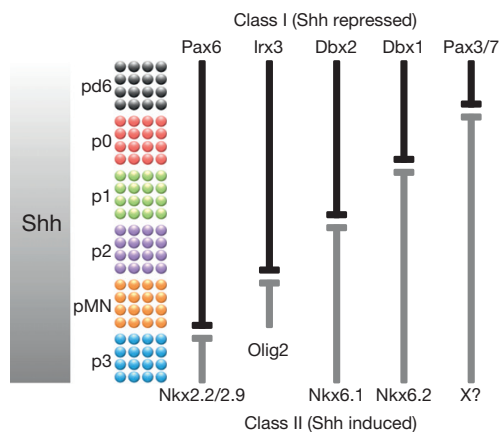


FIGURE 7.7 Transcriptional cross-repression sharpens boundaries between progenitor domains. Shh, found in a ventral to dorsal gradient, represses expression of Class I transcription factors and induces expression of Class II transcription factors. The Shh concentration needed to induce or repress each specific transcription factor defines their dorsal/ventral expression boundaries. Often the dorsal boundary of a Class II transcription factor is found at the ventral boundary of a Class I transcription factor. When this shared boundary is seen, these transcription factors typically inhibit each other's expression, which is termed cross-repression. Cross-repression ensures that only one of the competing factors is expressed in a particular cell, eliminating hybrid cell identities and sharpening the boundaries between the progenitor domains (pd6–p3). Adapted by permission of Macmillan Publishers Ltd from Lee SK and Pfaff SL (2001) *Transcriptional networks regulating neuronal identity in the developing spinal cord*. *Nature Neuroscience* 4 (supplement): 1183–1191.

boundaries between progenitor domains of the spinal cord (Muhr et al., 2001).

7.5.2 bHLH Factors

In addition to LIM-HD transcription factors setting up distinct boundaries through cross-repression, bHLH factors can occasionally repress LIM-HD factors. For example, the bHLH factor *Olig2*, which is expressed by the pMN domain, has been found to repress the LIM-HD factor *Irx3* (Mizuguchi et al., 2001; Novitch et al., 2001; Zhou and Anderson, 2002). Furthermore, while LIM-HD proteins are thought to specify neuronal subtypes, bHLH proteins typically regulate generic neuronal traits such as promoting axon and dendrite outgrowth, but bHLH factors can also specify cell fate (Bertrand et al., 2002; Lewis, 2006). The dual role of bHLH factors is exemplified by *Olig2*, which is important during neurogenesis, as well for the specification of MNs and oligodendrocytes derived from the pMN domain (Mizuguchi et al., 2001; Novitch et al., 2001; Pfaff et al., 1985; Zhou and Anderson, 2002).

Other bHLH factors can play dual roles as well. For example, when *Ngn2* is replaced by *Mash1* (*Ascl1*) by gene targeting, neuronal differentiation occurs normally, but the MN domain (which normally expresses *Ngn2*) is disrupted by the ectopic expression of V2 interneurons (which normally express *Mash1*), leading to the conclusion that *Mash1* and *Ngn2* specify different neuronal populations while functioning similarly in neurogenesis (Parras et al., 2002). The ability of *Mash1* to have the dual functions of promoting neurogenesis and specifying neuronal subtype was later attributed to the different helices of the protein, where Helix 1 is responsible for neurogenesis while both Helices 1 and 2 are responsible for neuronal subtype specification (Nakada et al., 2004). *Ngn2* has been found to function in neuronal specification through a different mechanism: phosphorylation of serine residues. While this phosphorylation is not needed for the neurogenic properties of *Ngn2*, it is required to promote MN specificity (Ma et al., 2008). It should also be noted that bHLH and LIM-HD factors do not necessarily work independently of each other; in some cases, bHLH and LIM-HD factors form heteromers to regulate neurogenesis and subtype specification (Lee and Pfaff, 2003).

7.5.3 Establishing Neural Identities through a Combinatorial Code

The transcription factors expressed in the progenitor domains drive expression of additional postmitotic transcription factors that further specify neuronal identity (Figure 7.9). V0 interneurons from the p0 domain express *Evx1*, V1 interneurons derived from the p1 domain express *En1*, the p2 domain gives rise to V2a (*Chx10+*) and V2b (*Gata3+*), *Hb9* is expressed by MNs from the pMN domain, and finally V3 interneurons from the p3 domain express *Sim1* (Goulding, 2009; Lewis, 2006). Loss of *Evx1* results in V0 interneurons taking on some phenotypic and genotypic characteristics of V1 interneurons, independently of upstream progenitor domain transcription factors (Moran-Rivard et al., 2001). Similarly, loss of *En1*, which is not required for early V1 interneuron differentiation, leads to pathfinding and functional defects in these neurons (Saueressig et al., 1999). Some of these transcription factors are sufficient for postmitotic cell-type specification as well. For instance, overexpression of *Hb9* is sufficient to drive ectopic MN development in the dorsal spinal cord (Tanabe et al., 1998).

Some of these transcription factors work in combination to specify neuronal subtypes. The proteins Lhx3, Isl1, and the nuclear LIM domain interactor (NLI) have been shown to form higher-order complexes. In this model, NLI dimers in the p2 domain are flanked by

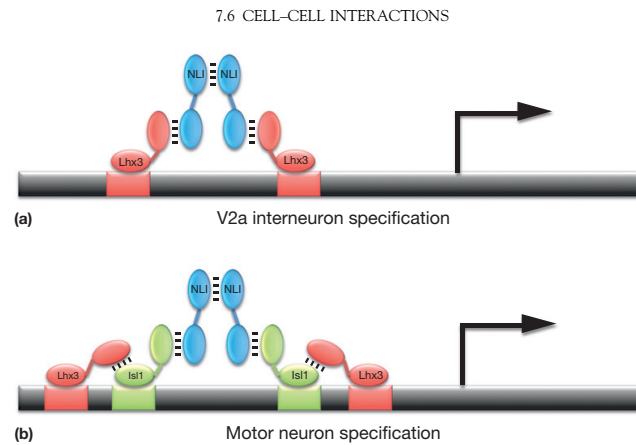


FIGURE 7.8 Example of a combinatorial transcription factor code. The expression of different combinations of transcription factors leads to specification of unique cell fates. In some cases, it has been shown that specific transcription factors physically interact to form higher-order transcriptional complexes that bind to novel regulatory sequences, which control distinct gene expression programs. (a) In the V2 progenitor domain, Lhx3 and NLI interact to form a tetramer that binds to specific DNA regulatory sequences, which results in specification of V2a interneuron identity. (b) In the pMN domain, Isl1 is coexpressed with Lhx3 and NLI. Isl1 prevents the formation of the V2a-specifying NLI–Lhx3 tetramer. Instead, an NLI–Isl1–Lhx3 hexamer forms. This new protein complex now binds to different DNA regulatory sequences, resulting in the expression of genes that specify motor neuron fate, instead of V2 interneurons. Adapted with permission from Elsevier from Thaler JP, Lee SK, Jurata LW, Gill GN, and Pfaff SL (2002) LIM factor Lhx3 contributes to the specification of motor neuron and interneuron identity through cell-type-specific protein–protein interactions. *Cell* 110: 237–249.

Lhx3 to form a tetramer that drives V2a identity (Figure 7.8). In the adjacent pMN domain, two Isl1 proteins bind to two NLI and two Lhx3 proteins to form a hexamer that drives MN identity (Lee et al., 2008; Thaler et al., 2002). In certain contexts, the LIM-HD factors Lhx3 and Isl1 require modulation by the bHLH factors Ngn2/NeuroM as well, illustrating how combinatorial expression patterns of transcription factors specify many different cell fates in the spinal cord (Lee and Pfaff, 2003).

7.6 CELL-CELL INTERACTIONS

While diffusible factors expressed within and outside the spinal cord play large roles in its organization, emerging studies are showing that cell–cell interactions within the cord also help determine its patterning and can give rise to a diverse population of neuronal subtypes.

7.6.1 Notch–Delta Signaling

The specification of V2a and V2b interneurons in the ventral spinal cord provides an example of cell-to-cell signaling. V2a neurons, which express the transcription factor *Chx10*, make up a population of glutamatergic interneurons, whereas V2b neurons, marked by *Gata3*, are composed of GABAergic interneurons. Two groups provided evidence for the involvement of the Notch–Delta signaling pathway in generating *Gata3*+ V2b neurons from p2 at the expense of *Chx10*+ V2a cells

(Del Barrio et al., 2007; Peng et al., 2007). In the canonical Notch–Delta pathway, Notch, a transmembrane receptor, binds the transmembrane ligand Delta/Jagged expressed by adjacent cells. Activated Notch is cleaved by the γ -secretase complex, and its intracellular domain (ICD) translocates into the nucleus. The ICD affects transcription of downstream genes in conjunction with CBF-1 and other proteins (Figure 7.4(c); Yoon and Gaiano, 2005). Studies performed primarily in *Drosophila* and *C. elegans* led to a model where lateral signaling mediated by the Notch–Delta interaction can generate cells with two distinct cell fates, despite coming from a population of progenitors with apparently equivalent cell fate (Greenwald and Rubin, 1992; Sprinzak et al., 2010).

In Presenilin (*PS1*) null embryos, where defective γ -secretase processing of Notch prevents ICD formation, *Chx10*+ cell numbers were increased while *Gata3* expression was lost. Similarly, ectopic expression of either *Delta4* or the ICD of *Notch* in chick spinal cords resulted in an increase of V2b neurons at the expense of V2a neurons, providing further evidence that Notch signaling promotes generation of V2b neurons from p2 (Del Barrio et al., 2007; Peng et al., 2007).

In the dorsal spinal cord, Notch signaling also plays a role in the choice between excitatory and inhibitory interneuron fate. The superficial dorsal horn includes glutamatergic excitatory dIL_B interneurons and GABAergic inhibitory dIL_A interneurons, both of which are derived from the dIL progenitor domain. Mizuguchi and colleagues showed that, in *Mash1* mutant mice, Delta1 expression and the Notch ICD are reduced, suggesting a

role for *Mash1* in regulating the Notch signaling pathway. In these mice, dIL_A neuron markers were downregulated while dIL_B neuron markers were upregulated. Consistently, overexpression of *Mash1* in chick spinal cord upregulated dIL_A genes and downregulated dIL_B markers. Interestingly, overexpression of *Delta1* resulted in upregulation of dIL_B genes, while dIL_A genes appeared unchanged. Similarly, in both *PS1* and *Delta1* mutants, although dIL_B gene expression was decreased, dIL_A gene expression was unchanged (Mizuguchi et al., 2006).

7.6.2 Retinoid Signaling

Another example of a cell–cell interaction that regulates spinal cord patterning is retinoid signaling in MN pools. In the brachial and lumbar levels of the spinal cord, LMC neurons innervate muscles in the limb. The LMC has ventral limb muscle-innervating medial LMC neurons (LMCm) and dorsal limb-innervating lateral LMC neurons (LMCl). During development, LMCm cells differentiate first and migrate out from the ventricular zone into the mantle zone. Subsequently, LMCl neurons are born and migrate out through the existing LMCm in an ‘inside-out’ manner. Studies by Sockanathan and colleagues showed that retinaldehyde dehydrogenase 2 (*Raldh2*), an enzyme responsible for RA synthesis, is expressed specifically in LMCm MNs and subsequently acts on differentiating LMCl MNs. In these experiments, brachial and thoracic spinal cord explants were cultured with retinol, the RA precursor. This resulted in increased numbers of ventral progenitor cells and MNs in brachial explants, but was not observed in thoracic explants, which suggests that expression of *Raldh2* in the MN pool at the brachial level may account for generation of RA, subsequently resulting in an increase in MN numbers. Using LMCl marker genes, they further showed that the expansion in the MN pool was due to an increase in LMCl neurons. Furthermore, overexpression of *Raldh2* caused the ectopic expression of LMCl markers in surrounding neurons, suggesting that diffusible RA has a non-cell-autonomous role in motor column specification (Sockanathan and Jessell, 1998).

In addition to being expressed in LMC, *Raldh2* is also expressed in the paraxial mesoderm. Using a Cre-lox system in mice to reduce the levels of *Raldh2* in a tissue-specific manner, the functions of *Raldh2* in the paraxial mesoderm and LMC were studied independently. In a mouse line with paraxial mesoderm-specific loss of *Raldh2*, the population of LMCl was reduced, while the LMCm population remained unchanged. However, when *Raldh2* expression was reduced specifically in the LMC, both LMCm and LMCl populations became smaller, and the timing of this was later than that of *Raldh2* reduction in the paraxial mesoderm. These results imply that tissue-specific *Raldh2* may function in the specification of LMCl via paracrine

RA signaling from the paraxial mesoderm as well as in the subsequent maintenance of both LMCm and LMCl populations through autocrine RA signaling from LMC MNs themselves (Ji et al., 2006).

7.7 GLIA IN THE SPINAL CORD

In addition to the different classes of neurons present in the spinal cord, there are two major types of glia: astrocytes and oligodendrocytes. Both cell types are found throughout the spinal cord. Historically, astrocytes have been thought of as cells which provide structural and metabolic support to their neuron neighbors, but additional astrocyte functions are continually being discovered. Oligodendrocytes are responsible for facilitating action potential conductance by myelinating axons.

7.7.1 Astrocytes

Traditionally, little effort has been put into the study of astrocyte diversity and any corresponding functional differences that arise from astrocytes derived from discrete progenitor domains. Recent work, however, has started to reveal that astrocyte diversity is much more extensive than previously appreciated (Hewett, 2009; Richardson et al., 2006). Astrocytes are generated in most of the spinal cord progenitor domains, with a notable exception of the pMN domain, which generates oligodendrocytes (Rowitch, 2004).

Generally, there is a difference between the fibrous white matter astrocytes that express high levels of glial fibrillary acidic protein (GFAP) and the protoplasmic astrocytes found in the gray matter that express low levels of GFAP (Hewett, 2009). The cause of this differential GFAP expression, and other molecular differences between the two subclasses, has yet to be determined. Additional work has shown that p1, p2, and p3 domains give rise to VA1, VA2, and VA3 fibrous astrocytes, respectively (Hochstim et al., 2008). These astrocytes occupy discrete, adjacent domains corresponding to the dorsoventral positioning of their respective progenitor domains and express unique combinations of Slit and Reelin. Thus, it appears at these early stages of research that there are parallels between neural and astrocyte patterning in the spinal cord.

It is interesting to note that there is evidence for functional coupling of astrocytes in discrete neural networks. For example, neurons within the rat somatosensory cortex form discrete network units called barrels (Hewett, 2009). Excitatory neurons within these barrels are highly connected with one another, and the astrocytes within each barrel are much more frequently connected via gap junctions to each other than to astrocytes in adjacent barrels (Houades et al., 2008). It will be interesting to see if astrocytes in individual motor pools display a similar functional

organization and whether there is, at its root, a developmental patterning mechanism that explains this organization.

7.7.2 Oligodendrocytes

Oligodendrocytes are found throughout the CNS. *In vivo* studies in spinal cord have identified at least two distinct progenitor domains that generate oligodendrocyte precursors (OLPs), including the pMN domain and at least one *Dbx+* domain (Fogarty et al., 2005; Richardson et al., 2006; Rowitch, 2004). The pMN domain expresses *Nkx6.1* and *Nkx6.2*, which are necessary for the expression of *Olig2*, a bHLH transcription factor required for OLP and MN generation (Lu et al., 2000; Novitsch et al., 2001; Rowitch, 2004).

Though oligodendrocytes and MNs share the same progenitor domain in the ventral spinal cord, they are generated at different time points, with neurogenesis preceding gliogenesis (Guillemot, 2007). Transcription factors play a role in this temporal switch. Studies by Zhou and colleagues showed that transient *Ngn1* and *Ngn2* expression in the pMN domain promotes neurogenesis, but when downregulated, gliogenesis is initiated (Zhou and Anderson, 2002). However, results from experiments performed by Sugimori and colleagues suggest a more complex mechanism involving combinatorial expression of transcription factors. In their model, coexpression of *Olig2* and *Ngn2* promotes the generation of MNs, while coexpression of *Mash1* and *Olig2* promotes the generation of oligodendrocytes, and the downregulation of *Ngn2* is only coincidental (Sugimori et al., 2007).

As mentioned earlier, while many of the OLPs generated in the spinal cord are from the pMN domain, there is at least one additional progenitor pool in the spinal cord. The idea that a separate, non-pMN-origin domain for OLPs existed was initially supported by the finding that OLPs could be generated *in vitro* from any dissected area of the spinal cord, though it was uncertain as to whether this was a phenomenon unique to *in vitro* conditions (Richardson et al., 2006). Another study then used a double knockout of *Nkx6.1* and *Nkx6.2* or separately a knockout of *Smo*, the mediator of Shh signaling. Either of these manipulations is sufficient to prevent MN and oligodendrocyte formation from the pMN domain; however, oligodendrocytes were still generated in the spinal cords of both of these mutants, indicating the presence of other OLP domains within the spinal cord (Cai et al., 2005). In a different series of experiments, mice expressing Cre recombinase under the control of *Dbx1*, a transcription factor expressed in the p0 and pd6 progenitor domains, were crossed to a Cre-dependent GFP reporter line. Cells expressing both GFP and *Olig2* were observed, indicating that a *Dbx+* progenitor domain for *Olig2*-expressing cells was present (Fogarty et al., 2005).

Interestingly, oligodendrocytes from the dorsal and ventral domains are thought to compete for survival (Richardson et al., 2006). Because ventral oligodendrocytes form and migrate to their final destination first, it is possible that they outcompete the dorsally generated oligodendrocytes for trophic factors in the environment. It is also possible that the ventral OLPs actively repress the dorsally derived OLPs as they migrate throughout the spinal cord. This competition hypothesis is supported by the fact that more oligodendrocytes are generated from dorsal progenitor regions when ventral OLPs are eliminated in the double knockout of *Nkx6.1* and *Nkx6.2* (Cai et al., 2005).

Despite the existence of distinct progenitor domains and molecular pathways regulating the formation of astrocytes and oligodendrocytes, there appear to be some similarities that are common to both types of glia. For example, the transcription factors *Sox9* and *NFIA* are necessary for both oligodendrocyte and astrocyte precursor generation (Stolt et al., 2003). These common transcription factors suggest there are parallels in the differentiation pathways of these two cell types. Of additional interest, a recent paper by Rompani and colleagues has provided evidence of a common progenitor for oligodendrocytes and astrocytes in the chick retina (Rompani and Cepko, 2010). While such a common progenitor has not yet been found in the spinal cord, its existence cannot be ruled out at this time.

7.8 HUMAN DISEASES OF SPINAL CORD PATTERNING

The number of genes and developmental processes that cumulatively serve to pattern the spinal cord is extensive and this number continues to grow. This begs the question: are there human developmental or genetic diseases that are associated with dysfunctional spinal cord patterning? Surprisingly, there is not a definitive answer to this question, but future research will almost certainly serve to better define diseases and syndromes with specific spinal cord patterning defects.

The lack of clarity on this issue can be explained by several factors. First, studies focused on cell-type identification in human spinal cords are rare, especially during embryonic stages when the transcription factors used to define cell types in mouse molecular genetic studies are expressed. The cell types and their unique sets of transcription factors shown in Figures 7.6, 7.7, and 7.9 can now be used to guide scientists studying human spinal cords in both health and disease. Second, every gene known to be important for spinal cord patterning is also expressed in non-spinal cord tissues. This accounts for the pleiotropic effects and/or embryonic lethality of mutations in these genes. Thus, many candidate diseases of spinal cord patterning may go unnoticed because dysfunctional gene products may result in spontaneous abortion or are

7. SPINAL CORD PATTERNING

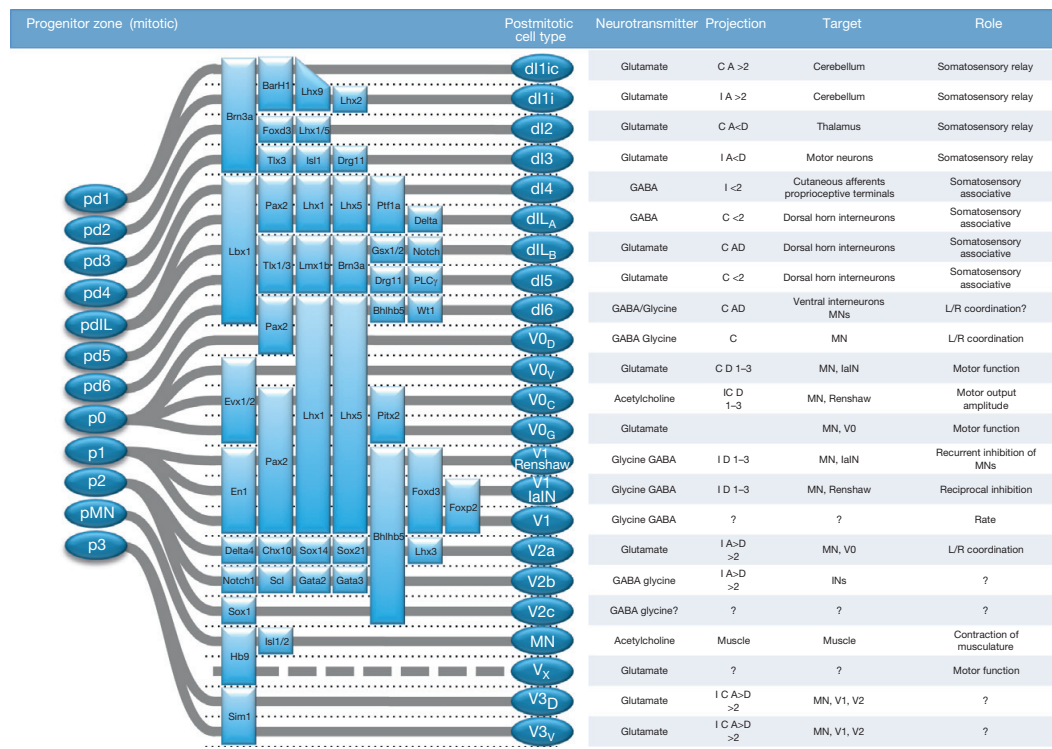


FIGURE 7.9 Diverse neuronal identities are specified by combinatorial transcription factor codes. Cells from the 12 spinal progenitor domains differentiate and migrate to their mature spinal positions. This process involves the expression of additional transcription factors as these cells become postmitotic. This figure depicts the combination of transcription factors that mark these cell types in an idealized spinal cord section. Projection code: I, ipsilateral; C, contralateral; A, ascending; D, descending; #, number of segments; V1-R, V1 Renshaw. Adapted with permission from Elsevier from Alaynick WA, Jessell TM, and Pfaff S (2011) *SnapShot: Spinal cord development*. Cell 146: 178-178.e1.

masked by greater defects in other tissues. For example, *Isl1* knockout mice exhibit a striking defect in MN generation, arrest in development at E9.5, and die by E11.5, but the latter two phenotypes are better explained by a dorsal aorta defect than a lack of MNs because *choline acetyltransferase* knockout mice, which lack MN activity, survive until birth (Pfaff et al., 1996). Hence, an opportunity to study the spinal cord patterning phenotype in the absence of other defects is limited. As a second example, mice and humans homozygous for mutations in *Chx10/Vsx2* (*Chx10*) share ocular developmental abnormalities typified by small eyes, retinal neuron differentiation defects, and congenital blindness. *Chx10* is expressed in multiple cell types in the developing eye, in addition to V2a interneurons in the ventral spinal cord (Burmeister et al., 1996; Ferda Percin et al., 2000). No obvious spinal cord phenotype, however, has been noted in either mice or humans. This may reflect any of several possibilities: (1) *Chx10* may be functionally redundant with another gene in the spinal cord and not in the eye; (2) the clinical issues related to blindness subvert the attention of both affected patients

and clinicians away from subtler locomotor defects; or (3) there is sufficient plasticity or compensation in the locomotor circuitry to mask a potential spinal cord patterning phenotype. Neural plasticity is another major issue that may have hindered identification of spinal cord patterning defects, in general.

The best example of a human disease that very likely harbors a spinal cord patterning defect, at least in some patients, is holoprosencephaly (HPE). HPE is characterized by abnormal formation and segmentation of midline structures in the CNS (Ming and Muenke, 1998). In the most extreme 'alobar' cases, no separation of the hemispheres and ventricles is seen. Surprisingly, 20% of these infants survive over 12 months. One in 250 conceptions and 1 in 8000 live births are affected, making it an extremely common CNS disorder, but the etiology is highly heterogeneous (Raam et al., 2011). About half of all HPE cases are associated with either a monogenic syndrome or chromosomal defect while 10% are caused by a mutation in one of four genes: *SHH*, *ZIC2*, *SIX3*, or *TGIF*. Specific causes of the remaining 40% of cases, apart

from risk factors, have not been defined. Autosomal-recessive, autosomal-dominant, and X-linked-recessive pedigrees have all been identified.

The simplest model of HPE is illustrated by mutations in *Shh*. In *Shh* knockout mice the dorsal spinal cord pattern is largely maintained but expanded at the expense of the most ventral cell types. Specifically, Isl1+ MNs are absent at all spinal cord levels and there is no morphologically distinct floor plate. V3 interneurons were not studied, but it is assumed that they were also absent. Furthermore, the optic vesicles are fused at the midline, modeling human HPE. A human–mouse difference, however, lies in the fact that the *Shh* heterozygous mutant mice have no phenotype (Chiang et al., 1996), while, as mentioned earlier, certain human pedigrees do show dominant inheritance of HPE (with variable penetrance and expressivity). Thus, ventral spinal cord defects are expected in severe postnatal cases of HPE.

Other diseases with a potential for concomitant but, as yet, undefined spinal patterning defects would include Currarino syndrome (caused by mutations in *Mnx1/Hlxb9*); Greig cephalopolysyndactyly syndrome and Pallister–Hall syndrome (*Gli3*); lambdoid synostosis, aniridia with or without cerebellar ataxia and mental retardation (*Pax6*); Wilms' tumor (*Wt1*); basal cell nevus syndrome (*Ptch1*); and medulloblastoma (*Ptch2*), because each of these genes have known roles in spinal cord patterning. Despite the challenges to clearly identifying patterning defects in humans, a number of other poorly defined congenital and developmental disorders associated with motor or sensory–motor processing defects may be associated with spinal cord patterning defects. These could, speculatively, include monogenic syndromes, chromosomal defects, autism spectrum disorders, and 'cerebral' palsies. Particular attention to polymorphisms in both coding and noncoding regulatory regions of the genome, gene dosage, and epigenetic alterations are warranted as part of future research efforts.

7.9 LESSONS FROM SPINAL CORD PATTERNING FOR DISEASE MODELING AND REGENERATIVE MEDICINE

While the role that spinal cord patterning defects play in human disease is incompletely defined at present, our understanding of the inductive signals that regulate cell fate within the spinal cord is actively being applied to the study of human disease through the directed differentiation of ESCs. ESCs represent the *in vitro* counterpart of the inner cell mass or primitive epiblast of the preimplantation blastocyst. These cells were first isolated from mouse embryos in 1981 and are regularly used in gene targeting studies to generate both knock-in and knock-out animals by placing genetically altered ESCs in

wild-type host blastocysts and then deriving engineered mouse lines from the modified ESCs. In fact, this mouse genetic technology has been instrumental in uncovering many of the mechanisms by which the spinal cord is patterned as discussed in this chapter. The property of ESCs that is important for the present discussion is that they are pluripotent, possessing the ability to differentiate into tissues from each of the three germ layers of the embryo, including ectoderm and its derivative neural tissues.

In 2002, Wichterle and colleagues first reported that mouse ESCs can be efficiently differentiated into spinal MNs (Wichterle et al., 2002). The method is to first direct ESCs toward neural progenitors by removing the signals that maintain ESCs in the pluripotent state, for example, leukemia inhibitor factor. These neural progenitors, without any further exogenous signals, differentiate into a variety of neural cell types that correspond to cells from a range of neuroanatomic locations. By recapitulating the inductive signals present *in vivo*, the neural progenitors can be directed to a number of fates *in vitro*. To generate MNs, RA is supplied to specify rostral spinal cord or hindbrain fate at the expense of more rostral brain tissue, and Shh is added to bias the progenitors to more ventralized lineages, including MNs. MNs generated using this method coexpress the MN markers *Hb9* and *Isl1*, the MMC marker *Lhx3*, and the cervical spinal markers *Hoxc5* and *Hoxc6*, but generally lack expression of the LMC marker *Lhx1* and the thoracic spinal cord marker *Hoxc8*. This combination of marker expression indicates that the majority of the ESC-derived motor neurons (ESC-MNs) generated by the Wichterle protocol are of a rostral cervical, MMC-like identity. These ESC-MNs were shown to be capable of engrafting into the spinal cord and growing axons with appropriate projection patterns and target innervation given their MMC-like identity. This work was later extended to human ESCs (Li et al., 2005), which are now regularly generated by many labs.

More recently, two groups developed protocols to generate additional subtypes of mouse and human ESC-MNs in RA-free conditions (Patani et al., 2011; Peljto and Wichterle, 2011). The rationale for eliminating RA from the differentiation protocol was yet again taken from lessons learned from the basic neurobiology of spinal cord patterning, which was that RA promotes a rostral spinal cord identity and precludes the generation of more caudal MN subtypes that are specified by members of the FGF family and Gdf11 discussed earlier (Dasen and Jessell, 2009; Figure 7.5). While these are still early days for *in vitro* MN subtype specification, one can now envision generating specific MN subpopulations to address particular experimental questions, such as differing susceptibility of MMC and LMC MNs to death in spinal muscular atrophy (SMA).

In this section, the generation of ESC-MNs is highlighted because these particular cells have been a major focus of research in the stem cell and spinal cord research communities. The choice of generating ESC-MNs, in particular, comes from the fact that they are essential for movement and survival and are selectively vulnerable in at least two devastating neurologic diseases, amyotrophic lateral sclerosis (ALS) and SMA. It should be noted that these differentiation protocols can be adapted to generate other spinal neuron classes. For instance, ventral interneuron classes such as Chx10+V2a interneurons are generated as ‘contaminant’ cells while following the ESC-MN differentiation protocol (Wichterle et al., 2002). In theory, the investigator can titrate Shh to enrich the culture for the desired class of neuron, or even eliminate the use of Shh entirely to selectively differentiate dorsal spinal cord interneuron classes. The addition of other morphogens at specific concentrations could also be useful. The current lack of focus on ESC-derived spinal cord cell types apart from ESC-MNs is that their functions are largely undefined in the context of both locomotor circuitry and human disease, but recent work has started to uncover important functions for several of these cell types (Alaynick et al., 2011; Goulding, 2009).

There are three reasons for pursuing this research. First, certain assays require large quantities of cells. In a 1-week differentiation, mouse ESCs can routinely generate tens of millions of purified MNs following fluorescent activated cell sorting. In contrast, a mouse spinal cord contains <50,000 MNs. Thus, ESC-derived cell types can be used in experiments that require large quantities of cells, including chromatin immunoprecipitation followed by massively parallel sequencing (ChIP-Seq) for the study of histone modifications or DNA:protein interactions, and cross-linking immunoprecipitation followed by massively parallel sequencing (CLIP-Seq) for the study of RNA:protein interactions. These facilitate the genome-wide interrogation of both pre- and posttranscriptional gene regulation, respectively. Second, a long-term goal is to develop cellular therapies in the setting of spinal cord disease, which may be treated by allogeneic stem cell transplants – a possibility which many scientific teams are now exploring. A final common motivation for using ESC-derived cell types is to model diseases by deriving ‘designer’ ESC lines harboring disease-associated alleles followed by their directed differentiation into the cell type of interest. In the event that these cells show a phenotype, this ‘disease in a dish’ can be probed for the root cause of disease or used to screen libraries for drugs that attenuate the phenotype. The field has been helped by the recent advent of induced pluripotent stem cells (iPS cells) (Takahashi and Yamanaka, 2006; Takahashi et al., 2007; Yu et al., 2007). These are generated when somatic cells

are reprogrammed to pluripotency by one of several methods, most commonly lentiviral transduction of fibroblasts with a panel of transcription factors known to regulate the pluripotent state, namely *Pou5f1*, *Sox2*, *Klf4*, and *c-Myc*. This strategy circumvents two difficulties when trying to model disease *in vitro* using hESCs. First, hESC genomes are difficult to manipulate and iPS cells already contain the relevant mutation without the need for gene targeting. Second, if iPS cells are derived from patients where a genetic etiology is not yet defined, as in the majority of cases of sporadic ALS, for example, the iPS cells will still contain the genetic makeup associated with that patient’s disease and may still therefore yield a valuable model. Notably, human iPS-derived MNs have now been derived from fibroblasts of both SMA (Ebert et al., 2009) and ALS patients (Dimos et al., 2008).

As further progress is made in understanding how individual cell types participate in locomotor circuitry and succumb to disease-related death, the stem cell and regenerative medicine communities will continue to draw on the principles in spinal cord patterning laid out in this chapter for insight into which cell types to generate and how to accomplish the task.

7.10 SUMMARY AND UNANSWERED QUESTIONS

The embryonic spinal cord forms a cylindrical structure that is exposed to an array of signals that specify the cell fate of uncommitted precursors. Many of the major signals are secreted factors that can be found in spatial gradients along the dorsoventral, rostrocaudal, and mediolateral axes. Together, these signals form a coarse three-dimensional grid, such that cells in the midst of this field will each be exposed to a unique combination of signals that direct cell fate. A mechanism of transcriptional cross-repression serves to sharpen the boundaries between each grid space and minimize hybrid cell identities, ultimately resulting in numerous neuronal subtypes, of which a large number have already been defined based on the unique combination of marker genes they express and their cell body position, morphology, pattern of connectivity, electrophysiological properties, and function. The outcome of this process is reflected in an elegant pattern of cell specification that underlies spinal circuit formation.

The amount of progress made in uncovering the basic biology behind spinal cord patterning is remarkable, but a great number of important questions remain. We leave the interested reader with this short list of some major questions and look forward to the answers in the future: (1) Beyond the dorsoventral patterning of the progenitor domains, is there further specification of postmitotic cells along this axis? (2) How does the spinal circuitry

change along the rostrocaudal axis? (3) What is the function of each neuronal subtype? (4) How is each subtype of cell interconnected with other subtypes? (5) Where are the DNA-binding sites and what genetic targets for the transcription factors are important for specifying cell identity? (6) How does the overexpression or deletion of a single transcription factor cascade into an entire fate change? (7) Is every cell within a particular neuronal subtype unique, or is there some cellular redundancy? (8) What really defines a neuronal subtype? (9) What is the extent of glial subtypes? Are they patterned in the same way that neurons are patterned? (10) How does time alter patterning and how is the precise temporal transition from neurogenesis to gliogenesis achieved? (11) Does the process of patterning a particular subtype make it prone to certain disease?

Glossary

Basic helix-loop-helix (bHLH) transcription factors Family of DNA-binding proteins that are characterized by a structural motif containing two alpha helices, one of which contains basic amino acids that facilitates DNA binding.

Combinatorial code A pervasive biological strategy for generating molecular complexity with a limited repertoire of factors. For example, many transcription factors operate as members of combinatorial codes that function coordinately to establish unique cellular identities.

Homeodomain A protein domain of approximately sixty amino acids that confers the ability to bind to specific DNA sequences; found in homeodomain transcription factors.

Interneuron Generic term for numerous classes of neurons whose cellular processes reside entirely within the central nervous system, unlike motor neurons.

LIM domain A protein domain important for mediating interactions with other LIM domain-containing proteins.

Motor column A collection of motor neurons found in roughly cylindrical structures that span many spinal segments and which innervate a group of muscles defined anatomically (e.g., the lateral motor column innervates limb muscles).

Motor neuron Special class of neuron that is defined by the presence of the cell soma within the central nervous system (brain or spinal cord) and an axon that targets muscle, gland, or postganglionic nervous tissue.

Motor neuron pool A cluster of motor neurons that collectively innervate a single muscle.

Patterning The process by which extrinsic and intrinsic signals regulate the development of unspecified precursor cells into an organized, functional structure replete with a myriad of diverse cell types.

References

Alaynick, W.A., Jessell, T.M., Pfaff, S.L., 2011. SnapShot: Spinal cord development. *Cell* 146 (1), 178–178.e1.

Alvarez-Medina, R., Cayuso, J., Okubo, T., Takada, S., Marti, E., 2008. Wnt canonical pathway restricts graded Shh/Gli patterning activity through the regulation of Gli3 expression. *Development* 135, 237–247.

Balaskas, N., Ribeiro, A., Panovska, J., et al., 2012. Gene regulatory logic for reading the Sonic Hedgehog signaling gradient in the vertebrate neural tube. *Cell* 148, 273–284.

Bel-Vialar, S., Itasaki, N., Krumlauf, R., 2002. Initiating Hox gene expression: In the early chick neural tube differential sensitivity to FGF and RA signaling subdivides the HoxB genes in two distinct groups. *Development* 129, 5103–5115.

Bertrand, N., Castro, D.S., Guillemot, F., 2002. Proneural genes and the specification of neural cell types. *Nature Reviews Neuroscience* 3, 517–530.

Briscoe, J., Novitsch, B.G., 2008. Regulatory pathways linking progenitor patterning, cell fates and neurogenesis in the ventral neural tube. *Philosophical Transactions of the Royal Society of London. Series B, Biological Sciences* 363, 57–70.

Brown, T.G., 1911. The intrinsic factors in the act of progression in of the mammal. *Proceedings of the Royal Society of London* 84, 308–309.

Burmeister, M., Novak, J., Liang, M.Y., et al., 1996. Ocular retardation mouse caused by Chx10 homeobox null allele: Impaired retinal progenitor proliferation and bipolar cell differentiation. *Nature Genetics* 12, 376–384.

Cai, J., Qi, Y., Hu, X., et al., 2005. Generation of oligodendrocyte precursor cells from mouse dorsal spinal cord independent of Nkx6 regulation and Shh signaling. *Neuron* 45, 41–53.

Carpenter, E.M., 2002. Hox genes and spinal cord development. *Developmental Neuroscience* 24, 24–34.

Chiang, C., Litingtung, Y., Lee, E., et al., 1996. Cyclopia and defective axial patterning in mice lacking sonic hedgehog gene function. *Nature* 383, 407–413.

Choe, A., Phun, H.Q., Tieu, D.D., Hu, Y.H., Carpenter, E.M., 2006. Expression patterns of Hox10 paralogous genes during lumbar spinal cord development. *Gene Expression Patterns* 6, 730–737.

Corcoran, R.B., Scott, M.P., 2006. Oxysterols stimulate Sonic hedgehog signal transduction and proliferation of medulloblastoma cells. *Proceedings of the National Academy of Sciences of the United States of America* 103, 8408–8413.

Dasen, J.S., de Camilli, A., Wang, B., Tucker, P.W., Jessell, T.M., 2008. Hox repertoires for motor neuron diversity and connectivity gated by a single accessory factor, FoxP1. *Cell* 134, 304–316.

Dasen, J.S., Jessell, T.M., 2009. Hox networks and the origins of motor neuron diversity. *Current Topics in Developmental Biology* 88, 169–200.

Dasen, J.S., Liu, J.P., Jessell, T.M., 2003. Motor neuron columnar fate imposed by sequential phases of Hox-c activity. *Nature* 425, 926–933.

Dasen, J.S., Tice, B.C., Brenner-Morton, S., Jessell, T.M., 2005. A Hox regulatory network establishes motor neuron pool identity and target-muscle connectivity. *Cell* 123, 477–491.

del Barrio, M.G., Taveira-Marques, R., Muroyama, Y., et al., 2007. A regulatory network involving Foxn4, Mash1 and delta-like 4/Notch1 generates V2a and V2b spinal interneurons from a common progenitor pool. *Development* 134, 3427–3436.

Dessaud, E., Yang, L.L., Hill, K., et al., 2007. Interpretation of the sonic hedgehog morphogen gradient by a temporal adaptation mechanism. *Nature* 450, 717–720.

Dimos, J.T., Rodolfa, K.T., et al., 2008. Induced pluripotent stem cells generated from patients with ALS can be differentiated into motor neurons. *Science* 321, 1218–1221.

Dubrule, J., Pourquie, O., 2004. fgf8 mRNA decay establishes a gradient that couples axial elongation to patterning in the vertebrate embryo. *Nature* 427, 419–422.

Duester, G., 2008. Retinoic acid synthesis and signaling during early organogenesis. *Cell* 134, 921–931.

Ebert, A.D., Yu, J., et al., 2009. Induced pluripotent stem cells from a spinal muscular atrophy patient. *Nature* 457, 277–280.

Ericson, J., Briscoe, J., Rashbass, P., van Heyningen, V., Jessell, T.M., 1997a. Graded sonic hedgehog signaling and the specification of cell fate in the ventral neural tube. *Cold Spring Harbor Symposia on Quantitative Biology* 62, 451–466.

7. SPINAL CORD PATTERNING

- Ericson, J., Rashbass, P., Schedl, A., et al., 1997b. Pax6 controls progenitor cell identity and neuronal fate in response to graded Shh signaling. *Cell* 90, 169–180.
- Ferda Percin, E., Ploder, L.A., Yu, J.J., et al., 2000. Human microphthalmia associated with mutations in the retinal homeobox gene CHX10. *Nature Genetics* 25, 397–401.
- Fogarty, M., Richardson, W.D., Kessaris, N., 2005. A subset of oligodendrocytes generated from radial glia in the dorsal spinal cord. *Development* 132, 1951–1959.
- Fuccillo, M., Joyner, A.L., Fishell, G., 2006. Morphogen to mitogen: The multiple roles of hedgehog signalling in vertebrate neural development. *Nature Reviews Neuroscience* 7, 772–783.
- Goulding, M., 2009. Circuits controlling vertebrate locomotion: Moving in a new direction. *Nature Reviews Neuroscience* 10, 507–518.
- Greenwald, I., Rubin, G.M., 1992. Making a difference: The role of cell-cell interactions in establishing separate identities for equivalent cells. *Cell* 68, 271–281.
- Grillner, S., Jessell, T., 2009. Measured motion: Searching for simplicity in spinal locomotor networks. *Current Opinion in Neurobiology* 19, 572–586.
- Guillemot, F., 2007. Cell fate specification in the mammalian telencephalon. *Progress in Neurobiology* 83, 37–52.
- Hewett, J.A., 2009. Determinants of regional and local diversity within the astroglial lineage of the normal central nervous system. *Journal of Neurochemistry* 110, 1717–1736.
- Hochstim, C., Deneen, B., Lukaszewicz, A., Zhou, Q., Anderson, D.J., 2008. Identification of positionally distinct astrocyte subtypes whose identities are specified by a homeodomain code. *Cell* 133, 510–522.
- Houades, V., Koulakoff, A., Ezan, P., Seif, I., Giaume, C., 2008. Gap junction-mediated astrocytic networks in the mouse barrel cortex. *Journal of Neuroscience* 28, 5207–5217.
- Hunter, C.S., Rhodes, S.J., 2005. LIM-homeodomain genes in mammalian development and human disease. *Molecular Biology Reports* 32, 67–77.
- Jessell, T.M., 2000. Neuronal specification in the spinal cord: Inductive signals and transcriptional codes. *Nature Reviews Genetics* 1, 20–29.
- Ji, S.J., Zhuang, B., Falco, C., et al., 2006. Mesodermal and neuronal retinoids regulate the induction and maintenance of limb innervating spinal motor neurons. *Developmental Biology* 297, 249–261.
- Lance-Jones, C., Omelchenko, N., Bailis, A., Lynch, S., Sharma, K., 2001. Hoxd10 induction and regionalization in the developing lumbosacral spinal cord. *Development* 128, 2255–2268.
- Lee, S., Lee, B., Joshi, K., Pfaff, S.L., Lee, J.W., Lee, S.K., 2008. A regulatory network to segregate the identity of neuronal subtypes. *Developmental Cell* 14, 877–889.
- Lee, S.K., Pfaff, S.L., 2001. Transcriptional networks regulating neuronal identity in the developing spinal cord. *Nature Neuroscience* 4 (Suppl), 1183–1191.
- Lee, S.K., Pfaff, S.L., 2003. Synchronization of neurogenesis and motor neuron specification by direct coupling of bHLH and homeodomain transcription factors. *Neuron* 38, 731–745.
- Lemons, D., McGinnis, W., 2006. Genomic evolution of Hox gene clusters. *Science* 313, 1918–1922.
- Lewis, K.E., 2006. How do genes regulate simple behaviours? Understanding how different neurons in the vertebrate spinal cord are genetically specified. *Philosophical Transactions of the Royal Society of London. Series B, Biological Sciences* 361, 45–66.
- Li, X.J., Du, Z.W., Zarnowska, E.D., et al., 2005. Specification of motoneurons from human embryonic stem cells. *Nature Biotechnology* 23, 215–221.
- Liem Jr., K.F., Jessell, T.M., Briscoe, J., 2000. Regulation of the neural patterning activity of sonic hedgehog by secreted BMP inhibitors expressed by notochord and somites. *Development* 127, 4855–4866.
- Liem Jr., K.F., Tremml, G., Jessell, T.M., 1997. A role for the roof plate and its resident TGFbeta-related proteins in neuronal patterning in the dorsal spinal cord. *Cell* 91, 127–138.
- Liu, J.P., Laufer, E., Jessell, T.M., 2001. Assigning the positional identity of spinal motor neurons: Rostrocaudal patterning of Hox-c expression by FGFs, Gdf11, and retinoids. *Neuron* 32, 997–1012.
- Liu, A., Niswander, L.A., 2005. Bone morphogenetic protein signalling and vertebrate nervous system development. *Nature Reviews Neuroscience* 6, 945–954.
- Lu, Q.R., Yuk, D., Alberta, J.A., et al., 2000. Sonic hedgehog-regulated oligodendrocyte lineage genes encoding bHLH proteins in the mammalian central nervous system. *Neuron* 25, 317–329.
- Ma, Y.C., Song, M.R., Park, J.P., et al., 2008. Regulation of motor neuron specification by phosphorylation of neurogenin 2. *Neuron* 58, 65–77.
- Ming, J.E., Muenke, M., 1998. Holoprosencephaly: From Homer to Hedgehog. *Clinical Genetics* 53, 155–163.
- Mizuguchi, R., Kriks, S., Cordes, R., Gossler, A., Ma, Q., Goulding, M., 2006. Ascl1 and Gsh1/2 control inhibitory and excitatory cell fate in spinal sensory interneurons. *Nature Neuroscience* 9, 770–778.
- Mizuguchi, R., Sugimori, M., Takebayashi, H., et al., 2001. Combinatorial roles of olig2 and neurogenin2 in the coordinated induction of pan-neuronal and subtype-specific properties of motoneurons. *Neuron* 31, 757–771.
- Moran-Rivard, L., Kagawa, T., Saueressig, H., Gross, M.K., Burrill, J., Goulding, M., 2001. Evx1 is a postmitotic determinant of v0 interneuron identity in the spinal cord. *Neuron* 29, 385–399.
- Muhr, J., Andersson, E., Persson, M., Jessell, T.M., Ericson, J., 2001. Groucho-mediated transcriptional repression establishes progenitor cell pattern and neuronal fate in the ventral neural tube. *Cell* 104, 861–873.
- Muroyama, Y., Fujihara, M., Ikeya, M., Kondoh, H., Takada, S., 2002. Wnt signaling plays an essential role in neuronal specification of the dorsal spinal cord. *Genes and Development* 16, 548–553.
- Nakada, Y., Hunsaker, T.L., Henke, R.M., Johnson, J.E., 2004. Distinct domains within Mash1 and Math1 are required for function in neuronal differentiation versus neuronal cell-type specification. *Development* 131, 1319–1330.
- Novitsch, B.G., Chen, A.I., Jessell, T.M., 2001. Coordinate regulation of motor neuron subtype identity and pan-neuronal properties by the bHLH repressor Olig2. *Neuron* 31, 773–789.
- Otaegi, G., Pollock, A., Hong, J., Sun, T., 2011. MicroRNA miR-9 modifies motor neuron columns by a tuning regulation of FoxP1 levels in developing spinal cords. *Journal of Neuroscience* 31, 809–818.
- Palmesino, E., Rousso, D.L., Kao, T.J., et al., 2010. Foxp1 and Ihx1 coordinate motor neuron migration with axon trajectory choice by gating Reelin signalling. *PLoS Biology* 8, e1000446.
- Parr, B.A., Shea, M.J., Vassileva, G., McMahon, A.P., 1993. Mouse Wnt genes exhibit discrete domains of expression in the early embryonic CNS and limb buds. *Development* 119, 247–261.
- Parras, C.M., Schuurmans, C., Scardigli, R., Kim, J., Anderson, D.J., Guillemot, F., 2002. Divergent functions of the proneural genes Mash1 and Ngn2 in the specification of neuronal subtype identity. *Genes and Development* 16, 324–338.
- Patani, R., Hollins, A.J., Wishart, T.M., et al., 2011. Retinoid-independent motor neurogenesis from human embryonic stem cells reveals a medial columnar ground state. *Nature Communications* 2, 214.
- Peljo, M., Wichterle, H., 2011. Programming embryonic stem cells to neuronal subtypes. *Current Opinion in Neurobiology* 21, 43–51.
- Peng, C.Y., Yajima, H., Burns, C.E., et al., 2007. Notch and MAML signaling drives Scl-dependent interneuron diversity in the spinal cord. *Neuron* 53, 813–827.
- Pfaff, S.L., Mendelsohn, M., Stewart, C.L., Edlund, T., Jessell, T.M., 1996. Requirement for LIM homeobox gene Is11 in motor neuron generation reveals a motor neuron-dependent step in interneuron differentiation. *Cell* 84, 309–320.

7.10 SUMMARY AND UNANSWERED QUESTIONS

- Pfaff, S.L., Zhou, R.P., Young, J.C., Hayflick, J., Duesberg, P.H., 1985. Defining the borders of the chicken proto-fps gene, a precursor of Fujinami sarcoma virus. *Virology* 146, 307–314.
- Raam, M.S., Solomon, B.D., Muenke, M., 2011. Holoprosencephaly: A guide to diagnosis and clinical management. *Indian Pediatrics* 48, 457–466.
- Rahnama, F., Shimokawa, T., Lauth, M., et al., 26.
- Richardson, W.D., Kessaris, N., Pringle, N., 2006. Oligodendrocyte wars. *Nature Reviews Neuroscience* 7, 11–18.
- Rompani, S.B., Cepko, C.L., 2010. A common progenitor for retinal astrocytes and oligodendrocytes. *Journal of Neuroscience* 30, 4970–4980.
- Roussou, D.L., Gaber, Z.B., Wellik, D., Morrissey, E.E., Novitch, B.G., 2008. Coordinated actions of the forkhead protein Foxp1 and Hox proteins in the columnar organization of spinal motor neurons. *Neuron* 59, 226–240.
- Rowitch, D.H., 2004. Glial specification in the vertebrate neural tube. *Nature Reviews Neuroscience* 5, 409–419.
- Saueressig, H., Burrill, J., Goulding, M., 1999. Engrailed-1 and netrin-1 regulate axon pathfinding by association interneurons that project to motor neurons. *Development* 126, 4201–4212.
- Shirasaki, R., Pfaff, S.L., 2002. Transcriptional codes and the control of neuronal identity. *Annual Review of Neuroscience* 25, 251–281.
- Sockanathan, S., Jessell, T.M., 1998. Motor neuron-derived retinoid signaling specifies the subtype identity of spinal motor neurons. *Cell* 94, 503–514.
- Sprinzak, D., Lakhanpal, A., Lebon, L., et al., 2010. Cis-interactions between Notch and Delta generate mutually exclusive signalling states. *Nature* 465, 86–90.
- Stolt, C.C., Lommes, P., Sock, E., Chaboissier, M.C., Schedl, A., Wegner, M., 2003. The Sox9 transcription factor determines glial fate choice in the developing spinal cord. *Genes and Development* 17, 1677–1689.
- Sugimori, M., Nagao, M., Bertrand, N., Parras, C.M., Guillemot, F., Nakafuku, M., 2007. Combinatorial actions of patterning and HLH transcription factors in the spatiotemporal control of neurogenesis and gliogenesis in the developing spinal cord. *Development* 134, 1617–1629.
- Takahashi, K., Tanabe, K., Ohnuki, M., et al., 2007. Induction of pluripotent stem cells from adult human fibroblasts by defined factors. *Cell* 131, 861–872.
- Takahashi, K., Yamanaka, S., 2006. Induction of pluripotent stem cells from mouse embryonic and adult fibroblast cultures by defined factors. *Cell* 126, 663–676.
- Tanabe, Y., William, C., Jessell, T.M., 1998. Specification of motor neuron identity by the MNR2 homeodomain protein. *Cell* 95, 67–80.
- Thaler, J.P., Lee, S.K., Jurata, L.W., Gill, G.N., Pfaff, S.L., 2002. LIM factor Lhx3 contributes to the specification of motor neuron and interneuron identity through cell-type-specific protein–protein interactions. *Cell* 110, 237–249.
- Timmer, J.R., Wang, C., Niswander, L., 2002. BMP signaling patterns the dorsal and intermediate neural tube via regulation of homeobox and helix–loop–helix transcription factors. *Development* 129, 2459–2472.
- Wichterle, H., Lieberam, I., Porter, J.A., Jessell, T.M., 2002. Directed differentiation of embryonic stem cells into motor neurons. *Cell* 110, 385–397.
- Wine-Lee, L., Ahn, K.J., Richardson, R.D., Mishina, Y., Lyons, K.M., Crenshaw 3rd, E.B., 2004. Signaling through BMP type 1 receptors is required for development of interneuron cell types in the dorsal spinal cord. *Development* 131, 5393–5403.
- Yoon, K., Gaiano, N., 2005. Notch signaling in the mammalian central nervous system: Insights from mouse mutants. *Nature Neuroscience* 8, 709–715.
- Yu, J., Vodyanik, M.A., Smuga-Otto, K., et al., 2007. Induced pluripotent stem cell lines derived from human somatic cells. *Science* 318, 1917–1920.
- Zhou, Q., Anderson, D.J., 2002. The bHLH transcription factors OLIG2 and OLIG1 couple neuronal and glial subtype specification. *Cell* 109, 61–73.

Chapter 1, in full, is a reprint of the material as it appears in Gifford, W. D., Hayashi, M., Sternfeld, M., Tsai, J., Alaynick, W. A., & Pfaff, S. L. (2013). Chapter 7 - Spinal Cord Patterning. Patterning and Cell Type Specification in the Developing CNS and PNS: Comprehensive Developmental Neuroscience (Vol. 1). Academic Press. <http://doi.org/10.1016/B978-0-12-397265-1.00047-2>. The thesis author was the second author of this paper.

Chapter 2

Rostrocaudal diversification of spinal neurons confers segment-specific spinal network architectures

Introduction

The spinal cord represents the final stage of generating motor behaviors, where descending commands or sensory inputs must be transformed into behaviorally-relevant pattern of motor neuron activity. Networks along the rostrocaudal axis of the spinal cord regulate diverse motor behaviors such as respiration, forelimb, trunk, and hindlimb movements, mediated by stringent innervations of motor neurons to muscle fibers. However, how the network properties of the central nervous system enable these diverse motor outputs remains elusive.

In a simplistic view, one possible explanation for the emergence of diverse motor outputs can be found in descending inputs originating from multiple regions of supraspinal structures innervating the spinal cord. Microstimulation and anatomical studies of motor cortex have identified distinct modules with projections to particular segments of the spinal cord that are sufficient to elicit movements in specific parts of the body (Tennant et al. 2011; Ramanathan, et al. 2015; Jeffery and Fitzgerald, 1999). Furthermore, anatomical studies in the brainstem have uncovered nuclei with preferential connections to forelimb or hindlimb motor neurons, with dedicated motor deficit following ablation (Esposito et al. 2014). It is, therefore, feasible to postulate that ensembles of activity in supraspinal structures, with connections to specific spinal levels, result in unique recruitment patterns of existing canonical spinal circuit elements along the rostrocaudal axis, thereby generating discrete network activity patterns underlying diverse motor behaviors.

An alternative, and not mutually exclusive, possibility for the emergence of diverse motor outputs may reside within spinal cord circuits. A series of transplantation studies in chick embryos has shown that forelimb and hindlimb regions of the spinal cords can maintain their behavioral roles even in ectopic segmental locations (Narayanan and Hamburger. 1971). This suggests that intrinsic properties of spinal cord circuits can contribute to behavioral roles of their resident segments. Another example of spinal neurons regulating region-specific motor behaviors comes from recent studies that uncovered that cervical spinal neurons communicate with supraspinal structures and underlie specialized motor output such as forelimb reaching behavior (Alstermark and Ekerot. 2013; Azim, et al. 2014; Pivetta et al. 2014). Together, these reports support the hypothesis that spinal circuits possess distinct circuit compositions that reflect the behavioral role

of their resident segments. However, neural substrates underlying these different spinal circuits along the rostrocaudal axis are poorly understood.

Decades of studies have identified numerous classes of spinal interneurons along the dorsoventral axis based on specific expression of transcription factors (Jessell. 2000; Alaynick et al. 2011; Goulding. 2009). Interestingly, these molecularly-defined interneurons can be found across the entirety of the rostrocaudal axis (Francius, et al. 2013) against the functional diversity of the spinal cord along the rostrocaudal axis. In this study, to account for this apparent disparity, we hypothesized that spinal interneurons are diversified further after their initial cell fate specification and investigated diversification of spinal cord network function by focusing on a network component V2a interneurons. Defined by the expression of transcription factor *chx10/vsx2*, V2a INs are the major excitatory neural type in the ventral spinal cord. Diversity of V2a INs has been implicated from previous studies based on marker gene expressions (Crone et al. 2008; Dougherty et al. 2013; Francius et al. 2013), morphological differences, and intracellular properties (Menelaou et al. 2013; Dougherty et al. 2010; Zhong et al. 2010; Al-Mosawie et al. 2007). Furthermore, subsets of cervical V2a INs have been shown to regulate forelimb reaching behaviors (Azim, et al. 2014, Pivetta et al. 2014). While these studies establish diversity within the V2a population, a comprehensive framework that links molecular, anatomical, and functional diversity across the spinal cord segments has not been established.

In this study, we show a cardinal spinal neuron class V2a interneurons are diversified with regard to their anatomical and functional connectivity with corresponding molecular diversification across the spinal segments. Viral tracing and optogenetic activation of V2a interneurons reveal that V2a interneurons exhibit distinct anatomical and functional connectivity schemes in cervical versus lumbar segments. RNA-sequencing analysis between cervical and lumbar V2a interneurons identifies distinct genetic signatures segregating the two segmental levels and reveals molecular diversification of conventional V2a interneuron marker genes during embryonic development. Finally, we identify that this molecular diversification corresponds to brainstem projection status of V2a interneurons enriched in cervical segments of the spinal cord. Our findings collectively reveal that, during embryonic development, a molecularly-defined single spinal network component undergoes diversification to support distinct motor outputs of

different spinal cord segments.

Results

To identify possible diversification of spinal circuitry along the rostrocaudal axis that may underlie diverse motor behaviors, we explored the possibility that a molecularly-defined class of spinal interneurons, V2a interneurons, displays heterogeneity in their molecular identity, anatomical and functional connectivity in different spinal segments.

We first set out to investigate the anatomical and functional connectivity of V2a interneurons along the rostrocaudal axis of the spinal cord. Given the differences in the degree of dexterity and the repertoire of usages between forelimbs and hindlimbs, we focused on cervical and lumbar segments in our current study.

V2a interneurons provide glutamatergic inputs to the ventral spinal cord circuits in cervical and lumbar segments

The V2a INs are characterized by their evolutionarily-conserved ipsilateral-projection patterns and glutamatergic neurotransmitter identity. However, there has been no comprehensive characterization of this class of spinal neurons across different segments of the spinal cord. Therefore, in setting up our study, we first expanded previous understanding of V2a INs by investigating whether spinal circuits in cervical and lumbar segments are composed of different composition of V2a interneurons.

To accomplish this, we indelibly labeled V2a INs with the fluorescent protein tdTomato using the cre-loxP system, where cre was driven by the endogenous locus of the canonical V2a marker gene *chx10* (*Chx10:cre* x *Ai9*). When we analyzed the segmental distribution of V2a interneurons, we found no differences between cervical and lumbar segments in cell number (cervical: 164 ± 13 cells/40um, lumbar: 185 ± 9 cells/40um, $p=0.25$, Supp Fig 1A). Fluorescent in situ hybridization against *vglut2* mRNA confirmed that V2a interneurons are glutamatergic regardless of spinal levels (Supp Fig1B, see also Supp Fig 4B). Together, these observations indicate that cervical and lumbar spinal networks contain quantitatively similar compositions of glutamatergic V2a INs.

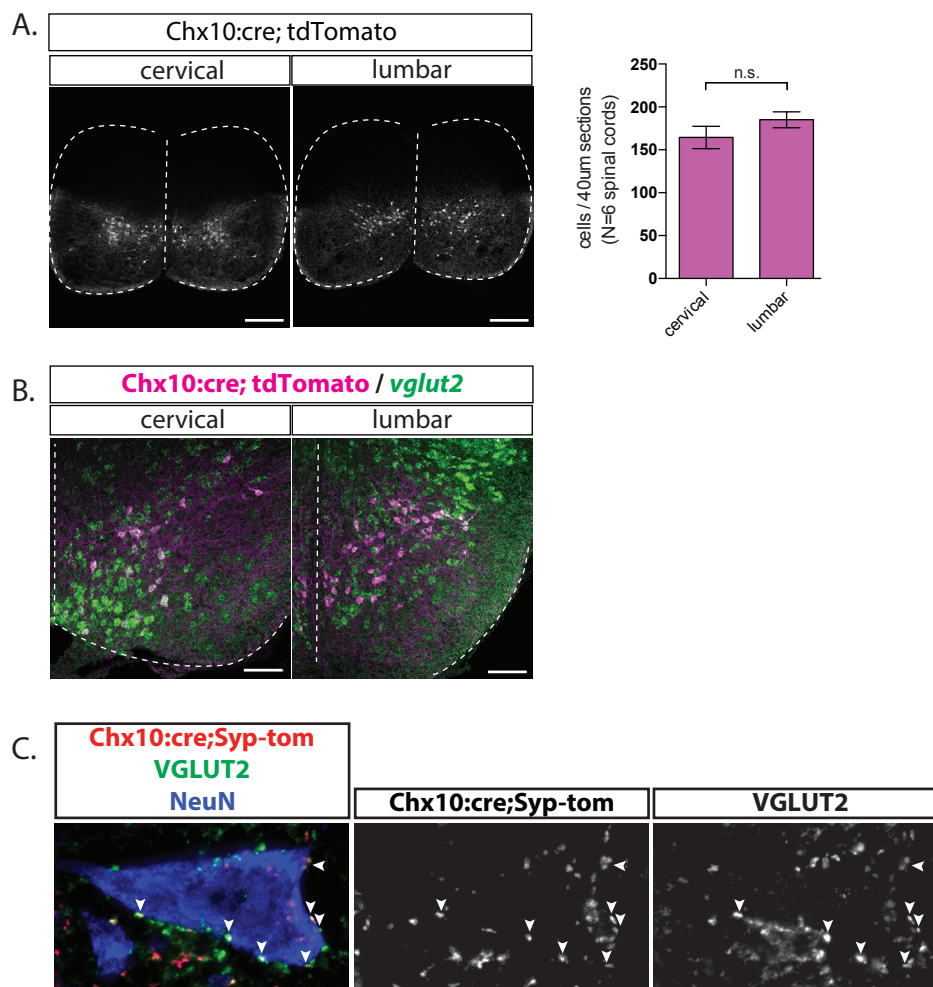


Figure 2.1: Basic characterization of V2a INs.

(A) Similar number of V2a spinal neurons reside in cervical and lumbar segments. Number of V2a interneurons was examined in cervical and lumbar segments. 164 ± 13 cells/40µm ($n=6$ animals from 2 litters, \pm SEM cells) were found in lower cervical segments, and 185 ± 9 cells/40µm ($n=5$ animals from 2 litters, \pm SEM cells) were found in lower lumbar segments in P1 Chx10:cre+ROSA-CAG:ls1:tdTomato+ spinal cords ($p=0.25$, t-test). 20µm cryosections. Scale bar:100µm.

(B) V2a spinal neurons exhibit glutamatergic identity in cervical and lumbar segments. Neurotransmitter status of V2a interneurons was examined in cervical and lumbar segments. Fluorescent in situ hybridization was conducted using a vglut2 probe on P1 Chx10:cre+ROSA-CAG:ls1:tdTomato spinal cord cryosections. Vglut2 signals overlapped with tdTomato+ cells in cervical and lumbar segments. Scale bar: 50µm. See also Supp Fig 4B for RNA-seq results.

(C) Fluorescent protein-tagged synaptophysin labels presynaptic terminals. VGLUT2 immunostaining was conducted to examine the nature of Syp-tdTomato signals. Presynaptic marker VGLUT2 (green) signals overlapped with Syp-tdTomato signals.

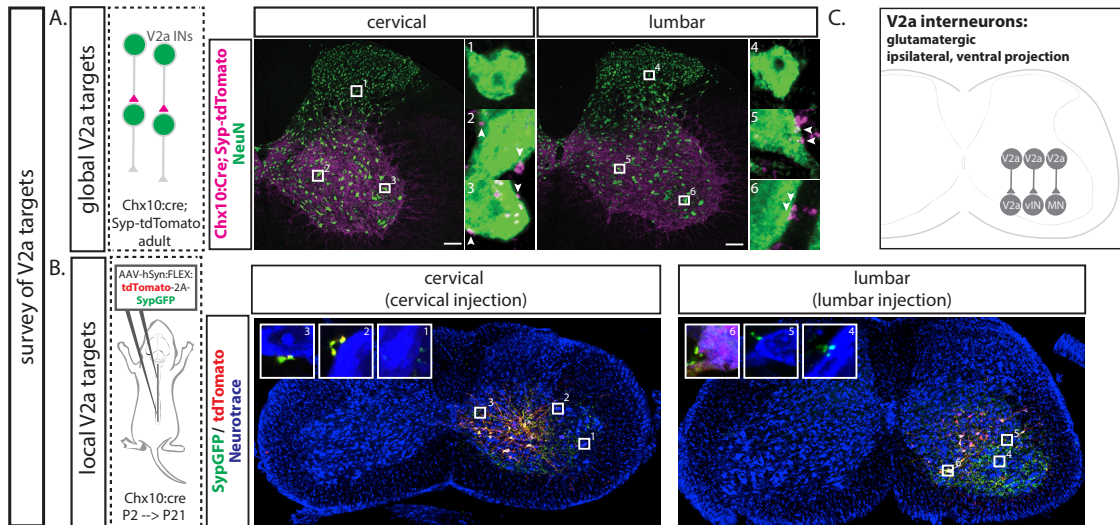


Figure 2.2: V2a spinal neurons are glutamatergic ventrally projecting neurons both in cervical and lumbar segments.

(A) V2a population projects broadly in the ventral spinal cord. Postsynaptic neurons of V2a interneurons were examined. Chx10:cre was crossed to ROSA-CAG:ls1:Synaptophysin-tdTomato reporter line to visualize putative presynaptic terminals of V2a interneurons as a population in the adult spinal cord. Postsynaptic neurons were identified by colocalization of synaptophysin (magenta) and NeuN (green). Synaptophysin was observed broadly in the ventral spinal cord. Numbered boxes correspond to the magnified images on the right. Both in cervical and lumbar segments, NeuN⁺ cells residing in the ventral spinal cords (motor neurons and interneurons) were surrounded by and colocalized with synaptophysin (2, 3, 5, 6). However, V2a-derived synaptophysin was mostly absent in the dorsal spinal cord (1,4). 30um cryosections. Scale bar: 100um.

(B) V2a spinal neurons project broadly in the ipsilateral ventral spinal cord within their resident segments. Local postsynaptic neurons of cervical or lumbar V2a interneurons were examined. AAV expressing tdTomato and SytGFP in a cre-dependent manner (AAV1-hSyn:FLEX:tdTomato-2A-SypGFP) was injected into either cervical or lumbar segments of Chx10:cre⁺ animals to visualize putative presynaptic terminals of local V2a interneurons. Both in cervical and lumbar segments, GFP signal was observed broadly in the ventral spinal cord of the ipsilateral side of injection. Numbered boxes correspond to magnified images on the top. Putative presynaptic terminals were observed onto motor neurons (1, 4), V2a interneurons (6), and other ventral interneurons (2, 3, 5) within the ipsilateral side. Viral injections were conducted at postnatal day 2 (P2) and tissue was collected at P21. 50um cryosections. Scale bar: 100um.

(C) Our anatomical studies indicate that similar number of glutamatergic V2a INs project broadly onto ipsilateral ventral spinal cord neurons both in cervical and lumbar segments.

We next surveyed synaptic targets of V2a interneurons in cervical versus lumbar segments. We examined the laminar distribution of synaptic outputs from the V2a population by genetically labeling presynaptic terminals with synaptophysin tagged with tdTomato (Syp-tdTomato; Chx10:cre x Ai34). Syp-tdTomato expression recapitulated the pattern of synaptic output revealed by the excitatory presynaptic marker VGLUT2 (Supp Fig 1C), suggesting this genetic method reliably labels presynaptic terminals and is suited to survey synaptic targets of V2a interneurons. We observed Syp-tdTomato signals distributed widely throughout the ventral spinal cord both in cervical and lumbar segments, and putative synaptic contacts were found on NeuN+ somata as well as outside of somata in lamina VII-IX (Figure 1A). Strikingly, we found little evidence of V2a synaptic output to the dorsal horn (Figure 1A).

Given diverse morphologies and axonal projections of V2a INs (Dougherty et al. 2010; Ni et al. 2014), we next examined the relationship between segmental location of V2a cell bodies and their output patterns in cervical and lumbar segments. To achieve this, we labeled the cell bodies of V2a INs with tdTomato and their presynaptic terminals by Syp-GFP by unilaterally-injecting AAV expressing tdTomato and Syp-GFP into cervical or lumbar segments of Chx10:cre neonates (Figure 1B). We observed tdTomato+ neurons extensively labeled around the injection sites. In addition to the population level analysis, local V2a output marked by Syp-GFP was broadly targeted to unilateral ventral spinal neurons including V2a-V2a interconnectivity (Figure 1B).

Together, these experiments show that cervical and lumbar V2a interneurons share common characteristics on their glutamatergic output throughout the unilateral ventral spinal cord neurons in their resident segments (Figure 1C).

V2a interneurons exhibit distinct connectivity schemes in cervical versus lumbar segments

Our anatomical characterizations show that V2a INs broadly project to neurons located in the ventral spinal cord. Of these synaptic targets of V2a interneurons we have uncovered, we focused on detailed anatomical connectivity between V2a interneurons and motor neurons. Although V2a interneurons have been shown to synapse onto motor neurons (Al-Mosawie et al. 2007; Stepien et al. 2010; Ni et al. 2014), whether V2a interneurons in cervical segments ver-

sus lumbar segments exhibit quantitatively distinct connectivity to motor neurons has not been elucidated. Delta-G rabies vector expressing GFP (Δ G-Rabies:GFP) together with AAV encoding glycoprotein (AAV:G) was injected into forelimb or hindlimb muscles of Chx10:cre; tdTomato neonates. $2.2\pm 0.4\%$ of forelimb premotor INs were V2a INs, whereas $4.9\pm 0.2\%$ of hindlimb premotor INs were V2a INs (Figure 2A, $p < 0.0001$). This statistical difference was maintained even after the data was further normalized by the number of rabies+ MNs or by the number of V2a INs (Supp Fig 2). Furthermore, this segmental anatomical connectivity difference of V2a INs is not generalized to all interneuron subtypes, as we found that cholinergic V0c INs comprised a similar portion of cervical and lumbar premotor neurons ($0.6\pm 0.1\%$ of forelimb premotor INs, $0.5\pm 0.1\%$ of hindlimb premotor INs, $p = 0.48$, Figure 2A). Together, our observations indicate that V2a INs exhibit higher anatomical connectivity to MNs in lumbar levels than at cervical levels.

In addition to synaptically targeting local circuitry, spinal neurons have also been shown to communicate with supraspinal structures such as the cerebellum and the brainstem (Alstermark and Ekerot. 2013; Azim, et al. 2014). In zebrafish, sub-population of V2a INs with ascending axons is enriched in rostral segments (Menelaou, et al. 2014). Furthermore, in mice, cervical premotor V2a INs are known to project to the Lateral Reticular Nucleus in the brainstem (Pivetta et al. 2014; Azim et al. 2014). These reports prompted us to investigate the segmental distribution of supraspinal projecting V2a INs. To retrogradely visualize V2a INs with ascending projection, Δ G-Rabies:GFP was injected into the brainstem of Chx10:cre; tdtomato neonates. $84.8\pm 5.6\%$ of all the brainstem-projecting V2a interneurons resided within cervical segments, indicating a strong cervical bias of V2a interneurons that project into the brainstem compared to lumbar V2a interneurons (Figure 2B).

Our anatomical characterizations together revealed that V2a INs provide excitatory drive to ventral spinal circuits independent of the spinal segment. However, we found that composition of target populations of V2a INs differentiates cervical and lumbar V2a INs: cervical V2a interneurons project into the brainstem more than lumbar segments, and lumbar V2a interneurons synapse onto motor neurons more than cervical V2a interneurons.

Activation of cervical and lumbar V2a interneuron evokes distinct motor outputs

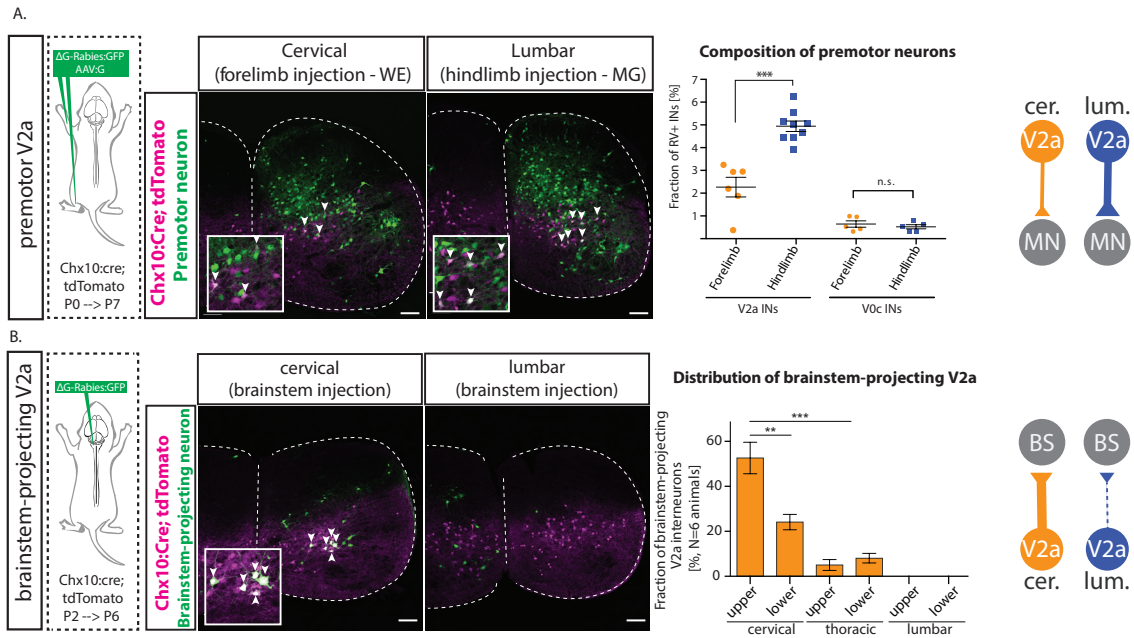


Figure 2.3: V2a interneurons exhibit distinct anatomical connectivity schemes in different spinal segments.

(A) Lumbar V2a neurons exhibit higher anatomical connectivity to motor neurons. Anatomical connectivity between motor neurons and V2a interneurons at cervical and lumbar segments was examined. ΔG -Rabies expressing GFP (ΔG -Rabies:GFP) and AAV expressing glycoprotein were co-injected into either forelimb or hindlimb muscles of Chx10:cre;ROSA-CAG:ls1:tdTomato+ animals to visualize spinal interneurons that synapse onto infected motor neurons. GFP+ neurons and GFP+tdTomato+ V2a interneurons were quantified across rostrocaudal extent of the labeling in the spinal cord (For forelimb injection, typically C1 to mid-thoracic segments. For hindlimb injection, typically mid-thoracic to upper sacral segments). $2.2 \pm 0.4\%$ ($n=6$ animals from 2 litters, \pm SEM%) of forelimb premotor interneurons were V2a interneurons, whereas $4.9 \pm 0.2\%$ ($n=9$ animals from 2 litters, \pm SEM%) of hindlimb premotor interneurons were V2a interneurons ($p < 0.0001$, t-test). ChAT+ V0c interneurons represented $0.6 \pm 0.1\%$ ($n=5$ animals from 2 litters, \pm SEM%) and $0.5 \pm 0.1\%$ ($n=5$ animals from 2 litters, \pm SEM%) at cervical and lumbar segments, respectively ($p=0.48$, t-test). Injections were conducted at P0 and tissue was collected at P7. 25 μ m cryosections. Scale bar: 100 μ m.

(B) Brainstem-projecting V2a interneurons predominantly reside in the cervical spinal cord. ΔG -Rabies:GFP was injected into brainstem of Chx10:cre+ROSA-CAG:ls1:tdTomato+ animals as a retrograde tracer to visualize spinal neurons projecting into the brainstem. GFP+tdTomato+ V2a interneurons were quantified along the rostrocaudal axis in the spinal cord. $84.8 \pm 5.6\%$ ($n=7$ animals from 2 litters, \pm SEM%) of all the brainstem-projecting V2a interneurons resided within cervical segments. Injections were conducted at P2 and tissue was collected at P6. 25 μ m cryosections. Scale bar: 100 μ m.

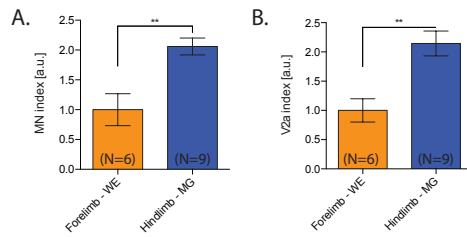


Figure 2.4: Distinct MN-V2a connectivity between cervical and lumbar segments.

(A, B) Distinct MN-V2a connectivity between cervical and lumbar segments is not dependent on the number of infected motor neurons or on the number of V2a INs. Data from figure 2A was further normalized by the number of motor neurons labeled by Δ G-Rabies:GFP (A) or by the number of V2a INs (B), and lumbar V2a interneurons had higher connectivity index per motor neuron or V2a INs than cervical V2a interneurons ($p=0.002$ (A), $p=0.003$ (B), t test).

Our observations so far raise the possibility that distinct connectivity schemes provide an anatomical basis for V2a INs to contribute to motor outputs in a distinct fashion in different spinal cord segments. To examine this possibility, we analyzed the properties of motor output evoked by the stimulation of the V2a population. We utilized mouse genetics (Chx10:cre x Ai32) to express ChR2 reproducibly in V2a interneurons. Reflecting segmental output pattern of V2a INs (Figure 1B), focal and unilateral stimulation of V2a INs within single cervical (typically C8) or lumbar segment (typically L5) resulted in motor neuron spikes in the same segmental ventral roots, indicating that V2a INs are sufficient to evoke intrasegmental motor outputs (Figure 3A).

However, analysis of the latency and reliability of these motor responses revealed significant differences between cervical and lumbar segments. Following repeated stimulations of cervical V2a INs (10 trials with 10 sec intervals), we found that $48 \pm 12\%$ ($n=12$ animals) of cervical photostimulation trials evoked motor neuron spikes, whereas $100 \pm 0\%$ ($n=13$ animals) of lumbar photostimulation trials evoked motor neuron spikes ($p=0.0001$). Moreover, lumbar motor neuron spikes were evoked at a shorter latency than cervical motor neuron spikes (cervical: 53.03 ± 2.93 ms; $n=9$ animals; lumbar: 31.19 ± 1.83 ms; $n=13$ animals, $p<0.0001$, Figure 3A). To exclude the possibility that distinct motor neuron responses between cervical and lumbar segments were due to differences in the optical recruitment of V2a interneurons, we synaptically isolated V2a INs (see Methods) and found no difference in the latency or reliability of cervical or lumbar V2a INs that were optically stimulated (Figure 3B). Given that similar numbers of glutamatergic V2a interneurons are present in cervical and lumbar segments (Supp Fig 1, also see next section), our data indicate that stimulation of lumbar V2a INs contribute to the motor neuron activity more reliably and robustly than cervical V2a INs.

To determine whether the weak recruitment of cervical motor neurons is a general property of cervical spinal circuits, we compared optically evoked motor responses following stimulation of dorsal excitatory interneuron population labeled with *Lmx1b:cre*. Here, optical stimulation of these INs generated robust motor responses from both cervical and lumbar spinal cords with no difference in the latency of these responses (Figure 3C). These results indicate that spinal circuits can robustly recruit both cervical and lumbar motor neurons, highlighting the distinct contribution of cervical and lumbar V2a INs to motor outputs.

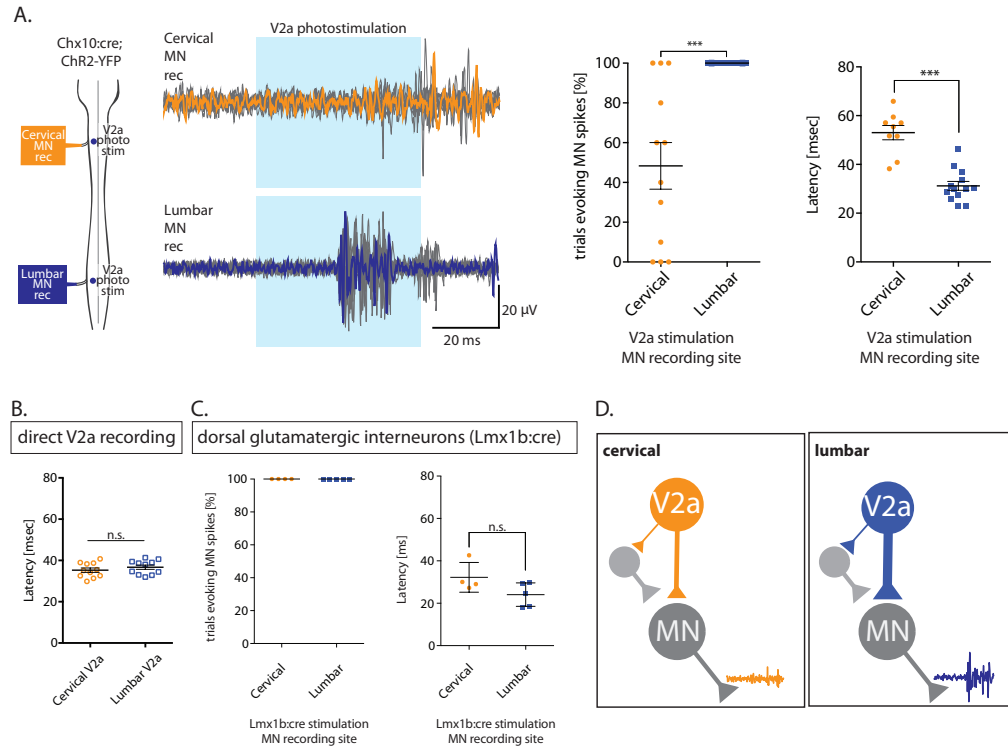
Figure 2.5: Activation of lumbar V2a interneurons results in more robust motor outputs than cervical V2a interneurons.

(A) Activation of lumbar V2a neurons results in more robust motor outputs than cervical V2a neurons. Contribution of V2a activations to motor outputs was examined. *Chx10:cre;ROSA-CAG:ls1:Chr2-YFP* at P2-4 were used to unilaterally-photostimulate V2a interneurons while recording motor output. Motor neuron spikes from a representative animal are shown. Orange (cervical) or blue (lumbar) trace indicates an average of 10 photostimulation trials, and gray traces indicate individual trials. Duration of photostimulation is shown in light blue boxes. $48\pm 12\%$ ($n=12$ animals from 5 litters, \pm SEM %) of cervical photostimulation trials evoked motor neuron spikes at cervical segments, whereas $100\pm 0\%$ ($n=13$ animals from 5 litters, \pm SEM %) of lumbar photostimulation trials evoked motor neuron spikes at lumbar segments ($p=0.0001$, t test). Of the photostimulation trials resulting in motor neuron spikes, cervical V2a photostimulation had a latency of 53.03 ± 2.93 ms ($n=9$ animals from 5 litters, \pm SEM ms), while lumbar V2a photostimulation had a latency of 31.19 ± 1.83 ms ($n=13$ animals from 5 litters, \pm SEM ms; $p<0.0001$, t test).

(B) Both cervical and lumbar V2a neurons are recruited at the same timing. Recruitment timing of V2a neurons upon photostimulation was examined. Spikes of V2a interneurons were recorded in the ventral spinal cords in the presence of CNQX and D-APV to eliminate synaptic transmission and isolate V2a interneuron spikes. Cervical photostimulation had latency of 36.72 ± 1.02 ms ($n=11$ units recorded from 3 animals, \pm SEM ms), and lumbar photostimulation had latency of 35.28 ± 1.07 ms ($n=11$ units recorded from 3 animals, \pm SEM ms, $p=0.34$, t test). Prior to application of CNQX and D-APV, MN spikes were recorded from these animals, and cervical V2a photostimulation had a latency of 59.47 ± 3.24 ms ($n=3$ animals, \pm SEM ms), while lumbar V2a photostimulation had a latency of 40.85 ± 2.80 ms ($n=3$ animals, \pm SEM ms; $p=0.01$, t test).

(C) Cervical and lumbar spinal networks can exhibit similar outputs. Contribution of dorsal glutamatergic interneuron activations to motor outputs was examined. Experiment was conducted as described in the previous figure, except *Lmx1b:cre* was used. $100\pm 0\%$ ($n=4$ animals from 2 litters, \pm SEM %) of cervical photostimulation trials evoked motor neuron spikes at cervical segments, and $100\pm 0\%$ ($n=5$ animals from 2 litters, \pm SEM %) of lumbar photostimulation trials evoked motor neuron spikes at lumbar segments. Cervical photostimulation had a latency of 32.23 ± 3.51 ms ($n=4$ animals from 2 litters, \pm SEM ms), while lumbar photostimulation had a latency of 24.07 ± 2.47 ms ($n=5$ animals from 2 litters, \pm SEM ms; $p=0.09$, t test).

(D) Our analyses reveal that both cervical and lumbar V2a INs are recruited at the same timing, but recordings from MNs show lumbar V2a INs are positioned to elicit MN spikes more reliably with a shorter latency. This may reflect the anatomical connectivity difference that we uncovered in Figure 2.



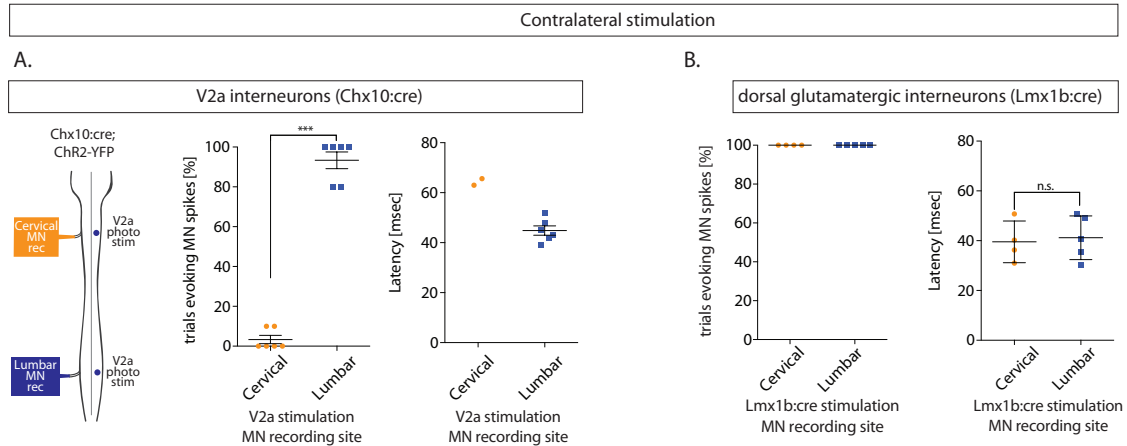


Figure 2.6: Contralateral stimulations.

(A) Activation of lumbar V2a neurons results in more robust motor outputs than cervical V2a neurons from the contralateral side. Contribution of V2a activations to contralateral motor outputs was examined. Contralateral side of the spinal cord was photostimulated while recording motor output. $3 \pm 2\%$ ($n=6$ animals, \pm SEM %) of cervical photostimulation trials evoked motor neuron spikes at cervical segments, whereas $93 \pm 4\%$ ($n=6$ animals, \pm SEM %) of lumbar photostimulation trials evoked motor neuron spikes at lumbar segments ($p < 0.0001$, t test). Of the photostimulation trials resulting in motor neuron spikes, cervical V2a photostimulation had a latency of 64.29 ± 1.31 ms ($n=2$, \pm SEM ms), while lumbar V2a photostimulation had a latency of 44.86 ± 1.87 ms ($n=6$ animals, \pm SEM ms).

(B) Cervical and lumbar spinal networks can exhibit similar outputs. Contribution of dorsal glutamatergic interneuron activations to contralateral motor outputs was examined. Experiment was conducted as described in the previous figure, except Lmx1b:cre was used. $100 \pm 0\%$ ($n=4$ animals from 2 litters, \pm SEM %) of cervical photostimulation trials evoked motor neuron spikes at cervical segments, and $100 \pm 0\%$ ($n=5$ animals from 2 litters, \pm SEM %) of lumbar photostimulation trials evoked motor neuron spikes at lumbar segments. Cervical photostimulation had a latency of 39.56 ± 4.19 ms ($n=4$ animals from 2 litters, \pm SEM ms), while lumbar photostimulation had a latency of 41.19 ± 3.92 ms ($n=5$ animals from 2 litters, \pm SEM ms; $p=0.79$, t test).

One of the hallmarks of spinal cord network function is the capability to generate rhythmic motor outputs underlying the locomotion. The locomotor outputs rely on left-right alternating network activity mediated by several classes of contralateral projecting spinal neurons (Talpalari et al. 2013; Kullandar, et al. 2003; Zhang, et al. 2008). V2a INs have been shown to indirectly regulate contralateral spinal cord activity via contralaterally-projecting V0 INs, and elimination of V2a INs results in left-right alternation at a high speed (Crone et al. 2008; 2009). We therefore next set out to investigate to what extent activity of V2a INs can serve as a functional basis for contralateral motor outputs in cervical and lumbar segments. We recorded motor neuron spikes in the same way as the previous experiments and photostimulated cervical or lumbar V2a INs from the contralateral side of the spinal cord. We found that only $3\pm 2\%$ ($n=6$ animals) of cervical photostimulation trials evoked contralateral motor neuron spikes, while $93\pm 4\%$ ($n=6$ animals) of lumbar photostimulation trials evoked contralateral motor neuron spikes ($p<0.0001$, Supp Fig 3A), indicating that lumbar V2a INs can contribute to the contralateral motor outputs and are better positioned to underlie locomotor outputs compared to cervical V2a INs. In contrast, optical stimulation of excitatory dorsal INs (*Lmx1b:cre*) generated robust contralateral motor responses from both cervical and lumbar spinal cords with no difference in the latency of these responses (Supp Fig 3B), highlighting the distinct contribution of cervical and lumbar V2a INs to contralateral motor outputs.

Together, our anatomical and functional studies demonstrate that V2a INs are positioned to contribute to the distinct motor patterns generated by cervical and lumbar spinal cord. We found that lumbar V2a INs are wired to support the network activity for robust motor neuron recruitment. In contrast, cervical V2a INs provide input to supraspinal structures with activating motor outputs less robustly, demonstrating how a given class of spinal interneurons can exhibit diverse contribution to motor outputs in different spinal segments.

Cervical and lumbar V2a interneurons exhibit distinct genetic signatures

Given the diversity of anatomical and functional connectivity schemes uncovered within a given class of spinal neurons between cervical and lumbar segments, we next set out to explore genetic signatures that may segregate cervical and lumbar V2a interneurons using RNA-sequenc-

ing. We reasoned that such identification would offer us a genetic entry point to access diverse V2a interneurons and offer us a general principle underlying diversification of spinal neural networks. Cervical and lumbar segments were collected from E15.5 Chx10:cre;tdTomato embryos, and tdTomato⁺ and – fractions were collected and were subjected for RNA-seq analyses (Figure 4A).

We first investigated the common molecular feature of V2a INs by focusing on genes enriched in tdTomato⁺ samples compared to tdTomato⁻ samples (Figure 4B). Both in cervical and lumbar segments, the canonical V2a IN marker gene *chx10/vsx2* exhibited the highest fold enrichment compared to tdTomato⁻ samples (Figure 4C,D). In addition, other known V2a IN marker genes such as *sox14*, *shox2*, *lhx3* and *lhx4* were consistently enriched in V2a INs with high level of expression, forming a cluster of genes away from the rest of the genes expressed, together with 2 non-coding RNAs (Figure 4C,D). Together, these observations indicate that canonical V2a IN marker genes differentiate V2a INs from the rest of the spinal cells both in cervical and lumbar segments.

We next compared genes differentially expressed between cervical and lumbar V2a interneurons. We found 48 genes enriched in cervical V2a compared to lumbar V2a and 51 genes enriched in lumbar V2a compared to cervical V2a. Given our earlier observations that lumbar V2a INs evoke motor output more robustly and reliably than cervical V2a INs (Figure 3), we examined genes known to confer neurotransmitter identities and did not find differential expression, indicating cervical and lumbar V2a interneurons exhibit similar neurotransmitter identity as a population (Supp Fig4B).

We next investigated constituents of cervical and lumbar V2a genetic networks and how they may differ from each other. Of the genes differentially expressed between cervical and lumbar V2a INs, we found that *hox* genes corresponding to rostral and caudal segments represented the highest enriched genes in cervical and lumbar samples, respectively (Figure 4E).

Surprisingly, despite our observations that conventional V2a marker genes segregate V2a INs from the rest of the cells in the spinal cord both in cervical and lumbar segments, we observed that conventional V2a IN marker genes *Chx10/Vsx2* and *Sox14* were expressed higher in lumbar segments than cervical segments (Figure 4F, Supp Fig 4C).

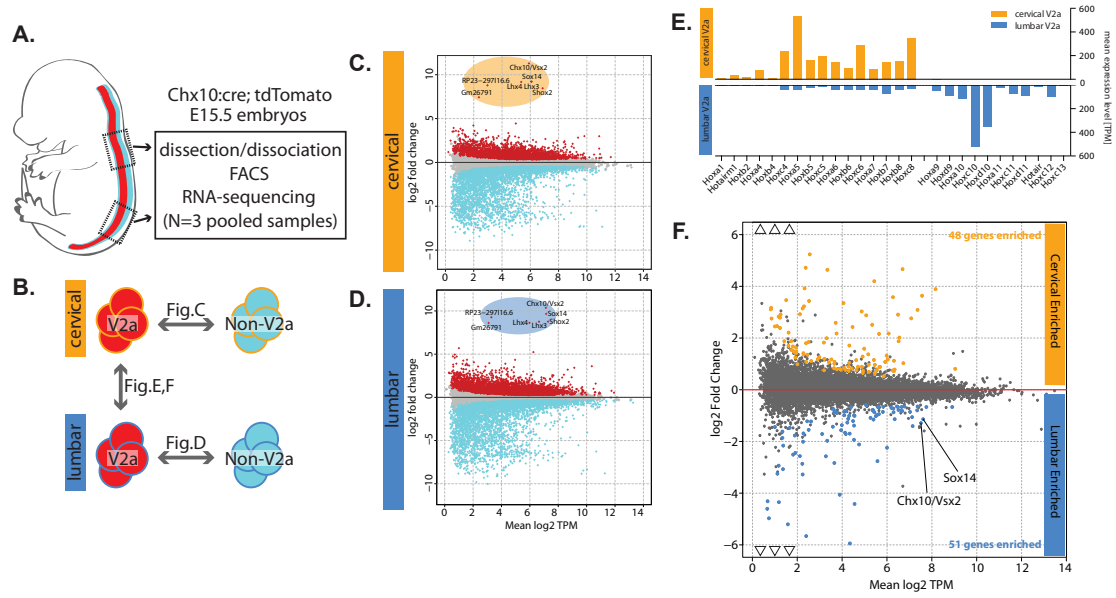


Figure 2.7: V2a interneurons exhibit distinct genetic signatures between cervical and lumbar segments.

(A) Experimental set up is shown. Cervical and lumbar segments were isolated from Chx10:cre;Rosa-CAG:ls1:tdTomato embryos at E15.5. Segments were enzymatically dissociated and sorted into tdTomato⁺ and tdTomato⁻ samples. Total RNA was subjected for library preparation and RNA-seq analyses.

(B) Schematics showing the analyses conducted. Genes enriched in V2a INs compared to tdTomato⁻ cells at cervical and lumbar segments were examined (Figure C, D). Furthermore, genes enriched in cervical V2a INs versus lumbar V2a INs were examined (Figure E, F).

(C,D) A similar set of genes characterizes V2a neurons in cervical and lumbar segments. Genes enriched in V2a INs compared to tdTomato⁻ cells in cervical (upper panel) and lumbar (lower panel) segments are shown. Both in cervical and lumbar segments, the same five transcription factors and two non-coding RNAs represented the top transcripts differentially expressed compared to tdTomato⁻ cells.

(E) Hox genes segregate cervical and lumbar V2a INs. Hox genes detected either in cervical or lumbar V2a INs are listed on the x axis. Expression level of hox genes in cervical V2a INs (upper panel) and lumbar V2a INs (lower panel) are shown.

(F) Conventional V2a marker genes are expressed more in lumbar segments than cervical segments. Differential gene expression plot between cervical and lumbar V2a interneurons is shown within the log₂ fold change of ± 6 . Plot with Full range of fold change is shown in supplemental figure 3A. Orange dots indicate genes enriched in cervical segments, and blue dots indicate genes enriched in lumbar segments with the P value of < 0.05 . Of the conventional V2a marker genes, Chx10 and Sox14 were enriched in lumbar V2a interneurons.

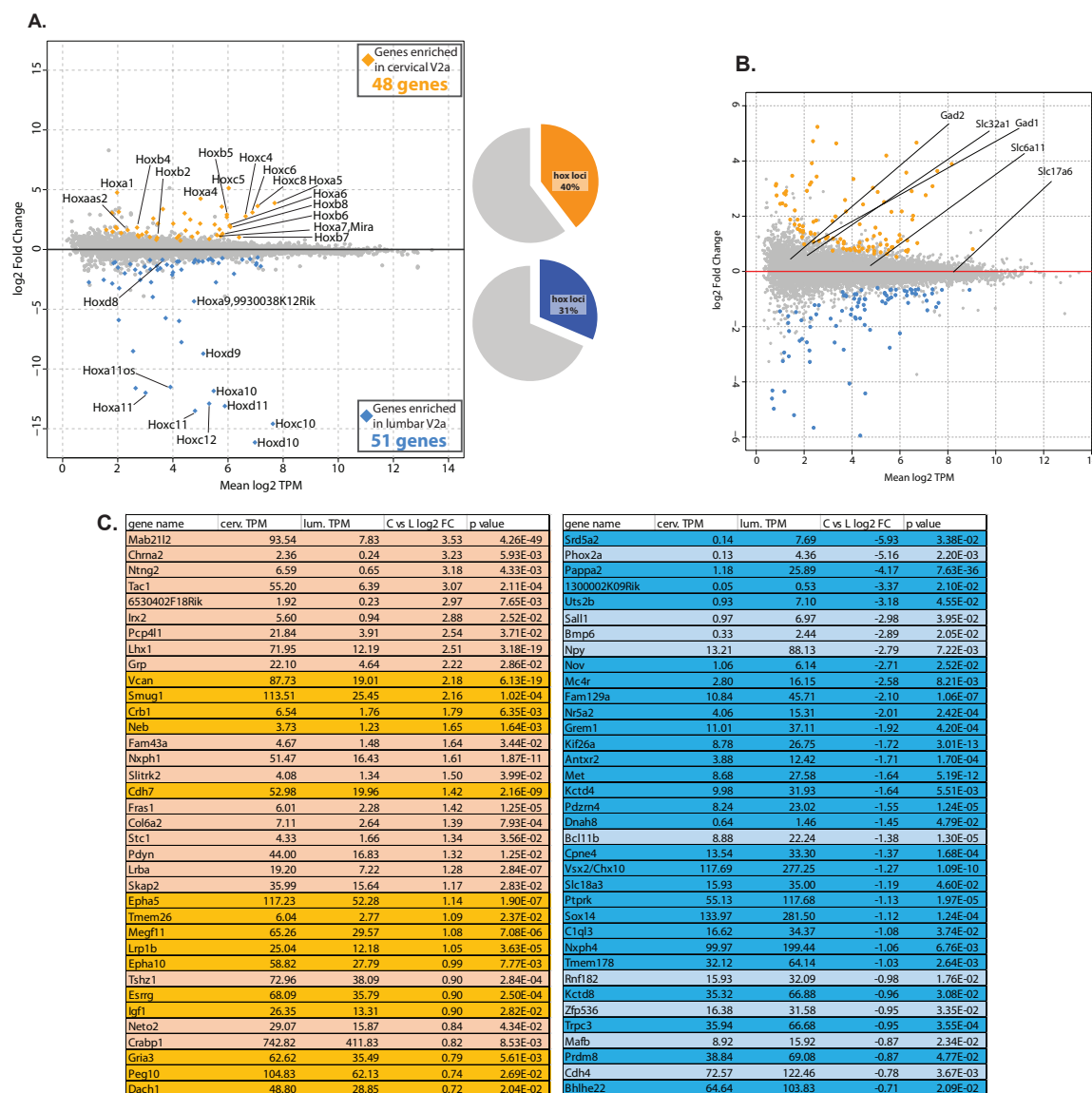


Figure 2.8: Supplemental RNA-seq data.

(A) Hox genes are differentially expressed in cervical and lumbar V2a INs. Differential gene expression plot between cervical and lumbar V2a interneurons is shown. Orange dots indicate genes enriched in cervical segments, and blue dots indicate genes enriched in lumbar segments with the P value of <0.05 . Hox genes are labeled. 40% of genes enriched in cervical V2a INs were genes expressed from hox loci, and 31% of genes enriched in lumbar V2a INs were genes expressed from hox loci.

(B) Genes that have been shown to confer neurotransmitter types are labeled. Slc17a6/vglut2, slc6a11/mGAT4, slc32a1/VGAT, gad1, and gad2 did not show differential expression, indicating cervical and lumbar V2a interneurons exhibit similar neurotransmitter types (see also Supp Fig 1B).

(C) List of genes differentially expressed in cervical V2a (orange) and lumbar V2a (blue). Hox genes are excluded in this list. Darker orange and blue indicate genes that are enriched in V2a compared to tdTomato- samples by more than 2-fold.

Together, our RNA-seq results indicate that, although the identical set of transcription factors characterize V2a interneurons as a population in cervical and lumbar segments, conventional V2a interneuron marker genes *chx10* and *sox14* were surprisingly expressed at a higher level in lumbar segments than cervical segments.

V2a interneurons are diversified with regard to conventional V2a interneuron marker genes

We reasoned that the differential expression of conventional V2a interneuron marker genes between cervical and lumbar segments may serve as a genetic entry point to further investigate the diverse connectivity schemes of V2a interneurons in cervical versus lumbar segments. Although RNA-seq reveals population level gene expression differences between cervical and lumbar segments, whether these differential expressions reflect heterogeneity among individual V2a INs is unknown.

We therefore conducted immunostaining against the V2a interneuron marker gene CHX10 to examine its protein expression in different spinal segments at a single cell resolution. In neonates, colocalization analysis identified that, at rostral levels in cervical segments, ~50% of V2a INs expressed detectable levels of CHX10 protein (identified with antibody labeling). Conversely, in lumbar segments ~90% of V2a INs expressed detectable levels of CHX10 protein (Figure 5A,B). These observations indicate that V2a INs exhibit rostrocaudal diversity with regard to the expression of the conventional marker gene *chx10*.

The disparity between V2a INs labeled with *Chx10:cre* reporter and CHX10 protein expression raises the possibility that, following initial specification of V2a identity, CHX10 is dynamically regulated in a subset of V2a INs. To examine this possibility, we took a time course of CHX10 during embryonic development. We found that in E11.5 spinal cords, all the V2a INs expressed CHX10. However, by E14.5, 50% of *tdTomato*⁺ V2a INs expressed CHX10 rostrally, and 90% of *tdTomato*⁺ V2a INs expressed CHX10 caudally, recapitulating our earlier observation at a postnatal time point and RNA-seq data at E15.5 (Supp Fig 5A,B, Figure 4). This developmental regulation of CHX10 expression prompted us to examine the time point where CHX10 expression reaches its mature state beyond postnatal stages. We found that a similar rostrocaudal pattern was present in adult spinal cords. Together, these data demonstrate that the rostrocaudal

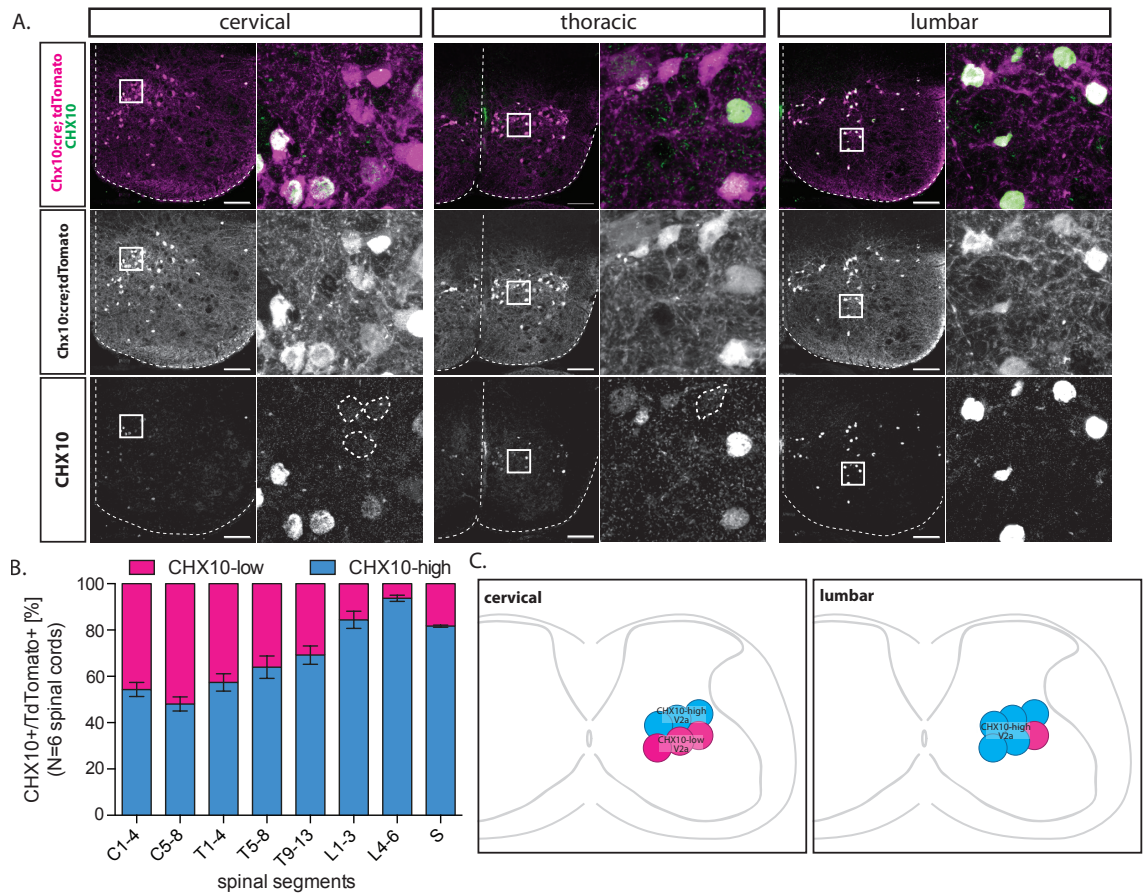


Figure 2.9: Conventional V2a interneuron marker CHX10 is differentially expressed between cervical and lumbar segments at a single cell level.

(A) A fraction of rostral V2a neurons lacks CHX10 expression. CHX10 protein expression was examined in V2a interneurons at a single cell resolution. V2a interneurons were visualized in *Chx10:cre;ROSA-CAG:ls1:tdTomato* animals, and CHX10 protein levels were determined through immunostaining. At cervical segments, CHX10 immunostaining did not label all the V2a interneurons, while at lumbar segments, CHX10 expression was observed in most of V2a interneurons at P1. 20um cryosections. Scale bar: 50um. Magnified regions are indicated with boxes on the left panels.

(B) CHX10 expression varies along the rostrocaudal axis. CHX10-high status was quantified along the rostrocaudal axis. At cervical segments, 50-60% of V2a interneurons had detectable level of CHX10 expression, while at lumbar segments more than 80% of V2a interneurons expressed detectable level of CHX10 (n=6 animals from 2 litters).

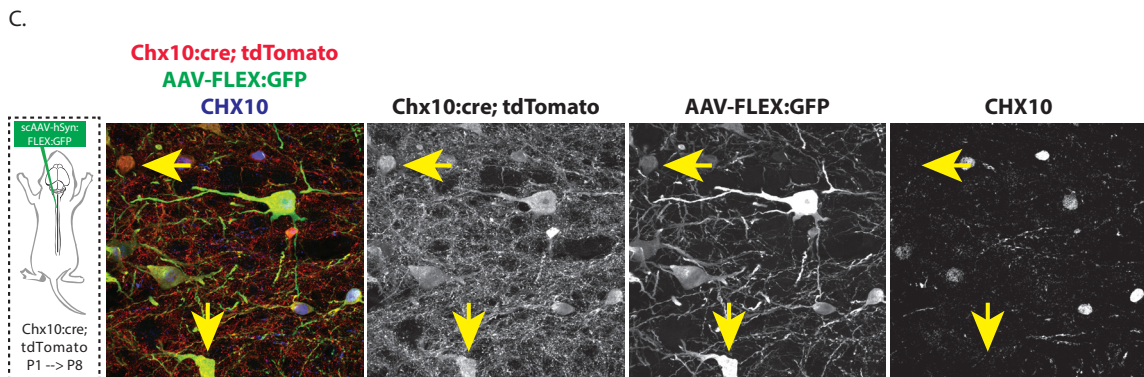
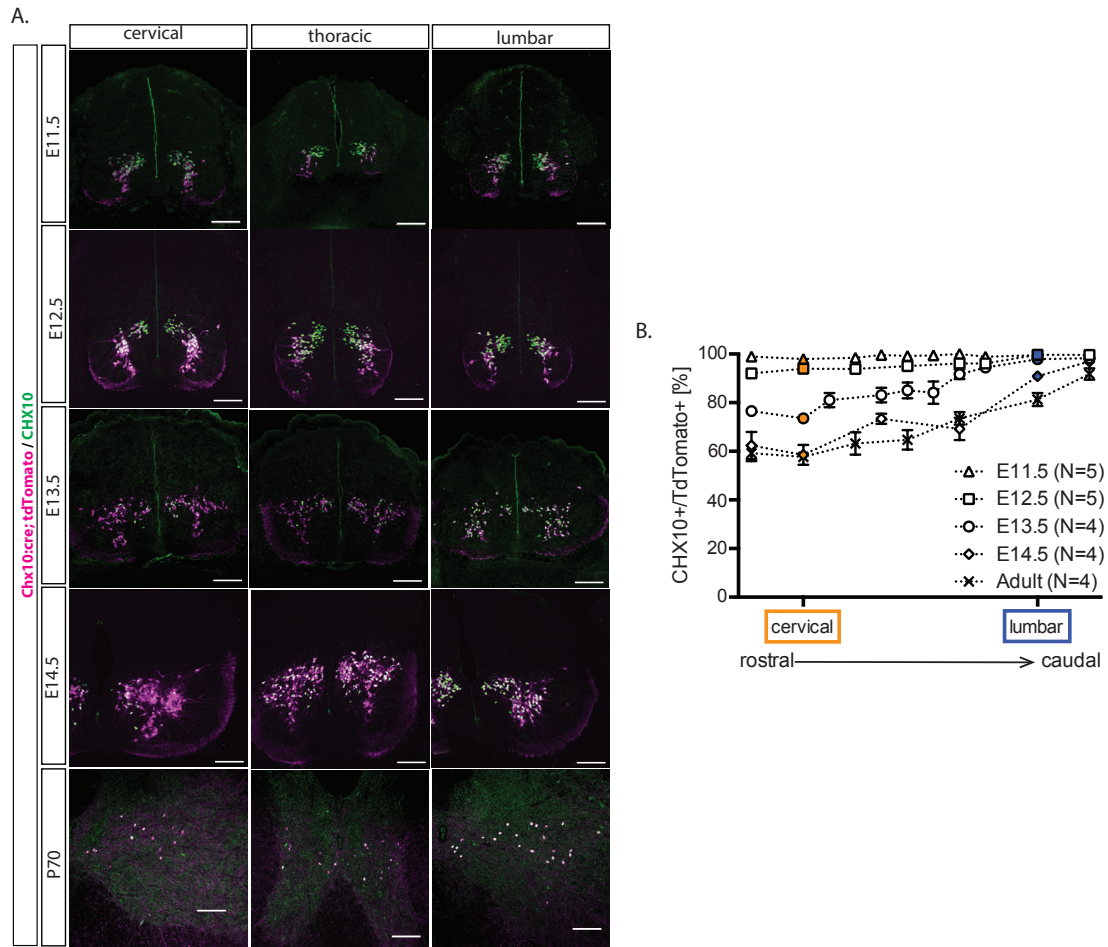
(C) Data shown here and our RNA-sequencing data (Figure 4F) reveal that at cervical segments, V2a interneurons are further diversified into conventional CHX10-high V2a interneurons and novel CHX10-low V2a interneurons.

Figure 2.10: Characterization of the V2a IN diversification.

(A) V2a diversification with CHX10 expression progressively takes place during embryonic development. Time course of CHX10 protein expression was examined during embryonic development into the adulthood. CHX10 immunostaining was conducted on *Chx10:cre+ ROSA-CAG:lsl:tdTomato+* cryosections from E11.5-E14.5 and P70 animals. 12um cryosections at E11.5-E13.5. 20um cryosections at E14.5 and P70. Scale bar: 50um at E11.5-14.5, 100um at P70.

(B) CHX10-high status was quantified along the rostrocaudal axis. Since the lengths of the spinal cords are different at different developmental stages, FOXP1 immunostaining was conducted to identify corresponding brachial/cervical and lumbar segments and align approximate rostrocaudal levels from different developmental stages (data not shown). At E11.5 and E12.5, vast majority of V2a interneurons expressed CHX10 protein, and progressive decrease of CHX10 expression was observed in some of V2a interneurons in rostral segments at E13.5 and E14.5. By E14.5 the rostrocaudal extent of CHX10 expression was consistent with postnatal and P70 spinal cords.

(C) V2a neurons can be labeled with AAV regardless of CHX10 expression level. A cre-dependent AAV encoding GFP (*scAAV1-hSyn:FLEX:GFP*) was injected into cervical segments of *Chx10:cre;tdTomato* neonates at P1 when the V2a diversification is complete. AAV labeled V2a neurons without detectable level of CHX10 (yellow arrows).



diversification of V2a INs occurs after the initial cell fate specification during embryonic development, and that it is maintained into the adulthood (Supp Fig 5A,B).

We next examined to what extent our antibody detection of CHX10 reflects the transcriptional activity of *chx10* locus. To address this, we used the activity of cre recombinase as a surrogate of *chx10* activity and injected AAV-hSyn:FLEX:GFP into *Chx10:cre*; *tdTomato* neonates. In addition to GFP+*tdTomato*+CHX10+ neurons, we also observed GFP+*tdTomato*+ neurons without detectable level of CHX10 (Supp Fig 5C), suggesting that V2a INs with undetectable level of CHX10 still possess low level of activity of *chx10* locus. We therefore name the V2a INs with detectable level of CHX10 as “CHX10high V2a” and V2a INs with undetectable level of CHX10 as “CHX10low V2a” (Figure 5C).

Our observations collectively show that, despite the fact that V2a INs are generated rather homogeneously along the rostrocaudal axis during embryonic development, *Chx10*, the conventional V2a IN marker gene, is itself dynamically regulated, serving as a molecular marker for the postmitotic diversification of V2a INs in cervical versus lumbar segments.

Other V2a marker genes exhibit diverse expression patterns

Given that other transcription factors characterize V2a INs in addition to *chx10* (Figure 4C,D), we next set out to investigate to what extent this rostrocaudal diversification is a general molecular strategy utilized in V2a INs. To this end, we investigated the protein expression of other V2a IN marker genes along the rostrocaudal axis.

Similarly to CHX10, 52±3% (n=7 animals from 2 litters, ±SEM %) of V2a interneurons were labeled with LHX3 antibody in cervical segments, whereas in lumbar segments, 91±4% (n=7 animals from 2 litters, ±SEM %; p<0.0001, t test) of the V2a interneurons were labeled with LHX3 antibody. Furthermore, more than 80% of CHX10-high V2a interneurons expressed LHX3 regardless of the spinal segments, highlighting the overlap between CHX10 and LHX3 across the spinal segments (Supp Fig 5-2A).

We next investigated the protein expression of LHX4. In cervical segments, 86±2% (n=8 animals from 2 litters, ±SEM %) of V2a interneurons were labeled with LHX4 antibody, whereas in lumbar segments, 96±1% (n=8 animals from 2 litters, ±SEM %; p=0.0016, t test) of the V2a

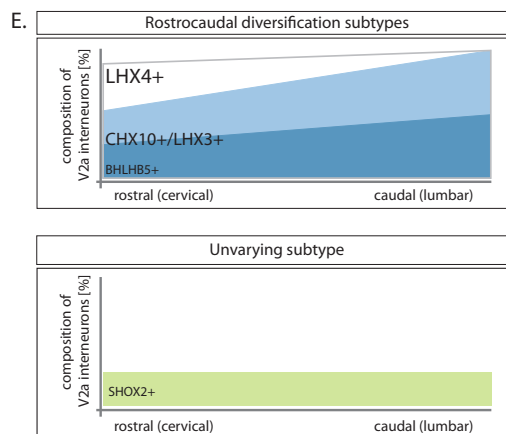
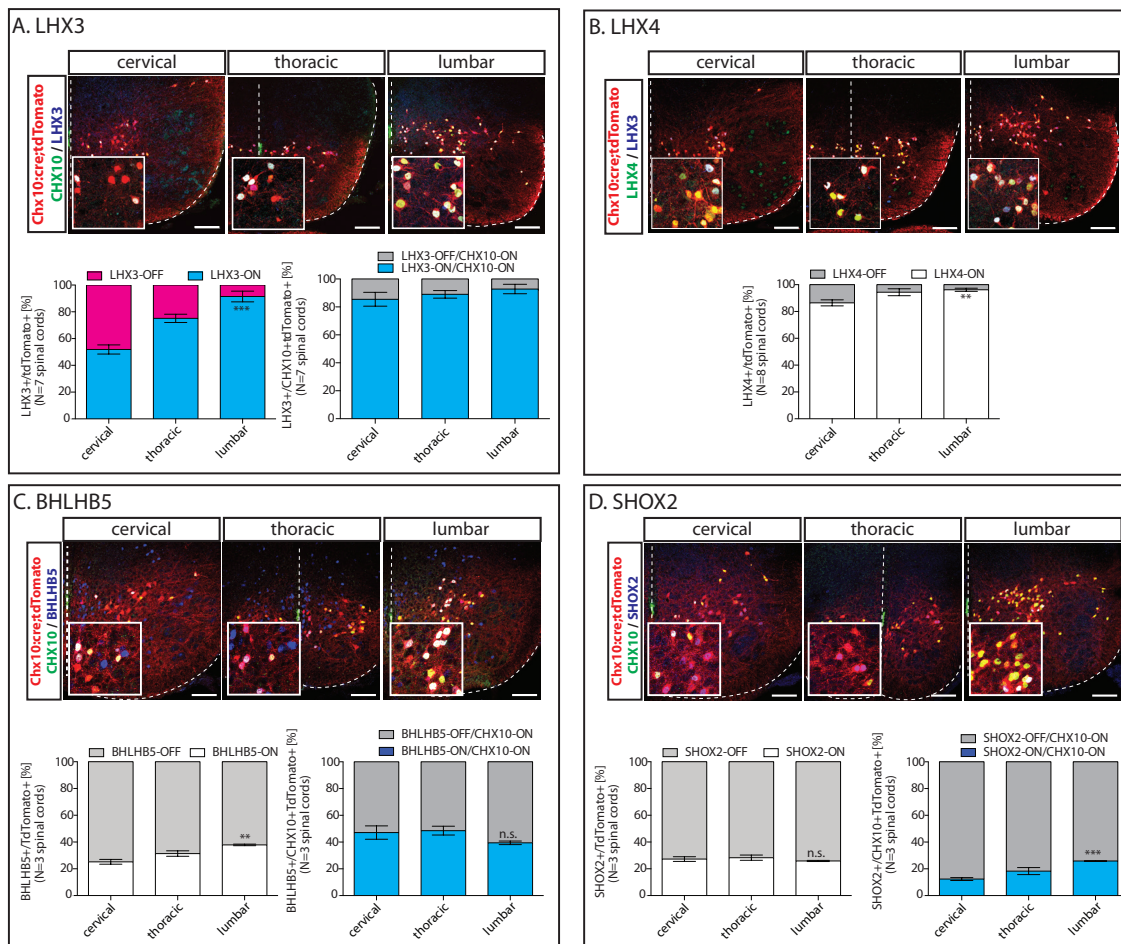
Figure 2.11: Other V2a interneuron marker genes are differentially expressed between cervical and lumbar segments.

(A) LHX3 expression resembles CHX10 expression in V2a interneurons. Protein expression of LHX3 was examined together with CHX10 in V2a interneurons. V2a interneurons were visualized in *Chx10:cre;ROSA-CAG:ls1:tdTomato* animals with immunostaining against CHX10 and LHX3. Similarly to CHX10, $52\pm 3\%$ ($n=7$ animals from 2 litters, \pm SEM %) of V2a interneurons were labeled with LHX3 antibody in cervical segments, whereas in lumbar segments, $91\pm 4\%$ ($n=7$ animals from 2 litters, \pm SEM %; $p<0.0001$, t test) of the V2a interneurons were labeled with LHX3 antibody. Furthermore, more than 80% of CHX10-high V2a interneurons expressed LHX3 regardless of the spinal segments. 20um cryosections. Scale bar: 50um

(B) LHX4 is expressed widely in V2a interneurons. Protein expression of LHX4 was examined together with LHX3 in V2a interneurons. In cervical segments, $86\pm 2\%$ ($n=8$ animals from 2 litters, \pm SEM %) of V2a interneurons were labeled with LHX4 antibody, whereas in lumbar segments, $96\pm 1\%$ ($n=8$ animals from 2 litters, \pm SEM %; $p=0.0016$, t test) of the V2a interneurons were labeled with LHX4 antibody. 20um cryosections. Scale bar: 50um

(C) BHLHB5 is mostly expressed within CHX10-high V2a interneurons. Protein expression of BHLHB5 was examined together with CHX10 in V2a interneurons. In cervical segments, $25\pm 2\%$ ($n=3$ animals, \pm SEM %) of V2a interneurons were labeled with BHLHB5 antibody, whereas in lumbar segments, $38\pm 1\%$ ($n=3$ animals, \pm SEM %; $p=0.0025$, t test) of the V2a interneurons were labeled. Furthermore, $47\pm 5\%$ and $39\pm 1\%$ of CHX10-high V2a interneurons expressed BHLHB5 in cervical or lumbar segments, respectively. Importantly, more than 90% of BHLHB5+ V2a INs expressed CHX10, indicating BHLHB5 labels a subset of Chx10-high V2a INs. 20um cryosections. Scale bar: 50um

(D) SHOX2 is expressed in a defined proportion of V2a interneurons. Protein expression of SHOX2 was examined together with CHX10 in V2a interneurons. In cervical segments, $27\pm 2\%$ ($n=3$ animals, \pm SEM %) of V2a interneurons were labeled with SHOX2 antibody, whereas in lumbar segments, $26\pm 0\%$ ($n=3$ animals, \pm SEM %; $p=0.47$, t test) of the V2a interneurons were labeled, indicating that this V2a marker gene is expressed in a defined fraction of V2a INs regardless of the spinal segments. 20um cryosections. Scale bar: 50um



interneurons were labeled with LHX4 antibody, indicating that LHX4 also exhibits rostrocaudal differences but with less magnitude than CHX10 or LHX3 (Supp Fig 5-2B).

We next examined the protein expression of BHLHB5. In cervical segments, $25 \pm 2\%$ ($n=3$ animals, \pm SEM %) of V2a interneurons were labeled with BHLHB5 antibody, whereas in lumbar segments, $38 \pm 1\%$ ($n=3$ animals, \pm SEM%; $p=0.0025$, t test) of the V2a interneurons were labeled. Furthermore, $47 \pm 5\%$ and $39 \pm 1\%$ of CHX10-high V2a interneurons expressed BHLHB5 in cervical or lumbar segments, respectively. Importantly, more than 90% of BHLHB5+ V2a INs expressed CHX10, indicating BHLHB5 labels a subset of Chx10-high V2a INs (Supp Fig 5-2C).

We next examined the protein expression of SHOX2. In cervical segments, $27 \pm 2\%$ ($n=3$ animals, \pm SEM %) of V2a interneurons were labeled with SHOX2 antibody, whereas in lumbar segments, $26 \pm 0\%$ ($n=3$ animals, \pm SEM %; $p=0.47$, t test) of the V2a interneurons were labeled, indicating that this V2a marker gene is expressed in a defined fraction of V2a INs regardless of the spinal segments (Supp Fig 5-2D).

Collectively, our colocalization studies show that multiple V2a marker genes exhibit rostrocaudal diversification, but each marker gene exhibits different expression patterns: LHX4 labels broader V2a populations, LHX3 labels similar subpopulation to CHX10, and BHLHB5 labels a subset of CHX10-high V2a INs (Supp Figure 5-2E). In contrast, SHOX2 is expressed in a defined fraction of V2a INs regardless of the spinal segments (Supp Figure 5-2E).

V2a diversification and molecular heterogeneity correspond to distinct anatomical pathways

Given our observation that the molecular diversification of V2a INs with regard to CHX10 is maintained into adulthood once it is established during embryonic development, we were interested to explore a functional correlate of the molecular diversification. To elucidate how V2a INs with distinct molecular marker genes may correspond to anatomical connectivity schemes, we revisited our anatomical connectivity experiments to examine whether V2a IN diversification corresponds to any of the connectivity that V2a interneurons exhibit. We focused our analyses on cervical segments given the heterogeneous V2a compositions with regards to their anatomical projection patterns as well as Chx10 expression.

We first labeled the brainstem-projecting V2a interneurons by injecting Δ G-Rabies:GFP

into the brainstem and asked what their CHX10 expression status is. We found that $83\pm 5\%$ of brainstem-projecting V2a interneurons were CHX10^{low} V2a INs, while $44\pm 3\%$ of all the V2a INs in the corresponding spinal segments were CHX10^{low} V2a INs ($p < 0.0001$, Figure 6A,C). Importantly, we found that the CHX10^{low} enrichment in this viral tracing study was not a direct result of viral infection down-regulating CHX10 expression (Supp Fig 6A). These observations collectively reveal the significant enrichment of CHX10^{low} identity within the brainstem-projecting status of V2a INs, uncovering a link between anatomical (brainstem-projection) and molecular (CHX10^{low} subpopulation) characteristics of V2a INs enriched in cervical segments.

Previous studies have shown that a subpopulation of V2a INs provides direct input simultaneously to the brainstem centers and forelimb motor neurons representing an efferent copy pathway (Azim et al. 2014; Pivetta et al. 2014). We therefore investigated whether there was also an enrichment of CHX10^{low} V2a INs in the cervical premotor population. Reflecting our observations for the supraspinal projecting V2a INs, we found that $71\pm 5\%$ of premotor V2a INs were CHX10^{low} INs (Figure 6B,C), raising the possibility that Chx10-low V2a subtype represents the efferent copy pathway among other V2a INs.

So far, of the anatomical connectivity that we tested, both brainstem-projecting and motor neuron-projecting status of V2a interneurons corresponded to CHX10^{low} status in cervical segments. Based on distributions of V2a synaptic terminals (Fig 1), we hypothesized that CHX10^{high} V2a INs provide inputs to ventral spinal interneurons. To investigate this possibility, we took advantage of Chx10 reporter line that expresses CFP under the endogenous chx10 promoter (Chx10:CFP). We first confirmed that CFP expression recapitulated the endogenous CHX10 protein (Figure 6D), indicating that Chx10:CFP line can be utilized to visualize processes of CHX10^{high} V2a interneurons. We then looked for VGLUT2+ CFP+ puncta surrounding ventral spinal neurons. Indeed we observed ventral spinal neurons with VGLUT2+CFP+ puncta, suggesting that CHX10^{high} V2a interneurons project onto ventral spinal neurons (Figure 6E). Together, our observations reveals that developmentally-imposed heterogeneous expression of Chx10 expression segregates connectivity schemes of V2a INs into supraspinal projection and intraspinal projection.

Figure 2.12: Molecular diversification of V2a interneurons corresponds to brainstem-projecting status.

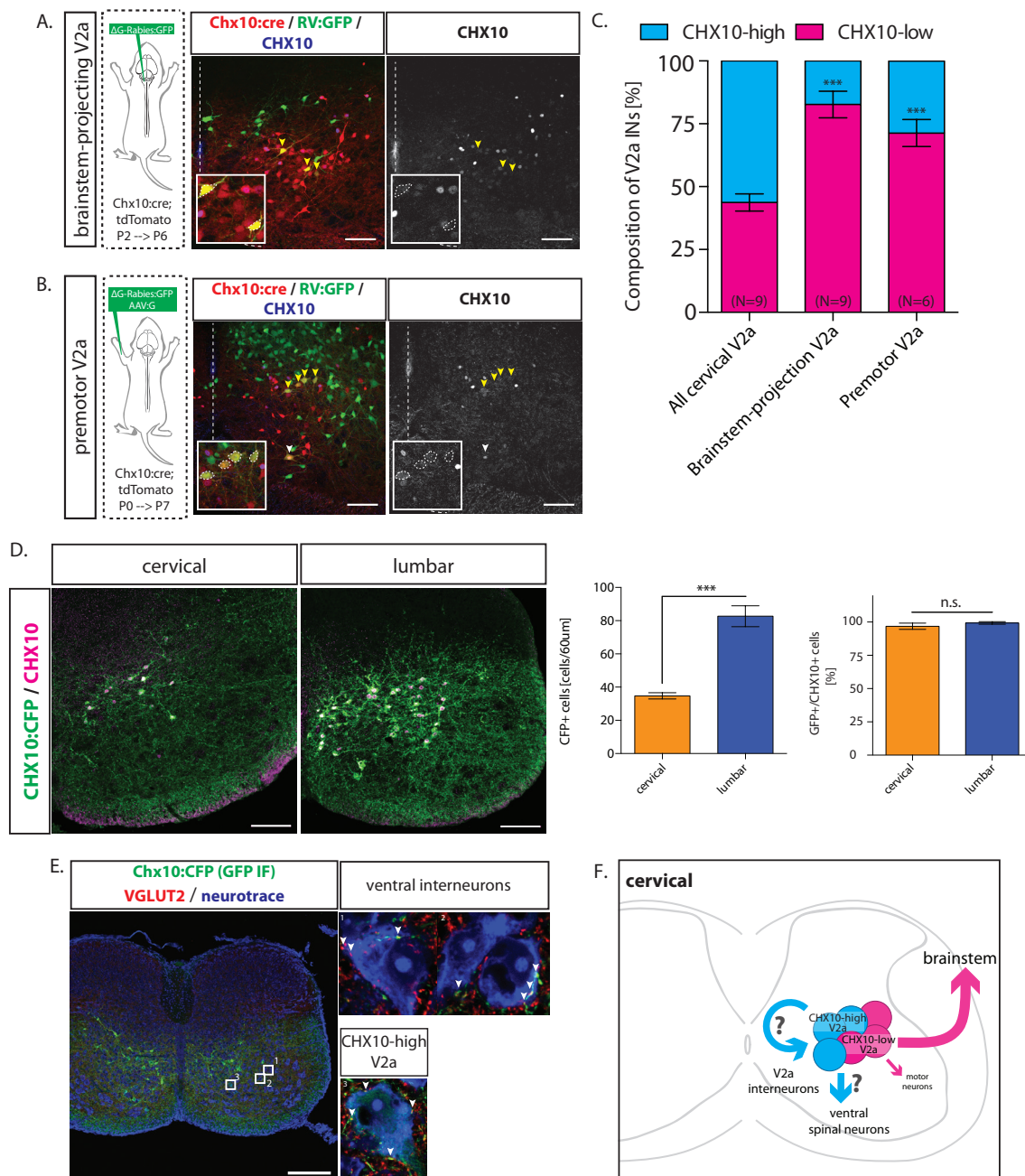
(A,C) Brainstem-projecting V2a neurons are predominantly composed of Chx10-low V2a neurons. Molecular identity of brainstem-projecting V2a interneurons was examined. CHX10 immunostaining was conducted on ΔG -Rabies:GFP+ tdTomato+ V2a interneurons. $83 \pm 5\%$ ($n=9$ animals from 3 litters, \pm SEM %) of brainstem-projecting V2a interneurons did not express a detectable level of CHX10, while $44 \pm 3\%$ ($n=9$ animals from 3 litters, \pm SEM %) of all the V2a interneurons in the corresponding sections did not express detectable level of CHX10 ($p < 0.0001$, t test), indicating significant enrichment of CHX10-OFF identity within the brainstem-projecting status of V2a interneurons. Yellow arrowheads: brainstem-projecting V2a interneurons without CHX10 expression. 25um cryosections. Scale bar: 50um.

(B,C) Cervical premotor V2a neurons are predominantly composed of Chx10-low V2a neurons. Molecular identity of premotor V2a interneurons was examined. CHX10 immunostaining was conducted on ΔG -Rabies:GFP+ tdTomato+ V2a interneurons. $71 \pm 5\%$ ($n=6$ animals from 2 litters, \pm SEM %) of premotor V2a interneurons did not express detectable level of CHX10 ($p=0.0005$, t test). Yellow arrowheads: premotor V2a interneurons without CHX10 expression. White arrowhead: CHX10-ON premotor V2a interneuron. 25um cryosections. Scale bar: 50um

(D) Chx10:CFP reporter line preferentially labels Chx10-high V2a INs. Expression patterns of CFP driven by the endogenous Chx10 promoter and endogenous CHX10 protein were examined at P3. More CFP+ were observed in lumbar segments compared to cervical segments ($n=7$ animals, $p < 0.0001$, t-test). In cervical segments, $96 \pm 2\%$ ($n=7$ animals, \pm SEM %) of CHX10+ cells were CFP+, and in lumbar segments, $99 \pm 1\%$ ($n=6$ animals, \pm SEM %) of CHX10+ cells were CFP+, highlighting how CFP expression recapitulates CHX10 expression. 20um cryosections. Scale bar: 50um.

(E) Chx10-high V2a neurons can project onto ventral spinal neurons. Putative postsynaptic neurons of CHX10-high V2a interneurons were examined. Putative postsynaptic neurons were visualized by colocalization between CFP (green), VGLUT2 (red), and neurotrace (blue). Numbered boxes correspond to magnified images on the right. Putative presynaptic terminals were observed onto ventral interneurons (1, 2) and Chx10-high V2a interneurons (3). 20um cryosections. Scale car: 100um.

(F) Working model of our current study is shown. V2a interneurons as a population project to motor neurons, ventral interneurons, V2a interneurons themselves, or the supraspinal structure such as the brainstem. Our viral tracing experiments in cervical segments reveal that V2a interneurons projecting into the brainstem or onto motor neurons are enriched with V2a interneurons without detectable CHX10 protein expression. Based on Chx10:CFP signal, we speculate that the remaining projection targets, such as ventral spinal neurons including V2a interneurons themselves, are enriched by CHX10-ON V2a interneurons, potentially segregating V2a interneurons into output pathways (i.e. motor neurons or supraspinal structures) and intraspinal recurrent pathways (i.e. ventral spinal neurons and V2a interneurons).



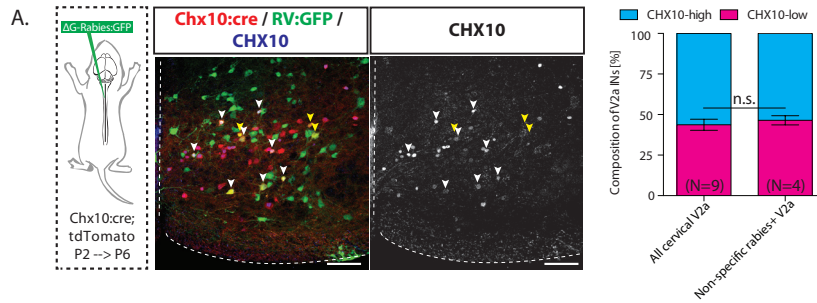


Figure 2.13: Rabies infection control experiment.

(A) Rabies infection does not downregulate CHX10 expression. Molecular identity of non-specific rabies+ V2a interneurons was examined. ΔG -Rabies:GFP was directly injected into cervical segments of the spinal cord to non-specifically label V2a interneurons. $46 \pm 2\%$ ($n=4$ animals from 1 litter, \pm SEM %) of ΔG -Rabies:GFP+ tdTomato+ V2a interneurons did not express detectable level of CHX10 ($p=0.63$, t test), indicating that rabies virus infection itself had little effect on CHX10 expression under our experimental condition. Yellow arrowhead: rabies+ V2a interneuron without CHX10 expression. White arrowhead: CHX10-ON rabies+ V2a interneuron. 25um cryosections. Scale bar: 50um.

Discussion

The spinal cord represents the final stage in generating motor outputs, where descending commands and sensory inputs are transformed into appropriate activity pattern of motor neurons to elicit behaviorally-relevant muscle contractions. The diverse behavioral outputs that the spinal cord mediates along the rostrocaudal axis raises the possibility that different spinal segments exhibit discrete network architectures that reflect diverse behavioral demands. One of the cardinal IN classes V2a INs plays important roles in multiple behavioral contexts: Whole body elimination of V2a INs results in locomotor deficits (Crone, et al. 2009), while forelimb-specific elimination of V2a INs results in forelimb reaching behavior deficits without locomotor defects (Azim, et al. 2014). We reasoned that these multiple behavioral defects the previous studies uncovered reflect cellular diversity of V2a INs and investigated V2a INs as a neural substrate that constitutes distinct network architectures in different segments. Here, we addressed how different spinal segments are composed of V2a INs with distinct molecular and connectivity schemes, underlying distinct operation of the spinal cord circuits in different segments.

We identified differential connectivity schemes and functional contributions of V2a INs in cervical versus lumbar segments. Through RNA-sequencing, we found that the conventional V2a IN marker gene *chx10* itself is dynamically regulated along the rostrocaudal axis in a graded manner during embryonic development. We found that the novel sub-population of V2a INs enriched in cervical segments (*CHX10^{low}*) preferentially communicates with supraspinal structures, diversifying the connectivity schemes that V2a INs exhibit in different spinal segments. Our findings collectively reveal that, during embryonic development, a molecularly-defined single spinal network component undergoes diversification along the rostrocaudal axis to support distinct motor outputs of different spinal cord segments. Our study establishes a framework of how diversification of spinal neurons along the rostrocaudal axis underlies distinct intrinsic network properties in different spinal segments.

Chx10-high/Chx10-low V2a INs and circuit operations in cervical and lumbar segments

Through RNA-sequencing, we have uncovered that the conventional V2a IN marker gene

Chx10 is surprisingly differentially expressed between cervical and lumbar segments. We find that lumbar V2a INs are mainly in a Chx10-high status, while cervical V2a INs include a novel Chx10-low subtype of V2a INs.

Based on our viral tracing studies, Chx10-low V2a IN subtype, which is enriched in cervical segments, represents V2a INs that project into the supraspinal structures. This pathway, named efferent copy pathway, is required for forelimb reaching behaviors that require precisions and online corrections in primates, cats, and rodents (Alstermark and Ekerot, 2013; Azim et al. 2014; Pivetta et al. 2014). Therefore, it is feasible to postulate that cervical networks contain quantitatively more anatomical substrates of V2a INs represented by Chx10-low status to support more modular network operations via supraspinal structures underlying forelimb movements.

Unlike cervical V2a INs, lumbar V2a INs exhibit more direct anatomical connectivity to MNs, and activity of lumbar V2a INs recruits both ipsilateral and contralateral motor outputs, while cervical V2a INs have limited contribution to motor outputs under our experimental set up (Figure 2, 3). Therefore, lumbar V2a INs may be better positioned to underlie autonomous network operation within the spinal cord and directly regulate the motor output to achieve stable and robust motor programs, which may accompany less precision via feedbacks from the supraspinal structures. This idea is supported by our observations. First, we did not observe supraspinal-projecting V2a INs from the lumbar segments. Secondly, Chx10-low V2a INs represent a small proportion of lumbar V2a INs.

In order to access the Chx10-high V2a INs, we took advantage of the fact that the Chx10:CFP line reflects the endogenous CHX10 protein expression and hence labels the Chx10-high V2a INs. Using this strategy, we observed that Chx10-high V2a INs can project to INs residing in the ventral spinal cord. The specific projection targets of Chx10-high V2a INs remains to be investigated in further detail. However, the enrichment of the Chx10-low status within supraspinal projecting V2a INs leads us to speculate that Chx10-high V2a INs in turn target INs in the ventral spinal cord, providing excitatory drive broadly within the spinal cord instead of communicating with the supraspinal structure. If this were the case, lumbar networks, that are predominantly composed of Chx10-high V2a INs, may be better suited to provide stronger excitatory drive to the ventral spinal cord than cervical networks, which have a higher proportion

of Chx10-low V2a INs. This, together with direct connection onto MNs, may establish a network basis for the robust and reliable motor outputs that we observed upon activation of lumbar V2a INs compared to cervical V2a INs (Figure 3).

How may V2a INs be involved in the operation of thoracic spinal networks? At a glance, the graded nature of V2a IN molecular diversity appears inconsistent with the drastic morphological changes at the periphery: namely the transition between limbs and trunk. However, forelimb movements are closely accompanied by contractions of trunk muscles for, for instance, stabilizing the body as animals reach an object. With this regard, the continuum of V2a IN molecular gradient between cervical V2a INs and thoracic V2a INs may make sense in order to achieve activating a variety of MNs during forelimb movements. Consistent with the graded nature of V2a INs along the rostrocaudal axis, our preliminary observation shows that activation of thoracic V2a INs results in thoracic MN spikes with a latency that is between cervical and lumbar (data not shown). Furthermore, our observations indicate that V2a INs project their axon across multiple segments. Indeed, forelimb or hindlimb premotor V2a INs can be found also in thoracic segments away from starter MNs (data not shown, Ni et al. 2014). This raises the possibility that the location of soma may not necessarily predict their contribution of motor outputs and that V2a INs in thoracic segments are also involved in regulation of cervical and/or lumbar segments.

Emergence of circuit diversity over the course of evolution

Given the developmental diversification of V2a INs and the importance of the supraspinal pathways in forelimb function, did this diversification mechanism play an instructive role in the emergence of forelimb functions over the course of evolution? While this pathway is necessary for the dexterous forelimb movement in primates, cats, and mice, spinal neurons seem to project into LRN also in species without dexterous digits such as ungulates (Alstermark and Ekerot. 2013; Azim, et al. 2014; Rao, et al. 1969). Furthermore, V2a INs in zebrafish readily exhibit supraspinal projection morphology specifically in the rostral segments (Menelaou, et al. 2014). We therefore speculate that the rostrocaudal diversification and the anatomical pathway are evolutionarily-conserved phenomena at least at a crude level, and they themselves may not

necessarily have instructed the emergence of dexterous forelimb movements. Perhaps it was novel computations in the supraspinal structures (in the brainstem, cerebellum, or cortex) that instructed the emergence of forelimb movements, together with morphological changes of peripheral digits that facilitated the movements.

Given the evolutionarily-conserved nature of the supraspinal projection, an alternative way to view this diversification of spinal neurons and corresponding network architecture may be that cervical spinal network may be generally better positioned to update supraspinal structures with the spinal network activity. Within the supraspinal structures, different sensory inputs or motor plans may be integrated together with the inputs from the spinal cord to shape final motor outputs that the animal is capable of doing using forelimbs (in mammals) or fins (in zebrafish). Indeed, LRN has been shown to receive inputs from multiple regions of CNS including sensorimotor cortex, red nucleus, superior colliculus, and other brainstem regions in addition to spinal cord (Alstermark and Ekerot. 2013; Pivetta et al. 2014).

Marker gene expression and cell types

In our current study, we utilized RNA-seq technology to uncover genes differentially expressed in different segments of the spinal cord, and we identified the conventional V2a IN marker gene *Chx10* itself as a postnatal marker for rostrocaudal diversification of V2a INs: V2a INs enriched in cervical segments contain a novel V2a subtype that express *chx10* at a low level. Interestingly, in our RNA-seq analysis, we did not find a V2a IN-specific gene that was enriched only in cervical segments. This raises the possibility that there is no single gene that marks *Chx10*-low V2a INs by itself and poses a limitation in identifying a potential cell type based solely on a single gene. Given the recent efforts into identifying novel cell types through combinatorial codes of transcription factors (Francius et al. 2014; Bikoff et al. 2016; Gabbitto et al. 2016; Wenick and Hobert, 2004), it would be intriguing to investigate whether including additional genes/transcription factors from our RNA-seq data set would allow us to genetically-access *Chx10*-low V2a INs or further subdivide V2a INs in general.

Molecular and developmental mechanisms underlying V2a diversification

What is the molecular mechanism underlying the rostrocaudal diversification of V2a INs during embryonic development? Our observations so far suggest that this may be achieved in a cell-autonomous manner, since we did not observe alteration of V2a diversification with regard to CHX10 expression after eliminating MNs (ChAT:cre x ROSA:lsl:DTA, data not shown) or proprioceptive inputs (Pv:cre x ROSA:lsl:DTA, data not shown). Moreover, alternation of notch pathway (Chx10:cre x ROSA:lsl:NotchICD) or hox accessory protein (Nestin:cre x Foxp1fl/fl) did not alter the CHX10 diversification (data not shown). Given the graded nature of V2a IN diversification (Supp Figure 5A), one candidate mechanism is that rostrocaudal morphogens, such as RA, FGF and GDF, set up the molecular nature of the V2a diversification progressively during embryonic development either in a hox-dependent or –independent manner.

Roles of chx10 gene in V2a INs

What are the molecular consequences of having Chx10 at high level in one population while the other population expresses at a low level? Given the distinct axonal projection and anatomical connectivity scheme correlated with the Chx10-low subtype, it would be intriguing if downregulation of chx10 were involved in regulating such events.

Transcription factor chx10/vsx2 has been studied in the retinal development, where it is expressed in the retinal progenitors, bipolar cells, and a subset of muller glia, and chx10 null animals exhibit microphthalmia (Burmeister et al. 1996). Overexpression of Chx10 in retinal progenitors generates ectopic bipolar cells at the expense of photoreceptor cells, while Chx10-VP16 results in the opposite, suggesting that repressive functionality of chx10 instructs bipolar cell fate (Levne-bar, et al. 2006). Direct or indirect downstream genes of chx10 have been identified during retinal development (Zou and Levine, 2012; Reichman et al. 2009; Rowan et al. 2004), but mechanistic insights into how chx10 regulates downstream gene networks and define the cellular behaviors of these cell types still remain elusive.

Chx10 homolog ceh-10 has been studied as a terminal selector gene in *C.elegans*, where it is involved in AIY neuron cell fate specification (Altun-Gultekin et al 2001). In this context, ceh-10 together with ttx-3 has been shown to regulate a battery of genes that characterize

the behavior of AIY neurons such as neurotransmitter receptors as well as *ceh-10* and *ttx-3* themselves (Wenick and Hobert, 2004). The cooperative nature of *ceh-10* and *ttx-3* in regulating downstream genes raises the possibility that *Chx10* works with other transcription factors to regulate downstream gene expression to confer the characteristics of V2a INs.

Graded nature of diversification is found elsewhere in the CNS

We report that the conventional V2a marker gene *Chx10* is enriched in lumbar V2a INs than cervical V2a INs. The fraction of *CHX10*⁺ V2a INs is graded along the rostrocaudal axis, rostral-low and caudal-high, and this expression profile is maintained in the adult mice. In addition to *CHX10*, other transcription factors expressed in V2a INs, including *LHX3*, *LHX4*, and *BHLHB5*, are also expressed in a graded manner with rostral-low and caudal-high (Supp Figure 5-2). Graded expression patterns of transcription factors have been reported elsewhere in the CNS. In the developing cortex, multiple transcription factors are expressed with a gradient within the progenitors (Greig, et al. 2013; O’Leary et al. 2007) and transiently in postmitotic neurons (Joshi, et al. 2008; Zembrzycki, et al. 2015). These transient expression of transcription factors at multiple developmental stages regulate ultimate cortical area identities with discrete anatomical connectivity. In adult mice, hippocampal CA1 pyramidal cells exhibit graded expression pattern of numerous transcription factors along the dorsoventral axis (Cembrowski, et al. 2015). Therefore, this graded expression pattern of transcription factors that we have uncovered may represent a molecular strategy and organizational principle underlying diversification of neurons across different regions of the nervous system both during development and in adult.

Author Contributions

M.H. and S.L.P. designed the study and wrote the manuscript. M.H. and C.A.H. designed and carried out the experiments with help from A.J.L. and K.L.H.. A.J.L. generated AAV-hSyn:FLEX:GFP plasmid. S.P.D. analyzed RNA-sequencing data. K.S. provided *Chx10:Cre* and *Chx10:lsl:CFP* line.

Acknowledgements

We would like to thank K. Lettieri, M. Gullo, L.C. Bachmann, M.J. Sternfeld, N.D. Amin, P.J. Osseward, Salk GT3 core (L. Lisowski, J. Naughton, J. Marlet, R. Armendariz, C. Ly), FCCF core (C. O'Connor, C. Fitzpatrick), NGS core (M. Ku) for technical support and advice; M. Goulding and R. Johnson for providing reagents. M.H. was supported by the Timken-Sturgis Foundation and the Japanese Ministry of Education, Culture, Sports, Science, and Technology Long-Term Student Support Program. C.A.H. was supported by a U.S. National Research Service Award Fellowship from U.S. National Institutes of Health NINDS. A.J.L. was supported by George E. Hewitt Foundation for Medical Research and Christopher and Dana Reeve Foundation. K.L.H. was supported as a National Science Foundation Graduate Research Fellow and by the Chapman Foundation. S.L.P. is supported as a Howard Hughes Medical Institute Investigator and as a Benjamin H. Lewis chair in neuroscience. This research was supported by funding from the Howard Hughes Medical Institute, the Marshall Foundation and the Sol Goldman Charitable Trust.

References

- Alaynick, W.A., Pfaff, S.L., and Jessell, T.M. SnapShot: spinal cord development. *Cell*. 146, 178-178. 2011.
- Al-Mosawie, A., Wilson, J.M., and Brownstone, R.M. Heterogeneity of V2-derived interneurons in the adult mouse spinal cord. *Euro. J. Neurosci*. 26, 3003-3015. 2007.
- Alstermark, B., and Ekerot, C.F. The lateral reticular nucleus: a precerebellar centre providing the cerebellum with overview and integration of motor functions at systems level. A new hypothesis. *J. Physiol*. 591, 5453-5458. 2013.
- Altun-Gultekin, Z., Andachi, Y., Tsalik, E.L., Pilgrim, D., Kohara, Y., and Hobert, O. A regulatory cascade of three homeobox genes, *ceh-10*, *ttx-3* and *ceh-23*, controls cell fate specification of a defined interneuron class in *C. elegans*. *Development*. 128, 1951-1969. 2001.
- Azim, E., Jiang, J., Alstermark, B., and Jessell, T.M. Skilled reaching relies on a V2a propriospinal internal copy circuit. *Nature*. 508, 357-363. 2014.
- Bertrand, V. and Hobert, O. Linking Asymmetric cell division to the terminal differentiation program of postmitotic neurons in *C.elegans*. *Dev.Cell*. 16, 563-575. 2009.
- Bikoff, J.B., Gabitto, M.I., Rivard, A.F., Drobac, E., Machado, T.A., Miri, A., Brenner-Morton, S., Famohure, E., Diaz, C., Alvarez, F.J., Mentis, G.Z., and Jessell, T.M. Spinal inhibitory interneuron diversity delineates variant motor microcircuits. *Cell*. 165, 207-219. 2016.
- Burmeister, M., Novak, J., Liang, M.Y., Basu, S., Ploder, L., Hawes, N.L., Vidgen, D., Hoover, F., Goldman, D., Kalnins, V.I., Roderick, T.H., Taylor, B.A., Hankin, M.H., and McInnes, R.R.

- Ocular retardation mouse caused by Chx10 homeobox null allele: impaired retinal progenitor proliferation and bipolar cell differentiation. *Nat. Genet.* 12, 376-384. 1996.
- Cembrowski, M.S., Bachman, J.L., Wang, L., Sugino, K., Shields, B.C., and Spruston, N. Spatial gene-expression gradients underlie prominent heterogeneity of CA1 pyramidal neurons. *Neuron.* 20, 351-368.
- Crone, S.A., Quinlan, K.A., Zagoraïou, L., Droho, S., Restrepo, C.E., Lundfald, L., Endo, T., Setlak, J., Jessell, T.M., Kiehn, O., and Sharma, K. Genetic ablation of V2a ipsilateral interneurons disrupts left-right locomotor coordination in mammalian spinal cord. *Neuron.* 70-83. 2008.
- Crone, S.A., Zhong, G., Harris-Warrick, R., and Sharma, K. In mice lacking V2a interneurons, gait depends on speed of locomotion. *J. Neurosci.* 29, 7098-7109. 2009.
- Dougherty, K.J. and Kiehn, O. Firing and Cellular Properties of V2a Interneurons in the Rodent Spinal Cord. *J. Neurosci.* 30, 24-37. 2010.
- Dougherty, K.J., Zagoraïou, L., Satoh, D., Rozani, I., Doobar, S., Arber, S., Jessell, T.M., and Kiehn, O. Locomotor rhythm generation linked to the output of spinal shox2 excitatory interneurons. *Neuron.* 80, 920-933. 2013.
- Esposito, M.S., Capelli, P. and Arber, S. Brainstem nucleus MdV mediates skilled forelimb motor tasks. *Nature.* 508, 351-356. 2014.
- Francius, C., Harris, A., Rucchin, V., Hendricks, T.J., Stam, F.J., Barber, M., Kurek, D., Grosveld, F.G., Pierani, A., Goulding, M., and Clotman, F. Identification of multiple subsets of ventral interneurons and differential distribution along the rostrocaudal axis of the developing spinal cord. *PLoS One.* 8, e70325. 2013.
- Gabitto, M.I., Pakman, A., Bikoff, J.B., Abbott, L.F., Jessell, T.M., and Paninski, L. Bayesian sparse regression analysis documents the diversity of spinal inhibitory interneurons. 165, 220-233. 2016.
- Goulding, M. Circuits controlling vertebrate locomotion: moving in a new direction. *Nat. Rev. Neurosci.* 10, 507-518. 2009.
- Grieg, L.C., Woodworth, M.B., Galazo, M.J., Padmanabhan, H., and Macklis, J.D. Molecular logic of neocortical projection neuron specification, development and diversity. *Nat Rev Neurosci.* 14, 755-769. 2013.
- Hagglund, M., Dougherty, K.J., Borgius, L., Itohara, S., Iwasato, T., and Kiehn, O. Optogenetic dissection reveals multiple rhythmogenic modules underlying locomotion. *PNAS.* 110, 11589-11594. 2013.
- Horsford, D.J., Nguyen, M.T., Sellar, G.C., Kothary, R., Arnheiter, H., and McInnes, R.R. Chx10 repression of mitf is required for the maintenance of mammalian neuroretinal identity. *Development.* 132, 177-187. 2004.
- Jeffery, N.D. and Fitzgerald, M. Lack of topographical organization of the corticospinal tract in the cervical spinal cord of the adult rat. *Brain Res.* 833, 315-318. 1999.
- Jessell, T.M. Neuronal specification in the spinal cord: inductive signals and transcriptional codes. *Nat. Rev. Genet.* 1, 20-29. 2000.
- Joshi, P.S., Molyneaux, B.J., Feng, L., Xie, X., Macklis, J.D., Gan, L. Bhlhb5 regulates the postmitotic acquisition of area identities in layers II-V of the developing neocortex. *Neuron.* 60,

258-272. 2008.

Kimura, Y., Okamura, Y., and Higashijima, S. Alx, a zebrafish homolog of Chx10, marks ipsilateral descending excitatory interneurons that participate in the regulation of spinal locomotor circuits. *J. Neurosci.* 25, 5784-94. 2006.

Kimura, Y., Satou, C., and Higashijima, S. V2a and V2b neurons are generated by the final divisions of pair-producing progenitor in the zebrafish spinal cord. *Development.* 135, 3001-3005. 2008.

Kimura, Y., Satou, C., Fujioka, S., Shoji, W., Umeda, K., Ishizuka, T., Yawo, H., and Higashijima, S.I. Hindbrain V2a Neurons in the Excitation of Spinal Locomotor Circuits using Zebrafish Swimming. *Curr. Biol.* 23, 843-849. 2013.

Kirilly, D., Gu, Y., Huang, Y., Wu, Z., Bashirullah, A., Low, B.C., Kolodkin, A.L., Wang, H., Yu, F. A genetic pathway composed of sox14 and mical governs severing of dendrites during pruning. *Nat. Neurosci.* 12, 1497. 2009.

Kullandar, K., Butt, S.J., Lebet, J.M., Lundfald, L., Restrepo, C.E., Rydstrom, A., Klein, R., Kiehn, O. Role of EphA4 and EphrinB3 in local neuronal circuits that control walking. *Science.* 299, 1889-1892. 2003.

Levine, A.J., Hinckley, C.A., Hilde, K.L., Driscoll, S.P., Poon, T.H., Montgomery, J.M., and Pfaff, S.L. Identification of a cellular node for motor control pathways. *Nat Neurosci.* 17, 586-593. 2014.

Livne-bar, I., Pacal, M., Cheung, M.C., Hankin, M., Trogadis, J., Chen, D., Dorval, K.M., and Bremner, R. Chx10 is required to block photoreceptor differentiation but is dispensable for progenitor proliferation in the postnatal retina. *PNAS.* 103, 4988-4993. 2006.

Ma, L.H. Gilland, E., Bass, A.H., and Baker, R. Ancestry of motor innervation to pectoral fin and forelimb. *Nat. Comm.*

Menelaou, E., Vandunk, C., and McLean, D.L. Differences in spinal V2a neuron morphology reflect their recruitment order during swimming in larval zebrafish. *J. Comp. Neurol.* 522, 1232-1248. 2014.

Narayanan, C.H., and Hanburger, V. Motility in chick embryos with substitution of lumbosacral by brachial and brachial by lumbosacral spinal cord segments. *J. Exp. Zool.* 178, 415-431. 1971.

Ni, Y., Nawabi, H., Liu, X., Yang, L., Miyamichi, K., Tedeschi, A., Xu, B., Wall, N.R., Callaway, E.M., and He, Z. Characterization of long descending premotor propriospinal neurons in the spinal cord. *J. Neurosci.* 34, 9404-9417. 2014.

O'Leary, D.D., Chou, S.J., and Sahara, S. Area patterning of the mammalian cortex. *Neuron.* 56, 252-269. 2007.

Pivetta, C., Esposito, M.S., Sigrist, M., and Arber, S. Motor-circuit communication matrix from spinal cord to brainstem neurons revealed by developmental origin. *Cell.* 156, 537-548. 2014.

Ramanathan, D.S., Conner, J.M., Anilkumar, A.A., and Tuszynski, M.H. Cholinergic systems are essential for late-stage maturation and refinement of motor cortical circuits. *J. Neurophysiol.* 113, 1585-1597, 2015.

Rao, G.S., Breazile, J.E., and Kitchell, R.L. Distribution and termination of spinoreticular afferents in the brain stem of sheep. *J. Comp. Neur.* 137, 185-196. 1969.

Reichman, S., Kalathur, R.K., Lambard, S., Ait-Ali, N., Yang, Y., Lardenois, A., Ripp, R., Poch, O., Zack, D.J., Sahel, J.A., and Leveill, T. The homeobox gene CHX10/VSX2 regulates RdCVF promoter activity in the inner retina. *Human Mol. Genet.* 19, 250-261. 2009.

Rowan, S., Chen, C.M., Young, T.L., Fisher, D.E., and Cepko, C.L. Transdifferentiation of the retina into pigmented cells in ocular retardation mice defines a new function of the homeodomain gene Chx10. *Development.* 131, 5139-5152. 2004.

Stepien, A.E., Tripodi, M., and Arber, S. Monosynaptic rabies virus reveals premotor network organization and synaptic specificity of cholinergic partition cells. *Neuron.* 68, 456-472. 2010.

Talpalar, A.E., Bouvier, J., Borgius, L., Fortin, G., Pierani, A., and Kiehn, O. Dual-mode operation of neuronal networks involved in left-right alternation. *Nature.* 500, 85-88, 2013.

Tennent, K.A., Adkins, D.L., Donlan, N.A., Asay, A.L., Thomas, N., Kleim, J.A., and Jones, T.A. The organization of the forelimb representation of the C57BL/6 mouse motor cortex as defined by intracortical microstimulation and cytoarchitecture. *Cereb. Cortex.* 21, 865-876, 2011.

Tripodi, M., Stepien, A.E., and Arber, S. Motor antagonism exposed by spatial segregation and timing of neurogenesis. *Nature.* 479, 61-66. 2011.

Wenick, A.S. and Hobert, O. Genomic cis-regulatory architecture and trans-acting regulators of a single interneuron-specific gene battery in *C.elegans*. *Dev.Cell.* 6, 757-770. 2004.

Zembryzycki, A., Perez-Garcia, C.G., Wang, C., Chou, S.J., and O'Leary, D.D.M. Postmitotic regulation of sensory area patterning in the mammalian neocortex by Lhx2. *PNAS.* 112, 6736-6741. 2015.

Zhang, Y., Narayan, S., Geiman, E., Lanuza, G.M., Velasquez, T., Shanks, B., Akay, T., Dyck, J., Pearson, K., Gosgnach, S., Fan, C., and Goulding, M. V3 spinal neurons establish a robust and balanced locomotor rhythm during walking. *Neuron.* 60, 84-96. 2008.

Zhong, G., Droho, S., Crone, S.A., Dietz, S., Kwan, A.C., Webb, W.W., Sharma, K., and Harris-Warrick, R.M. Electrophysiological Characterization of V2a Interneurons and Their Locomotor-Related Activity in the Neonatal Mouse Spinal Cord. *J. Neurosci.* 30, 170-182. 2010.

Zou, C. and Levine, E.M. Vsx2 controls eye organogenesis and retinal progenitor identity via homeodomain and non-homeodomain residues required for high affinity DNA binding. *PLoS Genet.* 8, e1002924. 2012.

Chapter 2 is an adaptation of a manuscript being prepared for submission. The working citation is: Hayashi, M., Hinckley, C.A., Driscoll, S.P., Levine, A.J., Hilde, K.L., Sharma, K., Pfaff, S.L. Rostrocaudal diversification of spinal neurons confers segment-specific spinal network architectures. The authors would like to thank K. Lettieri, M. Gullo, L.C. Bachmann, M.J. Sternfeld, N.D. Amin, P.J. Osseward, Salk GT3 core (L. Lisowski, J. Naughton, J. Marlet, R. Armendariz, C. Ly), FCCF core (C. O'Connor, C. Fitzpatrick), NGS core (M. Ku) for technical support and advice; M. Goulding and R. Johnson for providing reagents. M.H. was supported by the Timken-Sturgis Foundation and the Japanese Ministry of Education, Culture, Sports, Science, and Technology Long-Term Student Support Program. C.A.H. was supported by a U.S. National Research Service Award Fellowship from U.S. National Institutes of Health NINDS. A.J.L. was supported by George E. Hewitt Foundation for Medical Research and Christopher and Dana Reeve Foundation. K.L.H. was supported as a National Science Foundation Graduate Research Fellow and by the Chapman Foundation. S.L.P. is supported as a Howard Hughes Medical Institute Investigator and as a Benjamin H. Lewis chair in neuroscience. This research was supported by funding from the Howard Hughes Medical Institute, the Marshall Foundation and the Sol Goldman Charitable Trust.

Methods

Chapter 1 Methods

Chapter 1 does not contain experimental data.

Chapter 2 Methods

Mice.

The following strains of mice were used: ROSA-CAG:ls1:tdTomato (JAX, Ai9: <http://jaxmice.jax.org/strain/007905.html>); ROSA-CAG:ls1:Synaptophysin-tdTomato (JAX, Ai34D: <http://jaxmice.jax.org/strain/012570.html>); ROSA-CAG:ls1:ChR2-EYFP (JAX, Ai32: <http://jaxmice.jax.org/strain/012569.html>); Chx10:Cre (Azim et al. 2014); Chx10:CFP (Zhong, et al. 2010); Lmx1b:Cre (provided by R. Johnson, University of Texas MD Anderson Cancer Center). Mouse lines obtained from the JAX were maintained in B6 background, and the rest of the lines were maintained in CB6 background.

Viral tracing.

Aliquots of G-deleted Rabies:GFP and AAV1-hSyn:FLEX: tdTomato-2A-SypGFP (Addgene: #51509) were obtained from GT3 core at Salk Institute. The intramuscular injection and intraspinal injection are described elsewhere (Levine et al.). For the brainstem injection, Rabies:GFP was injected into various depths of rhombomere 8 and 9, which correspond to the posterior end of the developing cerebellum in early neonates (E18 and P4 reference atlas, Allen Brain Atlas). Spinal cords were collected 4-5 days after the injections.

Tissue preparation, immunohistochemistry and imaging.

Antibodies used were: Guinea pig anti-CHX10 (#717, 1:4000); Neurotrace-alexa647 (life technologies, 1:100); Guinea pig anti-VGLUT2 (Millipore, 1:3000); Rabbit anti-GFP (Lifetechnologies, 1:1,000); Goat anti-GFP (Millipore, 1:1,000); Rabbit anti-RFP (MBL, 1:1000); Rabbit anti-NeuN (Millipore, 1:1000); Rabbit anti-LHX3 (1:5000); Rabbit anti-LHX4 (1:5000); Guinea pig anti-LHX3 (1:5,000); Guinea pig anti-LHX4 (#721, 1:20,000); Guinea pig anti-SHOX2 (1:20,000); Goat anti-BHLHB5 (Santa Cruz).

Embryos were fixed with 2-4% PFA for 60-120 min. Postnatal spinal cords were

isolated and fixed with 4% PFA for 60-120 min. Adult mice were transcardially-perfused with PBS followed by 4% PFA. Adult spinal cords were dissected out and post-fixed with 4% PFA for 90 min. After the fixation, tissues were washed with PBS, equilibrated in 30% sucrose for 2hr – overnight, embedded in OCT, and subjected for cryosectioning onto glass slides (VWR). Immunohistochemistry was performed by incubating with primary antibodies (1-3 overnights, 4c) and fluophore-conjugated secondary antibodies (2hr, room temperature; life technologies, Jackson immuno). Sections were mounted with VectaShield (VECTOR) and coverslipped.

Optical stimulation and electrophysiology.

P2-4 spinal cords were isolated in 4°C oxygenated dissection ACSF (128 mM NaCl; 4 mM KCl; 21 mM NaHCO₃; 0.5 mM NaH₂PO₄; 3 mM MgSO₄; 30 mM d-glucose; and 1 mM CaCl₂), transferred to oxygenated room temperature recording ACSF (128 mM NaCl; 4 mM KCl; 21 mM NaHCO₃; 0.5 mM NaH₂PO₄; 1 mM MgSO₄; 30 mM d-glucose; and 2 mM CaCl₂) Suction electrodes were attached to the cervical (typically C8) or lumbar (typically L5) ventral roots, and cords were then allowed to recover and equilibrate to room temperature for ~20 min. A 20x 1.0 numerical aperture (NA) objective was used to deliver light through the dorsal surface, ipsilaterally to a region of 250um diameter. The illuminated area corresponds to approximately half a spinal segment at these stages. 50-ms light pulses were generated by a 200-W light source and high-speed mechanical (5 ms open time) shutter controlled by TTL signals from pclamp software.

Motorneuron responses were recorded via the ventral roots with a multiclamp 700B amplifier and filtered 300 Hz- 1kHz to isolate suprathreshold responses, unless otherwise noted. Latencies to motorneuron responses were measured offline from the onset of the stimulation. At each location, photostimulations were conducted 10 times with an interval of 10sec.

Extracellular recordings from V2a interneurons were conducted with borosilicate glass microelectrodes filled with recording ACSF (100-500 kΩ resistance) and amplified with a multiclamp 700B amplifier as described above. The dura mater was removed from the dorsal surface of the spinal cord, and the electrodes were slowly advanced through the spinal grey matter with a motorized micromanipulator (Sutter instruments). Optical stimulations were

triggered at ~25-50 μ m intervals to search for low latency/jitter spike responses. Consistent with the laminar distribution of V2a interneurons, we only detected optical responses for recording sites >250 μ m from the dorsal surface. Once V2a responses were identified 10 μ M CNQX and 20 μ M D-APV were bath applied to isolate direct responses from V2a interneurons. In a subset of experiments we further synaptically isolated V2a interneurons with 10 μ M CNQX, 20 μ M D-APV, 10 μ M picrotoxin and 1 μ M strychnine. Following synaptic isolation we continued to record responses from optically identified V2a interneurons at ~50 μ m intervals. At each location photostimulations were conducted 10 times with an interval of 10sec between stimulations. Responses were analyzed offline as described for motoneurons.

Following physiological recordings spinal cords were fixed by immersion in 4% PFA for 2 hrs.

RNA-seq sample preparation

Cervical and lumbar segments were dissected out in aCSF, and dissociation was conducted using Papain following manufacture's instruction (Worthington Biochemical). Via FACS, cells were collected directly into Trizol (Life Technologies). 5-6 embryos were used from each litter, which typically yielded ~20K cells. 3 litters were used to obtain biological replicates. Total RNA was isolated and digested with TURBO DNase (Life Technologies). Agilent Tape Station was used to determine RNA integrity (RIN) numbers prior to library preparation. Stranded mRNA-Seq libraries were prepared using the TruSeq Stranded mRNA Library Prep Kit according to the manufacturer's instructions (Illumina). Briefly, RNA with poly-A tail was isolated using magnetic beads conjugated to poly-T oligos. mRNA was then fragmented and reverse-transcribed into cDNA. dUTPs were incorporated, followed by second strand cDNA synthesis. dUTP-incorporated second strand was not amplified. cDNA was then end-repaired, index adapter-ligated and PCR amplified. AMPure XP beads (Beckman Coulter) were used to purify nucleic acid after each steps of the library prep. All sequencing libraries were then quantified, pooled and sequenced at single-end 150 base-pair using the Illumina NextSeq 500 at the Salk NGS Core. Raw sequencing data was demultiplexed and converted into FASTQ files using CASAVA (v1.8.2). Libraries were sequenced with a depth median of 37.8 million (IQR = 35.5 - 38.7

million).

TruSeq adapters were trimmed from reads. Only reads > 50bp were retained. Remaining reads were filtered, selecting for reads with > 15 average base quality. Trimming and filtering was performed with the BBMap (BBTools) package. For genome alignments, HISAT2 was used with default settings and the mm10 mouse genome release. For gene expression analysis, Sailfish was used with a combined gene annotation using UCSC, RefSeq and Ensembl annotations. To include quantification of the Cre sequence, we inserted the sequence into the gene annotation prior to building the Sailfish index for quantification in order to quantify its expression simultaneously with the rest of the mouse transcriptome.

Differential expression testing was performed by using DESeq2, edgeR and limma/voom. The maximum post-hoc corrected p-value from the three programs was taken as the final p-value at each gene (i.e. significant in all three programs). Each program was run in “glm” mode, and all conditions presented were included in the model. Genes were considered significant at $p < 0.05$.